Commensal *Candida albicans* colonization alters the host gastrointestinal tract environment with immune and neuroendocrine consequences for host health

A thesis submitted by

Laura Markey

in partial fulfillment of the requirements for the degree of

PhD

in

Molecular Microbiology

Tufts University

Sackler School of Graduate Biomedical Sciences

February, 2020

Advisor: Carol Kumamoto, PhD

Abstract

Candida albicans is the most common commensal fungus found in the human gut microbiota. *C. albicans* is also an opportunistic pathogen and the primary cause of nosocomial fungal infections. This research investigated interactions between *C. albicans* and the host during commensal colonization using a murine gastrointestinal colonization model, to define how *C. albicans* affects host health when present as a member of the gut microbiota. An acute colonization model demonstrated that *C. albicans* colonization interacted with the host gut-brain axis and resulted in increased production of the hormone corticosterone (CORT) and increased anxiety-like behavior. Metabolomics analysis of the gastrointestinal (GI) tract revealed increased lipid abundance in general and a subset of neuroactive lipids, endocannabinoids, in particular in the *C. albicans*-colonized mice. Gene expression analysis of the liver revealed changes in expression of host genes that regulate that lipid homeostasis and glucose metabolism in response to the increased lipids in the *C. albicans*-colonized GI tract. Pharmacological manipulation of the endocannabinoid system demonstrated that these changes in the GI tract were responsible for the altered CORT production and anxiety-like behavior and revealed a novel mechanism by which changes to the gut microbiota resulted in changes to the gut-brain axis.

Humans are likely colonized with *C. albicans* over a period of weeks to months, therefore a long-term colonization model was used to investigate the impact of continued *C. albicans* carriage. Using this model, *C. albicans* was shown to induce an immune response that was protective against challenge with the gastrointestinal pathogen *Clostridioides difficile*. In the context of long-term colonization, *C. albicans* was also

shown to influence the bacterial members of the gut microbiota and resulted in decreased resilience of the bacterial gut microbiota in response to antibiotic perturbation. Together these studies demonstrate that the fungus *C. albicans* plays an important role in modulating host health under conditions of homeostasis and in response to challenge with a bacterial pathogen or antibiotic disruption.

Acknowledgements

Thank you to my mentor Carol Kumamoto, for her enthusiastic support of a microbiology thesis project that while rooted in understanding the biology of C*andida albicans* spent quite a bit of time investigating the endocrinology of stress and behavioral neuroscience. I relished the opportunity to study so many different (but related!) topics during my PhD research, and relied on your guidance, knowledge and support all along the way.

Thank you also to my committee member and unofficial neuroscience mentor Jamie Maguire who provided much needed expertise in all things neuroscience and neuroendocrinology. We would not have known where to begin in our study of the gut-brain axis without your expansive institutional knowledge and experience.

Thank you to the other members of my unusually large committee, Bree Aldridge, John Leong, Joan Mecsas and Honorine Ward for your embrace of this project and your patience as it took various unexpected twists and turns. Our committee meetings, tricky as they were to schedule, were always a source of productive discussion, honest feedback and encouragement.

Table of Contents

List of Tables

List of Figures

List of Copyrighted Materials Used

Markey, Laura, Lamyaa Shaban, Erin Green, Katherine Lemon, Joan Mecsas and Carol Kumamoto. “Pre-colonization with the commensal fungus *Candida albicans* reduces murine susceptibility to *Clostridium difficile* infection.” Gut Microbes, 2018, Nov 9 (6): 497-509

List of Abbreviations

2-AG- 2-arachidonoylglycerol
ACTH- adrenocorticotropic hormone
AEA- anandamide, N-arachidonoylethanolamide
CB1- cannabinoid receptor 1
CB2- cannabinoid receptor 2
CDI- Clostridioides difficile infection
CORT- corticosterone
CRH- corticotropin releasing hormone
DAGL- diacylglycerol lipase
Efg1- enhanced filamentous growth
EPM- elevated plus maze
FAAH- fatty acid amide hydrolase
FADS1- acyl-CoA 8-3 desaturase, Δ5 desaturase
FADS2- acyl-CoA 6 desaturase, Δ6 desaturase
FASN- fatty acid synthase
FMT- fecal microbiota transplant
FST- forced swim test
G6Pase- glucose-6-phosphatase
GI- gastrointestinal
GR- glucocorticoid receptor
HPA- hypothalamus-pituitary-adrenal
IBD- inflammatory bowel disease
ITS2- internal transcribed spacer
LEFSE- Linear Discriminant Analysis effect size
LnEA- linolenoylethanolamide
LEA- linoleoylethanolamide
Lip4- lipase 4
MAGL- monoacylglycerol lipase
MR- mineralocorticoid receptor
NAE- N-acylethanolamide
NAPE- N-acyl-phosphatidylethanolamine
NAPE-PLD N-acyl-phosphatidylethanolamine phospholipase
OEA- oleoylethanolamide
OTU- operational taxonomic unit
PEPCK-C- phosphoenolpyruvate carboxykinase, cytosolic
PLB1- phospholipase B 1
PUFA- polyunsaturated fatty acid
PUFA- polyunsaturated fatty acid
PVN- paraventricular nucleus
QIIME- Quantitative Insights Into Microbial Ecology

SCD1- stearoyl-CoA desaturase
SCN- suprachiasmatic nucleus
SREBP1c- sterol regulatory element-binding protein 1
THC- tetrahydrocannabinol
TRPV1- transient receptor potential vanilloid

Chapter 1 Introduction

1.1 *Candida albicans* and the mammalian host

Candida albicans is a eukaryotic microbe found in the human oral and gut microbiome, is acquired shortly after birth[1] and stably colonizes ~60% of humans[2–4]. *C. albicans* is a pleomorphic fungus which grows as either budding yeast or filamentous hyphal cells[5] and can also exhibit non-sexual phenotypic switching, all of which contribute to its ability to generate highly variable populations[6]. It is able to adapt to a wide-range of environments within the mammalian host and can survive and colonize in niches with variation in pH, oxygen and carbon dioxide levels and nutrient availability. In addition to being a highly adapted commensal microbe, *C. albicans* can also cause severe disease in an immunocompromised host. When a human host undergoes a change in immune status, such as becoming neutropenic following treatment with chemotherapy or other immunosuppressive drugs, *C. albicans* already present in the gut can invade the tissue, enter the bloodstream (Candidemia) and seed a distal organ such as the kidney, causing severe damage (Candidiasis)[7,8].

Over the course of their shared evolutionary history, the mammalian immune system has evolved to control C. *albicans* levels in the gastrointestinal (GI) tract, preventing its spread and limiting the *C. albicans* load without eliminating *C. albicans* entirely. This balanced immune response results from the induction of both the inflammatory Th17 response and the induction of tolerogenic dendritic cells and regulatory T cells[9–12]. Mice deficient for any one of the various arms of the complex immune response to *C. albicans* can develop candidiasis, increased inflammation and dissemination. An inflammatory Th1 response is required to control *C. albicans* growth

in the GI tract and involves both IFN-γ and IL-12 signaling. Mice lacking the IFN-γ receptor as well as IL-12p40$^{-/-}$ mice both were unable to control gastrointestinal *C. albicans* infections, resulting in persistently high levels of *C. albicans* in the GI tract and the development of invasive abscesses in the stomach[13,14]. In systemic infection or oral mucosal infection models, an inflammatory IL-17/IL-23 response is also required for protection from *C. albicans* disease[15,16], although these cytokines are actually detrimental to host antifungal response in the GI tract[12]. In addition to the inflammatory immune response, appropriate control of *C. albicans* in the GI tract also involves the development of the anti-inflammatory and tolerogenic immune response mediated by regulatory T cells. In response to gastrointestinal *C. albicans* colonization, nTreg cells accumulate in the GI tract, produce IL-10 and increase IDO production, decreasing damaging neutrophil inflammation and inducing the development of tolerogenic dendritic cells[9,17]. The interaction between the host and *C. albicans* in the GI tract is a complex balance between sufficient inflammation and fungal killing to prevent tissue invasion and disease and limiting that inflammation to prevent the immune system from causing damage to the host.

In addition to allowing *C. albicans* to survive in the GI tract, this tolerant immune response is also beneficial to the host: the tolerogenic dendritic cells induced protect the host from experimental colitis[10] and the stimulation of the Th17 response is protective against subsequent challenge with the serious gastrointestinal pathogen *Clostridioides difficile*[18] as well as the common bacterial pathogen *Staphylococcus aureus*[19]. Through its immunoregulatory properties, *C. albicans* thus acts as a true mutualist, as it benefits from the host's limited response and the host benefits from its presence.

However, if *C. albicans* is present in the GI tract of an immunocompromised host or host with pre-existing damage and inflammation of the GI tract, it can have the opposite effect on the immune environment. Various studies of patients with inflammatory bowel disease (IBD) correlated symptom severity with the presence or increased abundance of *C. albicans*[20–22]. In rodent models of IBD or other types of GI tract disruption, the addition of *C. albicans* to the disrupted or inflamed GI tract worsened symptoms and delayed healing[23–25]. The contrast between the protective immune response stimulated in the healthy host and the detrimental immune response in a host with underlying GI tract disease demonstrates that *C. albicans* is poised to exploit a change in host health or immune status, and switch to acting as a pathogen.

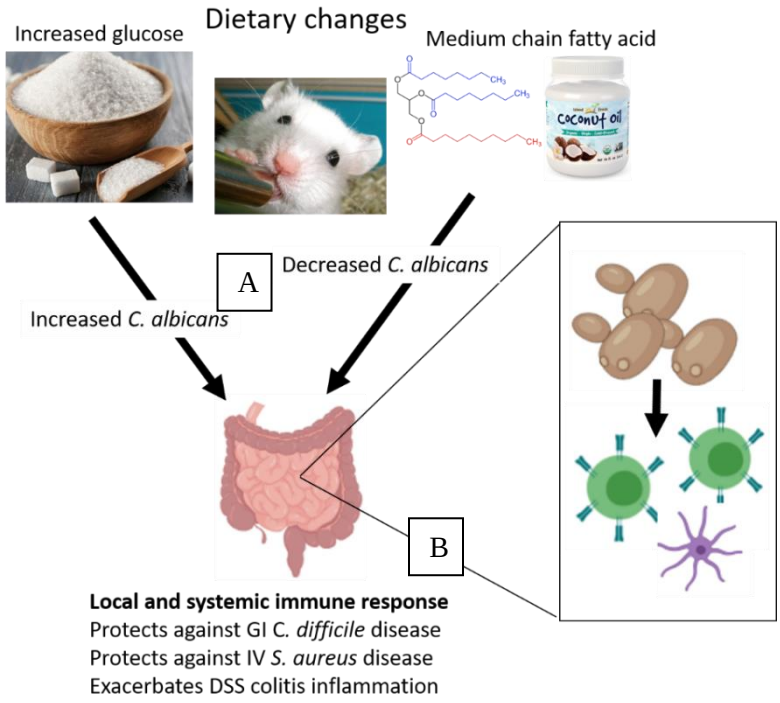

Figure 1.1: *C. albicans* interacts with the host gut environment. A) Changing host diet can affect the level of *C. albicans* colonizing the GI tract. Glucose supplementation increased *C. albicans* load while the addition of MCT oil to diet decreases *C. albicans* load. B) *C. albicans* stimulates an inflammatory immune response that is protective against infectious disease but can exacerbate pre-existing host inflammatory disease.

In addition to inducing changes in its host, *C. albicans* also changes its own transcriptional program in response to the host. Several transcription factors have been characterized as key regulators of commensal behavior as their regulatory targets include *C. albicans* metabolism, cell surface protein expression and cell morphology, are differentially regulated *in vivo* compared to laboratory growth and indeed are differentially regulated in pathogenic versus commensal mouse models[26–29]. One of these transcription factors, Efg1, is expressed at varying levels through the population of cells and allows the colonizing *C. albicans* to sense the immune status of the host. In a healthy host, cells with a low level of Efg1 are rapidly eliminated by the immune system, while cells with a high/stable level of Efg1 can persist[30]. In the absence of the immune response, the low Efg1 state outcompete the high Efg1 cells and have increased expression of metabolic genes allowing them to hypercolonize the GI tract[26,30]. Thus Efg` can act as an "immunosensor": variation in the Efg1 expression level in the population allows *C. albicans* to persist in the GI tract with the high Efg1 cells, and expand using the low Efg1 cells if the host becomes immunocompromised[31].

In addition to host-microbe interactions via the immune system, metabolic interactions between the host and *C. albicans* can affect the level of *C. albicans* in the GI tract and therefore its ability to cause disease. *C. albicans* is highly adapted to life in the GI tract and expresses an array of genes that allow it to utilize a range of host nutrients while colonizing the stomach through the large intestine. Although some of these environments have limited glucose availability (due to efficient host absorption and utilization) *C. albicans* can use long-chain fatty acids as a sole carbon source and efficiently convert them to glucose via β-oxidation followed by gluconeogenesis[32,33].

Changes in availability of host nutrients can significantly impact *C. albicans* carriage in the GI tract. A glucose-supplemented diet significantly increased the level of *C. albican*s in the GI tract of infant mice such that colonizing *C. albicans* was able to invade the stomach tissue after subsequent immunosuppression, while mice without glucose supplementation had significantly less invasion even after immunosuppression[34]. Conversely, an adult antibiotic-treated mouse model demonstrated that switching to a diet with limited long-chain fatty acids and rich in medium-chain fatty acids was sufficient to significantly decrease established *C. albicans* colonization of the GI tract[35] due to decreased *C. albicans* β-oxidation of lipids and thus decreased access to nutrients.

Understanding the connection between the mammalian host and *C. albicans* is clinically relevant, because *C. albicans* is the most common life-threatening fungal pathogen of humans[36,37]. Research into host-*C. albicans* interactions and how changes in host and microbe precede a switch from commensal to pathogenic behavior is therefore valuable and could help develop antifungal tools to prevent this switch from occurring. Previous research has focused largely on immune and to some extent the metabolic connections between *C. albicans* and the mammalian host. In light of the severe disease that gastrointestinal *C. albicans* is capable of causing should a host become immunocompromised, why is *C. albicans* the predominant fungal member of the human gut microbiome?

1.2 The gut microbiota protects the host from *Clostridioides difficile* disease

One well characterized way that bacterial members of the gut microbiota contribute to host health is through defense from gastrointestinal microbial pathogens. The bacterial gut microbiota is a major host defense mechanism against *C. difficile*

infection (CDI) and subsequent disease; CDI is a common, deadly and difficult to treat nosocomial infection. The diverse bacterial community of the gut microbiota limits available nutrients and physical space for *C. difficile* to infect the host, a phenomenon referred to as colonization resistance. More specifically, by transforming primary bile acids (compounds produced by the liver which aid in digestion of fat) to secondary bile acids in the intestine, the bacterial microbiota inhibits *C. difficile* spore germination and outgrowth[38]. Primary bile acids stimulate *C. difficile* spore germination, while secondary bile acids inhibit *C. difficile* vegetative growth[39]. Species of bacteria such as *Bacteroides sp., Clostridia sp*., and *Lactobacillus sp.* break down host-derived primary bile acids to secondary bile acids in the terminal ileum[40]. The bacterial microbiota is generally protective against gastrointestinal pathogens and specifically prevents CDI.

We also know that the gut microbiota is a key part of the normal host defense against *C. difficile* disease because disruption of the microbiota through treatment with antibiotics and exposure to *C. difficile* spores in a hospital setting are major risk factors for developing *C. difficile* disease. Although CDI can be treated with antibiotics, disease recurrence happens in 15-30% of patients[41]. Once one episode of recurrence has occurred, subsequent recurrences are likely to occur, as antibiotics successfully kill the pathogenic *C. difficile* bacteria but also kill commensal bacteria and limit the ability of the normal gut microbiota to recover.

Replacing the disrupted or eliminated gut microbiota of a CDI patient with a normal gut microbiota via fecal microbiota transplantation (FMT) has been widely successful in treatment of recurrent CDI, demonstrating that the normal gut microbiota is sufficient for protection from CDI disease[42–45]. However, the specific microbes involved

in this protection have not been identified- different bacterial species and combinations of species have all been shown to be capable of protecting the host from disease in rodent models[38,46]. Human FMT trials have utilized the transfer of complete gut microbiota communities, in as much as whole communities can be transferred from donor feces. Although the gut microbiota has been shown to play a role in many different aspects of human health, these FMT trials to treat recurrent CDI are the best example of how changing the gut microbiota is sufficient to improve host health.

The fungal members of the gut microbiota, or mycobiome, could also play a role in the success or failure of FMT as a treatment for CDI and may affect the overall efficacy of the microbiota in preventing CDI occurrence. In one study, researchers sequenced the internal transcribed spacer (ITS2) region of microbiota DNA samples from patients to define the mycobiome and identified a significant enrichment in nine fungal genera in patients with CDI compared to patients with diarrhea that did not have CDI[47]. Due to the limited reference genomes of fungi, only one of the nine enriched genera was identified: the *Penicillium* genus. Although not causal, this correlation suggested that an increase in commensal fungus abundance could be a feature of CDI. Other studies that sequenced the mycobiome have similarly found an overall enrichment of various fungal genera in patients with CDI diarrhea, including the most common commensal fungus *C. albicans*[48,49]. Studies that did not sequence the entire mycobiome, but only screened for the presence of *C. albicans* have found both negative[50] and positive[51,52] correlations between the presence of *C. albicans* and CDI, perhaps indicating that the effect of *C. albicans* on host CDI risk depends on additional host and microbial factors. This could

reflect a complex web of interactions that regulate *C. albicans* behavior as a commensal or an opportunistic pathogen in the GI tract environment.

1.3 The gut microbiota as an ecosystem

In investigating the effect of *C. albicans* colonization on the host and overall host health, we also wanted to understand how *C. albicans* interacts with the bacterial members of the gut microbiota. The bacterial gut microbiota is a complex and interconnected assemblage of bacterial species, which can vary widely from person to person in population composition but generally fulfills similar key metabolic functions[53]. Mammals are colonized shortly after birth with a simple gut microbiota, which then develops into the mature gut microbiota of adults by age one or two. During this period of acquisition, the community shifts in response to changes in diet such as the introduction of solid foods as well as illness and exposure to antibiotics[54]. Once matured, the gut microbiota of an adult is generally stable[55], although its composition can still be shifted by radical changes in diet such as becoming a vegan (or a vegetarian switching to eating meat)[56]. The process of acquisition, as well as the stability and diversity of the mature community, are likely regulated by interactions between bacterial species as well as collective interactions with the host. Many such interactions during acquisition and apparent equilibrium remain uncharacterized and could be key to our understanding of what makes a "normal" or "healthy" microbiota so beneficial to the host.

Although the role of individual bacterial species in affecting host health is largely unknown, overall diversity of the community is associated with improved human health[57,58] and with protection from CDI[59]. Diversity is clearly an important emergent property of the microbiota as a whole. It could be helpful to investigate other

characteristics of the microbiota as a whole entity that contribute to host health, in addition to ongoing studies focused on defining the role of key genera of commensal bacteria. The bacterial microbiota is a highly evolved, naturally-occurring and complex community of microbes, highly analogous to other natural ecosystems. To this end, the language and methodology of ecology provide a useful framework for analyzing the gut microbiota. The gut microbiota has been shown to regenerate itself after disruption by antibiotic treatment, a quality known as the resilience phenomenon. The classical ecological definition of resilience is the ability of a system to persist in the face of changes in the environment and return recognizably to its pre-disruption equilibrium[60]. Additional qualities of a complex ecosystem are also reflected in the gut microbiota community, including stability, the ability to resist perturbation and remain at equilibrium, and a more modern term, adaptive capacity, the ability to find resilience and stability across multiple stable states[61].

In investigating these underlying characteristics of the gut microbiota ecosystem, investigators often perturb the system and observe the response. The more resilient and stable a community is, the stronger the perturbation required to achieve disruption. In the context of the bacterial microbiota, perturbations can be short-term and severe, such as treatment with an antibiotic, or long-term and more subtle, such as a shift from an omnivorous to a vegan diet. Studies in humans and using rodent models have shown that a high dose of antibiotics is sufficient to disrupt the gut microbiota ecosystem, such that the gut microbiota shifts significantly in composition and diversity and remains different from the starting community even after a period of several months[55,62,63]. These studies demonstrate the limits to stability of the starting community, as it can be disrupted with a

severe enough perturbation, but also reflect the adaptive capacity of the microbiota- once the antibiotics are removed, although the community does not return to its starting state it does adopt a new, stable equilibrium state (rather than varying at random).

Adaptive capacity is often a trait that increases the health of an ecosystem in that it allows the community to reassemble even after a severe perturbation. In the case of the gut microbiota, the ability to adopt a separate but equally stable state can be a hindrance, as in the difficulty in treating a disease such as IBD in which the microbiota is present, stable, but characterized as "dysbiotic". One reason why FMT may have had such mixed results in the treatment of diseases such as IBD, in contrast to its overwhelming success in treating CDI, is the inherent stability and resilience of the dysbiotic IBD microbiota.

CDI patients are suffering from an infection with a single pathogen, *C. difficile*, which dominates the GI tract and causes disease symptoms. This population dominated by a single bacterial species is far less stable than a complex community such as a complete microbiota, therefore the addition of a stable collection of microbes through FMT is able to outcompete and eliminate the pathogen and treat CDI effectively. In order to effectively treat a disease like IBD, one would need to replace the existing stable but dysbiotic community with an equally stable and persistent "healthy" microbiota, which researchers have thus far been unable to accomplish. By continuing to characterize interactions between members of the healthy and dysbiotic gut microbiota, as well as with the host environment, we can better understand these bacterial ecosystems and develop new tools to push them from a dysbiotic stable state to a healthy stable state.

Previously researchers have demonstrated that *C. albicans* colonization alters the composition and diversity of the bacterial gut microbiota when mice are pre-treated with

antibiotics and then gavaged with *C. albicans*. Researchers identified overall separation in communities with and without *C. albicans* after three weeks of recovery from antibiotics (altered beta diversity) and specifically found that colonization with *C. albicans* inhibited recovery of Lactobacillus sp. and promoted recovery of *Enterococcus sp*.[64] These results indicated that *C. albicans* can affect how the gut microbiota recovers from antibiotic treatment. Additional research to characterize bacteria-fungal interactions in the context of the host environment would add another dimension to our understanding of the gut microbiota.

1.4 The gut-microbiota-brain axis

Several decades of investigation have demonstrated that the bacterial gut microbiota influences virtually every aspect of mammalian host health, including the gut-brain axis. The term gut-brain axis refers to the myriad bidirectional connections between the GI tract and the brain. These connections occur systemically, through the production of circulating mediators from enteroendocrine and immune cells in the GI tract, such as cytokines, hormones and metabolites, as well as through direct signaling from the GI tract environment to the brain via the enteric nervous system or the vagus nerve. Signals from the brain in turn can regulate activity in the GI tract, as the brain sends signals back down to the GI tract to regulate digestion, metabolism and motility[65,66]. Changes to the gut and the brain can affect the composition of the microbiota and changes in the microbiota can alter the GI tract environment and affect the local gut environment and the brain.

Specifically, researchers using mouse models have demonstrated significant changes in the composition of the gut microbiota in response to changes in the gut such as altered diet[67,68] or GI tract inflammation[69] and in response to changes in the brain such

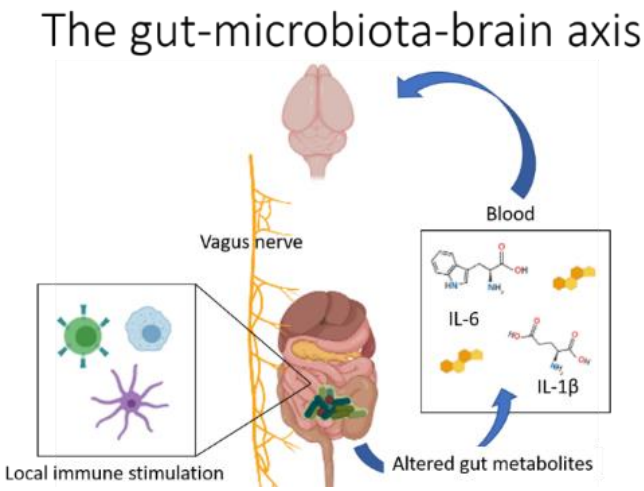

Figure 1.2: The gut-microbiota-brain axis. The gut (containing the microbiota) and the brain are connected by many pathways, three of which are highlighted here. A) The immune system can be stimulated by the microbiota and can interact with the brain either through inflammatory cytokines that circulate in blood (C) and interact with receptors at the blood-brain barrier or by interacting with receptors on afferent neurons in the gut that signal to the brain. B) The microbiota can change levels of neurotransmitters or other signaling compounds in the GI tract which interact with receptors on vagus nerve endings or afferent nerves of the enteric nervous system which signal directly to the brain. C) In addition to inflammatory cytokines, the microbiota can affect production of hormones or energy precursor metabolites in the GI tract, which then travel through the blood and signal at the blood-brain barrier.

as chronic psychological stress[70] or the induction of depression-like behavior[71]. Conversely, interventions that target the microbiota such as antibiotic treatment or repeated exposure to probiotic strains of bacteria alter permeability[72] and motility[73] of the GI tract, local and systemic metabolite abundance[74–77] and the production of hormones[73,78,79]. These changes to the microbiota can also change the brain, in that modifying the microbiota has been shown to alter anxiety-like[75,80–82] or depression-like behavior[83,84] as well as the acute psychological stress response[80,85,86]. Although many of these studies broadly disrupted the gut microbiota with antibiotics or compared germ-free

and specific-pathogen free animals, some research has been done to characterize the role of individual bacterial species in regulating the gut-microbiota-brain axis.

Probiotic *Lactobacillus sp*. and *Bifidobacteria sp*. have been shown to reduce the neuroendocrine stress response[86] and anxiety-like[87] and depression-like[84] behavior in rodent models. Limited human trials have demonstrated that daily probiotic consumption can sufficiently alter the gut microbiota to alleviate symptoms in the gut, in patients with ulcerative colitis[88] and irritable bowel syndrome[89,90], and in the brain, in patients with depression[91,92]. However, there have also been several human trials in which probiotic formulations did not affect health outcomes[93–95].

Reference	Species	Model	Intervention	Duration	Outcome
Bravo, 2011	Mouse	Normal/healthy	*Lactobacillus reuteri* (daily gavage)	28 days	Decreased anxiety/depression
Everard, 2013	Mouse	High-fat diet induced obesity	*Akkermansia muciniphila* (daily gavage)	28 days	Improved gut barrier function; normalized metabolic markers
Bercik, 2010	Mouse	*Trichuris muris* infection - induced chronic inflammation	*Bifidobacterium longum* (daily gavage)	10 days	Decreased anxiety
Kato, 2004	Human	UC patients with active disease	*Bifidobacteria*-fermented milk supplementing standard treatment	12 weeks	Improved clinical condition; significant increase in remission
Slykerman, 2017	Human	Postpartum women	*Lactobacillus rhamnosus* capsules	6 months	Decreased post-partum anxiety and depression (self-report survey 1 year after giving birth)
Kuisma, 2003	Human	UC patients at risk of pouchitis	*Lactobacillus* GG capsules	3 months	Did not reduce inflammation
Niv, 2005	Human	IBS patients	*Lactobacillus reuteri* tablets	6 months	Did not affect IBS symptoms

Table 1.1: Summary of probiotic intervention studies and outcomes. This table summarizes the findings of representative studies referenced in the text. Multiple studies using rodents have demonstrated improvement in either gut health, mental health or both. Studies in humans have had mixed results. It is relevant to note that the outcome of the Niv et al 2005 study showed comparable improvement in patients in the placebo and probiotic-treated groups, which is why the outcome is reported as "no effect".

Additional research is required to determine why certain patient populations respond to treatment while others are unaffected, and to understand the various interactions between the gut and the microbiota, or the gut, microbiota and brain that determine whether or not treatment is successful. Finally, the studies described above

required daily dosing with the probiotic bacterial strain(s), as it remains difficult to stably introduce desired bacterial species into the gut microbiota (in the absence of antibiotic treatment as is used when treating *C. difficile* infection with fecal microbiota transplant). Increased understanding of microbial community dynamics as well as their interactions with the host would improve our ability to make long-term changes to the microbiota to improve human host health.

One component of the gut-brain axis which can be affected by the gut microbiota is the hypothalamus-pituitary-adrenal (HPA) axis, is described in more detail below.

1.5 The hypothalamus-pituitary-adrenal axis

The HPA axis is important both as a regulator of homeostasis and in responding appropriately to acute psychological stress. In response to a stressor (and thus signals from various parts of the brain to the hypothalamus), neurons of the paraventricular nucleus (PVN) of the hypothalamus release the hormone corticotropin-releasing hormone (CRH). CRH binds to receptors on the pituitary leading to the systemic release into the bloodstream of adrenocorticotropin releasing hormone (ACTH). ACTH binds to receptors on the adrenal gland,

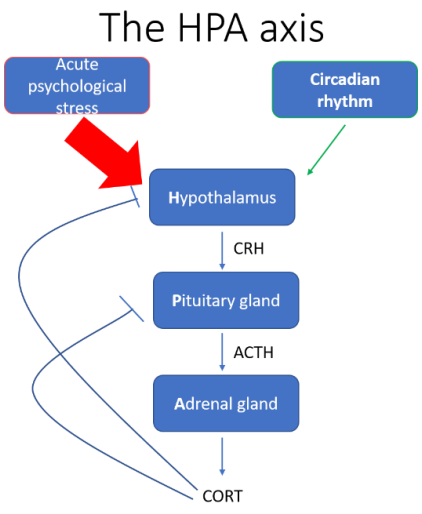

Figure 1.3: The hypothalamus-pituitary-adrenal axis. This pathway regulates production of the glucocorticoid hormone corticosterone, produced both in response to acute stress and under basal conditions. In response to stimulation, the paraventricular nucleus of the hypothalamus releases the hormone corticotrophin-releasing hormone (CRH), which interacts with the pituitary gland and triggers the release of adrenocorticotropin releasing hormone (ACTH), which circulates systemically and interacts with the adrenal gland to increase release of the hormone corticosterone (CORT). In addition to many targets described below, CORT negatively regulates its own production.

resulting in the systemic release of corticosterone in rodents or cortisol in humans (referred to generally as CORT). CORT circulates throughout the body and has pleiotropic regulatory effects, as nearly every cell in the body expresses receptors for CORT[96]. CORT regulates metabolism, immune cell function, reproduction and skeletal growth, to coordinate normal host function, initiate an effective stress response and limit the extent of the stress response[97].

There are two receptors for CORT, the mineralcorticoid receptor (MR) and the glucocorticoid receptor (GR). MR has a 10-fold higher affinity for CORT than GR, allowing cells to respond to low basal levels of circulating CORT via the MR to regulate homeostatic processes, and to respond to high concentrations of CORT via the GR to stimulate stress responsive pathways[98]. GR is a cytoplasmic protein with a central DNA-binding domain which contains two zinc finger binding motifs that recognize and target DNA sequences with the consensus binding sequence AGAACAnnnTGTTCT[99]. The ligand-binding C-terminal domain of GR has a hydrophobic pocket which interacts with CORT as well as additional regions that interact with coregulators[100]. Once in the nucleus, activated GR can bind to DNA directly to increase or decrease gene transcription, regulating cell processes on the order of minutes to hours. In addition to regulating various processes in tissues throughout the body, CORT also forms a classic negative feedback loop and negatively regulates its own production at the level of the brain, pituitary and adrenal gland[96].

One set of transcriptional targets for stress-induced CORT and GR is energy metabolism: CORT induces global metabolic changes to fuel the stress response. CORT increases hepatic gluconeogenesis, stimulates lipolysis in fat cells and increases free

amino acids by inhibiting protein synthesis[97,101,102]. Either directly, or in response to the CORT-induced increase in blood glucose, stress levels of CORT also increase insulin secretion, leading to further systemic metabolic changes and limiting the levels of stress-induced blood glucose[101]. CORT also blocks glucose uptake in the brain, skin and adipose tissue, while not inhibiting uptake in the muscle. This inhibition of glucose uptake increases catabolism in those tissues, freeing up substrates for gluconeogenesis in the liver and kidneys as well as altering the physiology of those tissues[103]. These actions increase energy availability and help the organism respond to a threat.

Glucocorticoids like CORT are widely used as anti-inflammatory drugs in the human population to treat a range of conditions. CORT enacts these anti-inflammatory properties by decreasing transcription of proinflammatory cytokines and reducing activation and proliferation of immune cells[104,105]. GR bound to CORT increases transcription of IκB, the inhibitor protein that inactivates the pro-inflammatory

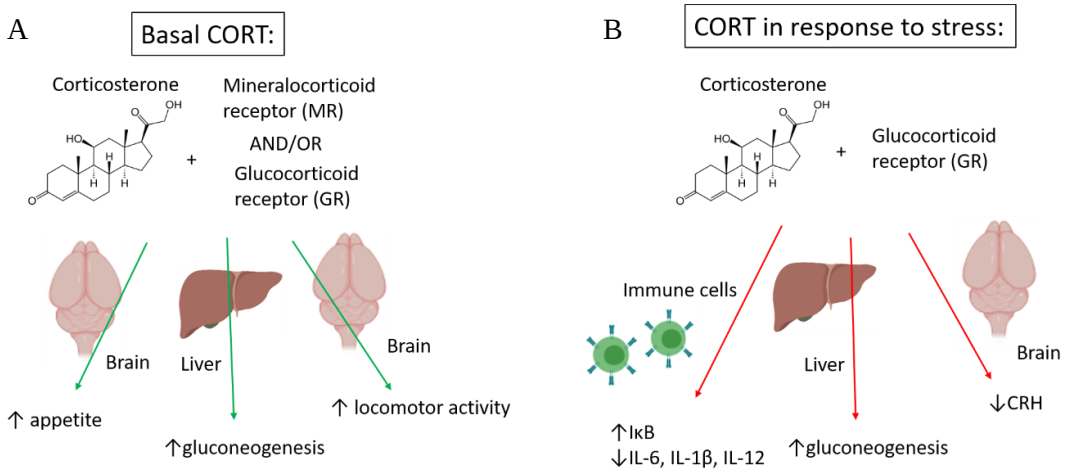

Figure 1.4: CORT is a broad transcriptional regulator. A) Under basal conditions CORT can bind to receptors in multiple regions of the brain to stimulate homeostatic behaviors such as appetite/feeding and locomotor activity. It also stimulates gluconeogenesis in the liver under both basal and stress-induced (B) conditions. B) In response to stress CORT negatively regulates its own production by decreasing CRH production in the brain. It also plays an important anti-inflammatory role in controlling stress-induced immune stimulation.

transcription factor NF-κB, resulting in a decrease in transcription of many pro-inflammatory factors including IL-6, IL-1, IL-2, IL-12, nitric oxide synthase, and COX-2[106,107]. This anti-inflammatory activity is a key way in which CORT limits the duration of the physiological response to stress: in part in response to the immediate release of catecholamines, the immune system is activated in response to psychological stress resulting in the release of pro-inflammatory cytokines into circulation 5-10 minutes after stress initiation[108,109]. The transcriptional anti-inflammatory downregulation in response to the increase in CORT (minutes to hours after stressor) ensures that inflammation in response to stress does not persist after the resolution of a stressor. In this way, CORT regulates the return to homeostasis. In addition to being a key part of the acute stress response, CORT is also an important regulator of basal, homeostatic processes. In the absence of stress, CORT release is regulated by the circadian rhythm: the roughly 24h long biological cycle controlled by the master circadian "clock" located in the suprachiasmatic nucleus (SCN) of the hypothalamus, which helps an organism coordinate life under stable conditions such as the sleep/wake times, activity and eating schedules. The major external cue for the circadian rhythm is light, which enters the retina and signals via nerve cells to the SCN. Within the SCN, various transcription factors referred to as clock-controlled genes increase or decrease in response to this stimulation. The SCN then signals to the PVN via the release of vasopressin, which stimulates CRH release in diurnal mammals (like humans) and inhibits CRH release in nocturnal mammals (like rodents)[110]. This regulation leads to a gradual increase in circulating CORT over the course of the inactive period, peaking immediately prior to waking and the active period, and gradually decreasing over the course of the active period.

Additional stimuli, such as limiting access to food to normally inactive (daylight) hours in rodents, can alter circadian rhythmicity of peripheral organs including the adrenal gland implying that there is a secondary "clock" present in the adrenal gland regulating basal CORT release[111].

Circadian control of CORT is an important mechanism by which the central circadian clock regulates homeostatic processes. Basal levels of CORT stimulate appetite[101,112], locomotor activity and regulate metabolism in liver, adipose and muscle cells[97,113,114]. Disruption of the circadian secretion of CORT is correlated with mood disorders[115–117], obesity and metabolic syndrome[114,118]. Long-term treatment with glucocorticoid drugs is associated with metabolic disorders such as insulin resistance and diabetes, obesity and cardiovascular disease[119]. In patients with adrenal insufficiency, replacement with a high dose of exogenously administered CORT has significant adverse metabolic effects, while replacement with low doses that more closely mimic the circadian rhythm of CORT production (in small studies) appeared to be an effective treatment with fewer side effects[119]. Together these results demonstrate the importance of CORT as a regulator of homeostasis, and the importance of its circadian rhythm.

Rodent studies have demonstrated that disruption of either basal CORT secretion or altered regulation of the HPA axis response to stress can result in changes in anxiety-like or depression-like behavior. As a hormone that can regulate both the gut and the brain, CORT is a key mediator of the gut-brain axis. In addition to external cues, the circadian release of CRH from the hypothalamus is gated by the endocannabinoid system. One endocannabinoid, anandamide, is a negative regulator that limits CRH

release in response to input from the SCN to provide a "brake" on basal CORT production. The endocannabinoid system is described further below.

1.6 The endocannabinoid system

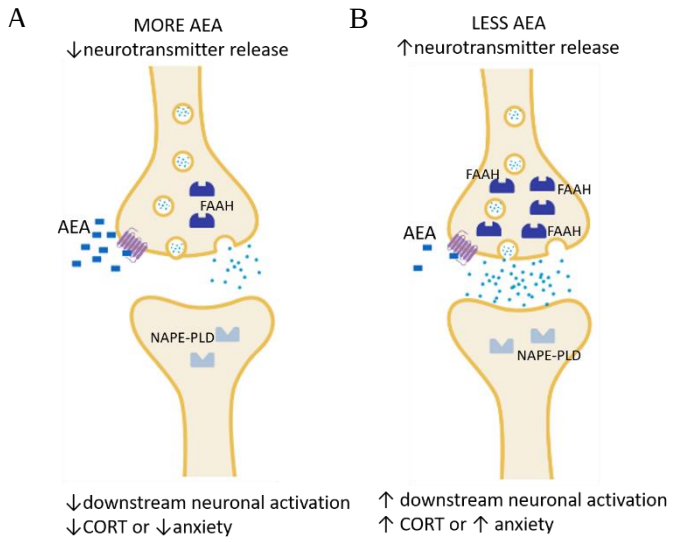

Figure 1.5: AEA signaling through CB1 limits activation at neuronal synapses. Under basal conditions (A) AEA is synthesized in the post-synaptic cell by NAPE-PLD in response to neuronal activation. It interacts with CB1 present on the pre-synaptic cell to inhibit further neurotransmitter release providing a tight negative feedback loop. In the context of neurons in the PVN, this limits production of CORT or anxiety-like behavior. In response to stress (B) there is increased activity and abundance of the AEA-degrading enzyme FAAH, which decreases the AEA available to signal and increases activation of downstream neurons.

Researchers studying the major psychoactive component of marijuana, (-)-trans-Δ^9-tetrahydrocannabinol (THC) discovered the cannabinoid receptors CB1[120,121] and CB2[122], distributed on neurons throughout the body, and responsible for the numerous and well-documented effects of THC: altered mood, nausea suppression, pain relief and appetite-stimulation[123]. Additional research revealed the endogenous ligands for these receptors, collectively referred to as the endocannabinoids, of which *N*-arachidonoylethanolamine (aka anandamide, AEA)[124] and 2-arachidonoylglycerol (2-

AG)[125] are the best characterized. CB1 and CB2 are G-protein coupled receptors, which when activated inhibit the activity of adenylyl cyclase and initiate mitogen-activated kinase activity within the pre-synaptic neuron, decreasing neurotransmitter release[126,127]. AEA and 2-AG are synthesized in the post-synaptic cell in response to calcium influx after neuronal activation and rapidly diffuse across the synapse to bind to CB1 and/or CB2 receptors on the pre-synaptic cell, limiting further neurotransmitter release. After acting at the receptor, AEA and 2-AG are internalized and degraded by intracellular enzymes fatty acid amide hydrolase (FAAH) and monoacylglycerol lipase (MAGL) respectively[128]. AEA interacts selectively with CB1 receptor while 2-AG is a moderate agonist at both the CB1 and CB2 receptors. In addition to differential affinity, varying levels in different tissues of AEA and 2-AG allow for variable endocannabinoid control of neurotransmission in various contexts.

The amount of AEA and 2-AG available for signaling is regulated by both the degradative and synthetic enzymes, although the synthetic pathway(s) of AEA remain incompletely understood. 2-AG is synthesized by sequential hydrolysis of membrane phospholipids and the rate-limiting step is carried out by the enzyme diacylglycerol lipase (DAGL)[129]. One of multiple pathways that results in the synthesis of AEA is the cleavage of the precursor N-arachidonoyl phosphatidylethanolamine (NAPE) by the phospholipase NAPE phospholipase D (NAPE-PLD)[130–132]. Pharmacological inhibition of either class of enzymes is effective at modulating tissue levels of endocannabinoids both *in vitro* and *in vivo*[133–137], and they are major targets for drug development. These inhibitors have also been an important tool in demonstrating the range of behavioral phenotypes and biological systems regulated by the endocannabinoid system using rodent

models. Synthetic agonists and inhibitors that target the CB1 and CB2 receptors directly have also been used to elucidate the role each plays in regulating various processes. In addition to these pharmacological tools, the successful generation of knockout mice lacking CB1, CB2, FAAH, MAGL, DAGL, or NAPE-PLD have also been used to determine the role of each part of the endocannabinoid system in regulating host physiology.

In addition to enzymatic activity, substrate availability also influences endocannabinoid levels present in various tissues. Both AEA and 2-AG are lipid signaling molecules built from arachidonic acid-containing phospholipids; therefore metabolic changes that alter availability of arachidonic acid can also affect production of AEA and 2-AG. The synthetic enzyme NAPE-PLD does not have a substrate preference for phospholipids with a particular length/degree of unsaturation acyl chain[138], such that the species of N-acylethanolamine synthesized reflects available fatty acids in the membrane phospholipids. Arachidonic acid is a ω-6 polyunsaturated fatty acid (PUFA, 20:4n-6). It can be synthesized in mammals from the essential fatty acid precursor, ω-6 linoleic acid (18:2n-6), and is also itself present in the diet. Feeding studies in various rodent models have shown that feeding a diet enriched with 18:2n-6 or 20:4n-6 fatty acids increased production of AEA in various tissues throughout the body including intestines, liver and brain[139,140] while conversely feeding a diet enriched in ω-3 fatty acids resulted in decreased AEA levels, as it is inefficient to convert ω-3 to ω-6 acyl groups[139,141] . These studies demonstrate that fatty acid availability in the GI tract can affect endocannabinoid synthesis throughout the body.

Endocannabinoid CB1 receptors have been found throughout the brain and central nervous system, as well as on peripheral afferent nerves. They broadly regulate neurotransmitter release in response to various stimuli, and can therefore play a major role in regulating many aspects of host physiology. Under basal conditions, AEA signaling within the amygdala limits excitation of neurons that regulate hypothalamus PVN activity, limiting CRH release from the hypothalamus and functioning as a brake on the circadian input from the SCN[142]. In mice lacking CB1, or treated with a CB1 antagonist to decrease AEA/CB1 signaling, mice have increased circulating ACTH and CORT, especially prior to the diurnal peak in basal CORT production[143,144]. When an acute stressor is sensed, CRH signaling in the amygdala increases activity of the degradative enzyme FAAH, decreasing the amount of AEA available to signal, increasing activity of the downstream neurons and increasing CRH release from the hypothalamus to the pituitary[145]. Regulation by 2-AG is observed during the acute stress response, as exposure to CORT increases 2-AG levels in the brain (possibly through inhibition of MAGL) and leads to increased 2-AG signaling and decreased input to the hypothalamus, limiting the duration of the CORT response[146]. Endocannabinoid system signaling is an important regulator of basal CORT, the initiation of the stress-induced CORT response, and rapid negative feedback control of stress-induced CORT.

As would be expected for a major regulator of the HPA axis, the endocannabinoid system has also been shown to be involved in regulating mood in humans, and emotional behavior such as anxiety-like behavior in rodent models. The CB1 knockout mouse has increased anxiety-like behavior in the elevated plus maze (exploratory model for anxiety)[147,148] as well as increased social anxiety[149]. Similar results have been shown

pharmacologically using specific CB1 antagonists. Increasing CB1 signaling, either genetically with the FAAH knockout mouse, or pharmacologically, through inhibition of FAAH or by administration of a CB1 agonist has the opposite, anxiolytic effect[148,150,151] although these studies have varied based on the strain of mouse used and laboratory conditions[152,153]. Intriguingly, and in accordance with observations in the human population after marijuana consumption, this anxiolytic effect in mice is biphasic: small increases in AEA /CB1 signaling alleviate anxiety while high doses of AEA or FAAH inhibitors actually increase anxiety[154]. The transient receptor potential vanilloid type-1 channel (TRPV1) has been shown to bind AEA, as well as other endocannabinoids in vitro[155,156], and to have an opposing effect to CB1 in regulating emotional behavior. Inhibition of TRPV1 channels decreased anxiety-like behavior in rodents[157] and TRPV1 knockout mice were insensitive to an IL-1B-induced model of anxiety[158]. Therefore at low doses, AEA (and increased AEA through FAAH inhibition) increase CB1 signaling, decreasing anxiety; but at high doses, FAAH inhibition also increases levels of other endocannabinoids that signal through TRPV1 (and are not CB1 agonists), and AEA is present at a high enough threshold that the pro-anxiety TRPV1 signal overrides the anti-anxiety CB1 signal[159]. The ratio of different endocannabinoid compounds in various tissues, as well as the expression level and sensitivity of the different receptors all can potentially alter the degree of activation at the synapse and therefore host phenotypes.

1.7 Summary and major research questions investigated in this thesis

The thesis research that follows investigates the ability of the fungus *C. albicans*, a normal member of the gut microbiota, to affect host health both within the GI tract and systemically. Although the role of bacterial members of the gut microbiota has been

investigated extensively, research into the effect of *C. albicans* on the host has largely focused on its interactions within the GI tract. One research project builds on this research, characterizes the host response to *C. albicans* colonization of the GI tract and demonstrates that the *C. albicans*-dependent immune changes therein have functional consequences: the host is protected from *C. difficile* disease. Another project goes beyond the GI tract and investigates the effect of *C. albicans* colonization on the host as a whole organism by focusing on changes to the gut-brain axis. This research demonstrates that *C. albicans* colonization alters host behavior in response to a stressful situation as well as basal stress hormone production.

Untargeted metabolomics analysis as a part of this project also demonstrated a broad metabolic effect of *C. albicans* on host lipid homeostasis, as well as a specific effect on the abundance of endocannabinoid precursors in the GI tract and systemic endocannabinoid signaling. These host phenotypes integrate multiple organ systems. Therefore by affecting them *C. albicans* colonization has a global impact on host health. Finally, a third project focuses on the bacterial members of the gut microbiota rather than the host response and investigates how the introduction of *C. albicans* into the microbial community changes the structure of the gut microbiota as well as important emergent qualities such as resilience and stability.

Because *C. albicans* is a part of the normal human gut microbiota from infancy, we propose that the *C. albicans*-dependent changes we observed are actually a part of normal human development, and likely influence what we think of as “normal” immune, endocrine and metabolic states in a healthy adult. As we have evolved with *C. albicans* in our GI tract over millennia, the changes we characterized in the *C. albicans*-colonized

mouse likely do not represent a pathogenic consequence of exposure to a microbe, but rather reveal how *C. albicans* influences normal, healthy host development.

Chapter 2 The commensal fungus *Candida albicans* dysregulates the host hypothalamus-pituitary-adrenal axis and anxiety-like behavior through alteration of the host endocannabinoid system and the gut-brain axis[1].

[1] Markey, Laura, Laverne Melon, Andrew Hooper, Jamie Maguire and Carol Kumamoto. "The commensal fungus *Candida albicans* dysregulates the host hypothalamus-pituitary-adrenal axis and anxiety-like behavior through alteration of the host endocannabinoid system and the gut-brain axis." To be submitted to PNAS

2.1 Introduction

Anxiety disorders are the most prevalent mental health disorder worldwide, with a lifetime prevalence of 5-7% of the human population, based on large population studies[160,161]. This number includes a range of disorders including generalized anxiety disorder, social anxiety disorder, specific phobias and panic disorder. The etiology of anxiety disorders is complex and incompletely understood, although many different genetic and environmental factors have been shown to be involved[162]. One integrative aspect of host health that has been shown to affect anxiety-like behavior is the gut-microbiota-brain axis. The gut-microbiota-brain axis refers to communication between the gut and the brain through multiple host systems such as the immune system, metabolism and direct neuronal connections via the vagus nerve and the enteric nervous system. Constant communication between the periphery and the brain is required for normal homeostasis. When normal communication is disrupted changes in host health as a whole can result.

Researchers using germ-free or antibiotic-treated mouse models have demonstrated that the absence of the gut microbiota leads to dysregulation of the hypothalamus-pituitary-adrenal (HPA) axis, one component of the gut-brain axis, as well as changes in anxiety-like behavior[75,82,85]. The endocrine output of the HPA axis, corticosterone (CORT), regulates transcription of genes in the immune, neuroendocrine, metabolic and cardiovascular systems. Under basal conditions CORT release is regulated by the circadian rhythm and under these conditions circulating CORT helps to maintain homeostasis. CORT is also a key part of the acute psychological stress response and increased CORT release is essential for rapidly mounting an effective response to stress.

Dysregulation of the HPA axis and CORT production is correlated with many different pathologies including disruption of the gut-brain axis and mental health disorders such as anxiety and depression.

Previous studies have shown that the gut microbiota plays a role in regulating the gut-brain axis. The addition of probiotic bacterial species including *Bifidobacterium sp*. and *Lactobacillus sp*. has been shown to decrease anxiety-like behavior and normalize HPA axis function in mice[86,163–166], indicating that these neuroendocrine phenotypes can be modulated by the presence or abundance of specific bacterial species within the gut microbiota. Investigation into the contribution of the gut-microbiota-brain axis to mental health could reveal novel regulators of anxiety-like behavior and offer mechanistic insight into the etiology of the disease.

Candida albicans is a commensal fungus that colonizes the gastrointestinal (GI) tract of ~60% of the human population[4,167,168]. Although a major colonizer of humans, its role as a member of the normal gut microbiota is largely uncharacterized. Previous researchers have shown that gastrointestinal *C. albicans* colonization induces local and systemic immune changes which are protective against future systemic *C. albicans* infection and disease[19], and against infection with bacterial pathogens such as *C. difficile*[18] and *S. aureus*[19]. The research that follows demonstrates that *C. albicans* affects host health beyond the GI tract. We show that *C. albicans* dysregulates HPA axis activation and increases anxiety-like behavior in a mouse model by altering endocannabinoid metabolism in the GI tract.

The mammalian endocannabinoid system regulates both the HPA axis and emotional behavior, among other host systems. It consists of two major lipid signaling

molecules, N-arachidonoylethanolamide (AEA) and 2-arachidonoylglycerol (2-AG) and their receptors CB1 (distributed throughout the nervous system) and CB2 (present primarily on immune cells)[120,121,124]. AEA and 2-AG are produced in response to activation in post-synaptic neurons, and act at CB1 on pre-synaptic neurons to limit neurotransmitter release. AEA and 2-AG levels are regulated by substrate availability and expression and activity of their synthetic and degradative enzymes[128,139]. Using genetic and pharmacological tools researchers have demonstrated that decreased CB1 signaling results in increased basal and stress-responsive CORT[143] as well as increased depression-like and anxiety-like behavior[148,150].

C. albicans is acquired as a fungal member of the gut microbiota soon after birth [3,169,170] and thus could play a role in both the development and maintenance of the gut-brain axis. We used an acute murine model of gastrointestinal *C. albicans* colonization to assess the ability of *C. albicans* to interact with the host gut-brain axis. We found that *C. albicans* colonization activated the host HPA axis and increased anxiety-like behavior via manipulation of the endocannabinoid system.

2.2 Methods

2.2.1 Animals

Five-week-old female C57BL/6 mice (Jackson Laboratory) were cohoused in a large cage (24”x17”) and given sterile food, water and bedding. Mice were allowed to acclimate to Tufts Animal Facility for three days during which time they were handled daily. If mice were to be given an intraperitoneal injection of drug/vehicle prior to a behavioral test, mice were also given an intraperitoneal injection of sterile normal saline (0.9% w/v) daily during this acclimation period.

The day prior to inoculation with *C. albicans* or mock-inoculation, mice were transferred to standard cages with three or four mice per cage. On this day (day -1) fresh fecal pellets were collected, homogenized in PBS and the homogenate plated on YPD-SA agar (YPD agar plus 100µg/ml streptomycin and 50µg/ml ampicillin) and incubated at 37°C for 2 days to confirm that mice were negative for cultivable fungi. The following day mice were inoculated orally with *C. albicans* ($5x10^7$CFUs/mouse) or mock-inoculated with PBS and moved to a fresh sterile cage (day 0). On day one, fresh fecal pellets were collected from all mice and plated on YPD-SA to confirm colonization with *C. albicans*. On day two, mice were put through a behavioral test, transferred from cages of four to cages of two (cages of three were not subdivided) and placed in fresh sterile cages. On day three in most experiments, mice were sacrificed in the afternoon two to four hours prior to lights out. In experiments investigating the effect of the circadian rhythm on CORT production, animals were sacrificed at various other timepoints as noted in the text. Animals were rapidly anesthetized with open-drop exposure to isoflurane and then sacrificed via decapitation.

All experiments were done in compliance with Tufts University IACUC guidelines.

2.2.2 Strains and growth conditions

C. albicans strain CKY101[171] was used for all experiments. For preparation of mouse inoculum, cells were grown at 37°C in YPD (1% yeast extract (BD), 2% peptone (Difco) 2% glucose (Sigma Aldrich)) for 24 hours. They were then washed twice with sterile PBS (phosphate-buffered saline) and resuspended in 2% (w/v) sucrose in PBS at a concentration of $2x10^9$ cells/ml. 25µl ($5x10^7$ cells) of this cell suspension was fed to

mice for gastrointestinal colonization. 25µl of a 2% sucrose solution in PBS was fed to mice for mock-inoculation.

2.2.3 Drug treatment

URB597 (Sigma Aldrich) and URB937 (Cayman Chemical) were dissolved in 18:1:1 normal saline:PEG400:Tween80 (Sigma Aldrich) and administered to mice via intraperitoneal injection at a dosage of 0.1-1mg/kg bodyweight four hours prior to behavioral testing or sacrifice.

2.2.4 Restraint stress

Mice were placed in a 50ml conical tube with two airholes enclosed with a rubber stopper for 30 minutes. After this restraint, mice were placed back in their home cage and either immediately anesthetized and sacrificed or allowed to recover in the home cage for 30 or 60 minutes and then anesthetized and sacrificed.

2.2.5 Elevated Plus Maze

Behavioral testing in the Elevated Plus Maze (EPM) was performed as described in Walf et al 2013[172]. Mice were moved from their housing room to the testing room at least one hour prior to testing. The EPM was sprayed with 70% ethanol and thoroughly dried. A mouse was then removed from its home cage, placed in the center of the EPM facing an open arm and allowed to explore for five minutes. After testing the mouse was placed in a fresh sterile cage. The EPM was sprayed with 70% ethanol prior to each trial. All trials were recorded with a video-camera from above and scored after the fact by a blinded observer for the number of open arm entries and the duration of time spent in the open arms. A mouse was scored as having entered an open arm when all four paws crossed into the open arm

2.2.6 Forced Swim Test

Behavioral testing in the forced swim test was performed as described in Can et al 2012 [173]. Mice were moved from their housing room to the testing room at least one hour prior to testing. A 5L beaker was sprayed with disinfectant and wiped dry, then filled with 10cm of 22°-25°C tap water. A mouse was removed from its home cage and placed in the beaker of water for a six-minute trial which was recorded by video-camera from the side and scored after the fact by a blinded observer. Trials were monitored to ensure mice remained floating throughout. After testing, mice were placed in a fresh sterile cage. FST videos were manually scored for the number of seconds spent floating immobile.

2.2.7 Bacterial microbiota analysis

The cecum, including contents, was dissected from mice after sacrifice on day three and was immediately frozen on dry ice. Microbial DNA was extracted using the QIAamp DNA Stool Mini Kit (Qiagen) following the manufacturer's protocol. Briefly, cecum samples were lysed by beadbeating (samples combined with 500mg 0.1mm diameter zirconia/silica beads) in Qiagen lysis buffer ASL, and the lysate was treated with InhibitEX tablets followed by enzymatic digestion with proteinase K (>500mAU/ml) and RNaseA (1mg/ml) and column DNA purification. Libraries were prepared from each sample and sequenced as described[174]. Briefly, PCR amplification of the V4 region of the 16S rRNA gene was performed with primers that included adapters for Illumina sequencing and twelve base barcodes. Two hundred fifty bp paired-end sequencing was performed using an Illumina MiSeq. Base calling was performed using CASAVA 1.8 and the resulting fastq files were used as input for downstream analysis

using QIIME (1.8.0)[175]. Briefly, the paired-end reads from the fastq files were joined, barcodes extracted and then demultiplexed. The operational taxonomic units (OTUs) were determined using a closed reference approach by aligning reads to the Greengenes Database (version 13_8) at 99% identity. The Greengenes phylogenetic tree was used to define the phylogenetic relationship between OTUs. The resultant OTU tables contained the relative abundance of bacterial taxa in each sample. These tables were used to calculate overall diversity within each sample. To compare the composition and diversity of samples to each other taking into account phylogenetic relatedness, the OTU tables were used to calculate the weighted UniFrac distance matrix, which was summarized with Principal Coordinate Analysis. Permanova analysis was performed using QIIME.

2.2.8 Measurement of hormones and cytokines in serum

Trunk blood was collected into serum separator blood collection tubes (BD) after sacrifice by decapitation and allowed to sit at room temperature for up to three hours. Tubes were then spun at 10,000xg for 10 minutes to separate serum. Serum was divided into aliquots and frozen at -80C.

Serum corticosterone was measured using a Corticosterone ELISA Kit (Enzo Life Sciences) following the manufacturer's small volume protocol including the serum displacement reagent. Serum cytokines were measured using a multiplex ELISA (Quanterix) following manufacturer's protocol.

2.2.9 Immunohistochemistry for cFOS in hypothalamus slices

Brains were rapidly dissected and fixed in 4% (w/v) paraformaldehyde in PBS for 24h at 4C. They were then cryopreserved by incubation in 10% (w/v) sucrose in PBS for 24h followed by 24h incubation in 30%(w/v) sucrose in PBS. Brains were rapidly frozen in

isopentane chilled on dry ice and stored at -80C. They were sectioned into 40µm sections using a cryostat and gross anatomical landmarks were used to identify sections containing the PVN of the hypothalamus. Sections of interest were incubated with 1:5000 dilution of rabbit anti-mouse cFos antibody (Sigma Aldrich F7799) for 72h, then stained using anti-rabbit IgG (VectaStain Elite ABC Kit) and streptadvidin-Alexa488 (Molecular Probes). Sections were then mounted onto glass slides and imaged using a Zeiss microscope with Apotome attachment.

2.2.10 Untargeted metabolomic analysis of cecum contents

The cecum was dissected after sacrifice on day three and contents were squeezed into a tube and immediately frozen in dry ice/ethanol bath and stored at -80C. Extraction of metabolites and untargeted metabolomic analysis were performed by Metabolon. As per their report: samples were prepared using the automated MicroLab STAR® system from Hamilton Company. To remove protein, dissociate small molecules bound to protein or trapped in the precipitated protein matrix, and to recover chemically diverse metabolites, proteins were precipitated with methanol under vigorous shaking for 2 min (Glen Mills GenoGrinder 2000) followed by centrifugation. The resulting extract was divided into five fractions: two for analysis by two separate reverse phase (RP)/UPLC-MS/MS methods with positive ion mode electrospray ionization (ESI), one for analysis by RP/UPLC-MS/MS with negative ion mode ESI and one for analysis by HILIC/UPLC-MS/MS with negative ion mode ES (additional fraction saved as back-up). All methods utilized a Waters ACQUITY ultra-performance liquid chromatography (UPLC) and a Thermo Scientific Q-Exactive high resolution/accurate mass spectrometer interfaced with a heated electrospray ionization (HESI-II) source and Orbitrap mass analyzer operated at

35,000 mass resolution. The MS analysis alternated between MS and data-dependent MS^n scans using dynamic exclusion. The scan range varied slighted between methods but covered 70-1000 m/z. Raw data was extracted, peak-identified and QC processed using Metabolon's hardware and software

Mass spectrometry data was log-transformed and statistical analysis of the results was performed using MetaboAnalyst 4.0[176,177].

2.2.11 Real-time quantitative PCR analysis

For measurement of gene expression, mice were sacrificed on day three and tissues were frozen at -80°C in RNALater (Invitrogen). RNA was purified from tissues using QIAzol for lysis and extraction with a Qialyzer, followed by column purification using the Ambion Purelink Mini kit (Invitrogen). cDNA was synthesized using SuperScript III (Invitrogen) with oligo-dT priming and the manufacturer's protocol. qPCR reactions were performed using SYBR Green Master Mix (Applied Biosystems) and a LightCycler 480 II (Roche) instrument. Standard curves were generated and all results normalized to the level of GAPDH expression in each sample. All primers are listed in table 2. When described in text, expression levels were normalized to the experimental mean of the control group.

2.3 Results

2.3.1 A single oral inoculation with *Candida albicans* is sufficient to establish gastrointestinal colonization without inflammatory disease

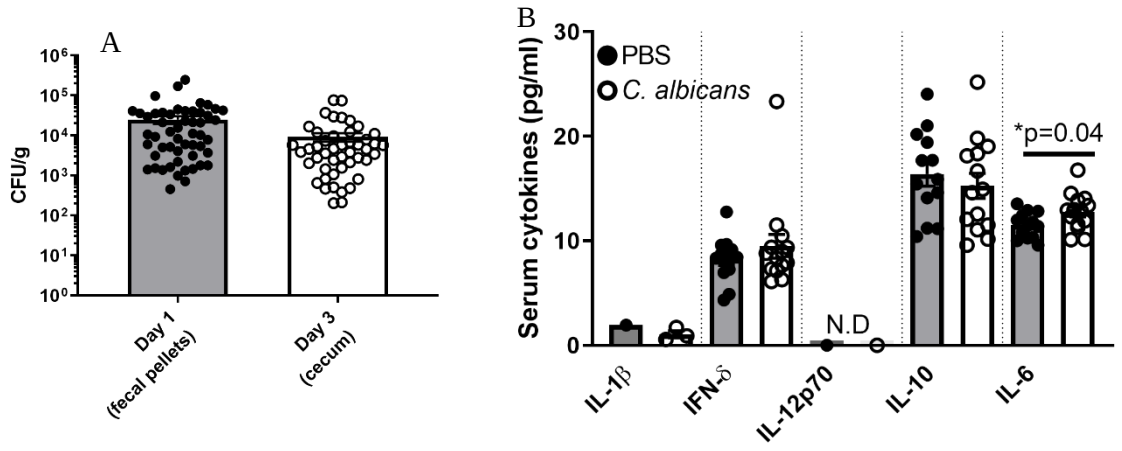

Figure 2.1: *C. albicans* colonizes for three days and does not cause systemic inflammation. Mice were either mock-inoculated or inoculated orally with *C. albicans.* Fecal pellets were collected one day after inoculation to confirm colonization with *C. albicans.* After mice were sacrificed on day 3, cecum contents were collected to quantify *C. albicans* levels in the GI tract and trunk blood was collected to measure cytokines in serum. A) Fecal pellets (gray bar) and cecum contents (white bar) homogenates were plated on YPD-SA and colony forming units counted. (day 1 N=98, day 3 N=77). B) Multiplex ELISA was used to measure circulating cytokines in serum from trunk blood collected after sacrifice. Black bars represent mock-colonized mice, white bars represent *C. albicans*-colonized mice. PBS N=13, C. albicans N=14. Symbols indicate mice; bars indicate average and SEM. Student's T-test, *p<0.05

For the work that follows, we used a novel acute colonization model to investigate the effects of *C. albicans* inoculation on the mammalian host. 5-week-old female mice (typically 23 mice per cohort) were cohoused for three days and acclimated to our facility. They were then either inoculated with a single dose ($5x10^7$ CFUs) of *C. albicans* (strain CKY101) or mock-inoculated with buffer. Mice were not treated with antibiotics because antibiotic treatment has been shown to affect the neuroendocrine phenotypes of interest. *C. albicans* was measurable in the fecal pellets after 24h and up to 3 days after

inoculation (Fig. 2.1A) and was detected throughout the gastrointestinal tract, as observed in previous models which utilized antibiotic treatment prior to *C. albicans* inoculation (Supplemental Fig. 1). No culturable fungi were detected in mice given the mock-inoculation. We assessed behavior after two days of colonization and mice were sacrificed after three days of colonization.

C. albicans-colonized mice did not exhibit symptoms of illness (ruffled fur, hunched posture, etc) or lose significant weight (<1% of bodyweight change, Supplemental Fig. 2). We used a multiplex ELISA to measure inflammatory cytokines in the serum after sacrifice and measured low levels of circulating inflammatory cytokines IL-1β, IFN-γ, IL-10 and IL-6 in mock-inoculated (Fig. 2.1B, black bars) and *C. albicans*-colonized mice (open bars). Systemic *C. albicans* infection and invasive disease results in a characteristic IL-12 response which was not detected in the serum of the *C. albicans*-colonized mice in our model. There was a small but significant increase in IL-6 in *C. albicans*-colonized mice, however, this increased level is substantially lower than that reported by other researchers as induced in mice with GI tract disease[178,179]. We concluded that our model resulted in stable colonization of mice with *C. albicans* in the GI tract that was not associated with disease or inflammation, modeling commensal gastrointestinal colonization.

Although we did not disrupt the bacterial microbiota with antibiotics, it is possible that the addition of *C. albicans* into the gut microbiota could alter the composition or diversity of the bacterial gut microbiota. Previous work by Erb-Downward *et al* demonstrated that colonization with *C. albicans* in the absence of antibiotic treatment had a small effect on the composition of the bacterial microbiota after seven days of

colonization[180]. We therefore analyzed the bacterial microbiota of the cecum of mice sacrificed after three days of *C. albicans* colonization. We used 16s rRNA DNA sequencing and the QIIME analysis pipeline to characterize the bacterial microbiota and found that the composition and diversity of the bacterial gut microbiota was not significantly altered by the introduction of *C. albicans* in this acute model of

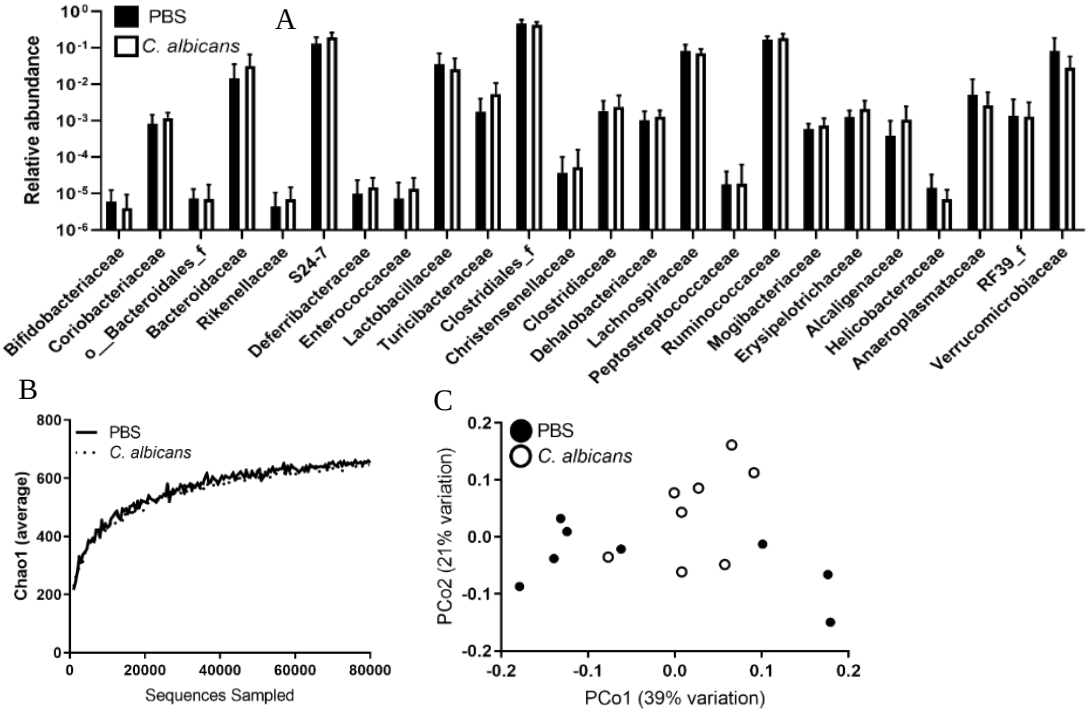

Figure 2.2: *C. albicans* introduction results in minimal change to the bacterial gut microbiota. Mice were mock-inoculated or inoculated with *C. albicans*. After three days of colonization, mice were sacrificed without stress and the cecum was collected, DNA extracted and used for Illumina sequencing of the 16s rRNA DNA and microbiota analysis. A) The average relative abundance of each bacterial family is shown (figure shows families detected with a median greater than 0 in at least one group). The abundance in the mock-colonized microbiota is represented by black bars and in the *C. albicans*-colonized microbiota as white bars. Bars indicate average and standard deviation B) Rarefaction of microbiota data was performed to measure Chao1 diversity from 500-80,000 sequences sampled (500 sequence steps). Average Chao1 score at each sequencing depth is represented by lines; average Chao 1 of mock-colonized microbiota is the solid line, *C. albicans*-colonized the dashed line C) Principal coordinates analysis of weighted UniFrac scores was performed. Principal coordinates 1 and 2 are shown. Each symbol represents a mouse microbiota; black circles are mock-colonized microbiota and open circles are *C. albicans*-colonized microbiota. N=8 per group for all analyses.

colonization (Fig. 2.2A, PBS control microbiota indicated by black bars/line/circles and *C. albicans*-colonized microbiota by white bars/dotted line/open circles). The relative abundance of bacterial taxa was compared at several levels (Mann-Whitney U test and linear discriminant analysis effect size (LEFSE) analysis[181]) and no taxa were significantly different when comparing their relative abundance in the mock-colonized microbiota with that of the *C. albicans*-colonized microbiota (Fig. 2.2A, family-level taxa summary shown). The overall diversity of the microbiota as quantified by averaging the Chao1 score for the microbiota of mice with and without *C. albicans* colonization was not significantly different (Fig. 2.2B).

We analyzed beta diversity using weighted UniFrac analysis and summarized the results using principal coordinates analysis (Fig. 2C, PBS control microbiota=black circles and *C. albicans*-colonized microbiota=open circles). The phylogenetic distance between the microbiota of individual mice varied, but PERMANOVA analysis of the complete principal coordinates analysis found that there was not significant separation of populations based on *C. albicans* colonization (pseudo-F statistic=1.7306, p=0.117, 999 permutations). These results demonstrate that mice inoculated with *C. albicans* in the absence of antibiotic pre-treatment resulted in stable colonization and minimal disruption of the bacterial microbiota in the absence of active disease.

2.3.2 *C. albicans* colonization increases anxiety-like behavior in the EPM

We assessed the effect of gastrointestinal *C. albicans* colonization on host emotional behavior using standard behavioral tests for anxiety and depression to determine whether *C. albicans* colonization altered behavioral outputs of the gut-microbiota-brain axis. On the second day post-inoculation mice were subjected to a

single behavioral test, either the elevated plus maze (EPM) test for anxiety-like behavior[172] or the forced swim test for depression-like behavior[182]. The EPM consists of two open, aversive arms and two closed arms. Mice were allowed to explore the EPM for a 5-minute trial which was video-recorded and scored by a blinded observer for time spent and entries into the closed and open arms. Anxiety-like behavior is quantified as avoidance of the aversive open arms. Occupation of arms is expressed as percentage arm time, calculated as the time spent in specified arms divided by the total time spent in both open and closed arms. *C. albicans* colonization significantly increased anxiety-like

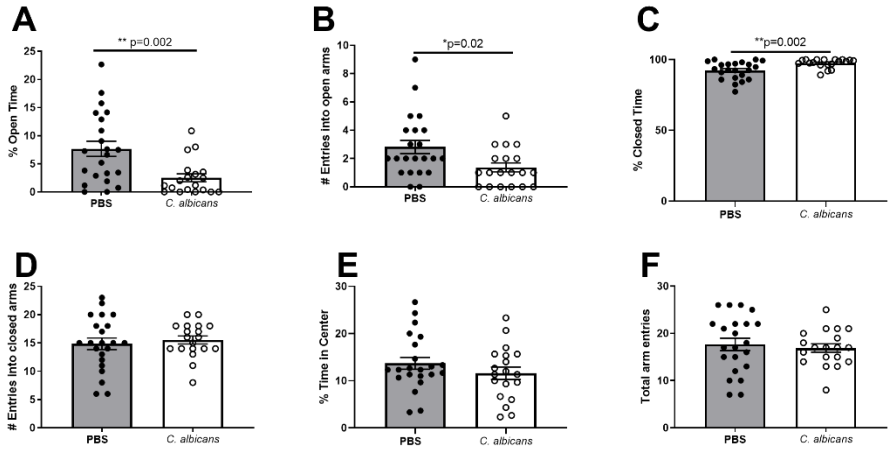

Figure 2.3: *C. albicans* colonization changes behavior in the EPM. Mice were placed in the EPM for a 5-minute trial which was later manually scored by a blinded observer. A) % of time in open arms was calculated as open arm time/total time spent in all arms*100. B) Number of entries into open arms, where entry required all 4 paws to cross into the arm. C) % of time in closed arms calculated as closed arm time/total time spent in arms. D) Closed arm entries. E) Center time was calculated by subtracting total arm time from 300s. % center time calculated as center time/300s. F) Entries into both open and closed arms. Symbols represent mice and bars indicate average and SEM. PBS N=22, *C. albicans* N=19 Welch's t-test **p<0.01, *p<0.05

behavior in the EPM. *C. albicans*-colonized mice spent significantly less time in and made fewer entries into the open arms of the elevated plus maze compared to the mock-colonized mice (Fig. 2.3A and B, PBS=black bars and *C. albicans*-colonized=open bars, Welch's t-test, $p<0.05$). There was a significant increase in the percentage of time spent

in the closed (safe) arms in the *C. albicans*-colonized mice but no difference in the number of entries into the closed arms (Fig 2.3C and D). There was no effect of *C. albicans colonization* on the duration of time spent in the center or on the total number of entries into all arms of the maze (Fig. 2.3, E-F), indicating that *C. albicans* colonization did not alter overall activity but specifically affected anxiety-like behavior. This increased avoidance of the open arms demonstrates an increase in anxiety-like behavior in the *C. albicans*-colonized mice.

` The forced swim test (FST) for depression was used to examine the effect of *C. albicans* colonization on a second aspect of emotional behavior, again after two days of colonization. Mice were placed in a 5L beaker with 10cm of 22°C water for a six-minute trial which was video-recorded and later scored by a blinded observer for time spent swimming versus time spent floating. This assay measures behavioral despair, as depression-like behavior in this assay is quantified by an increase in the amount of time spent floating immobile rather than actively swimming and seeking escape.

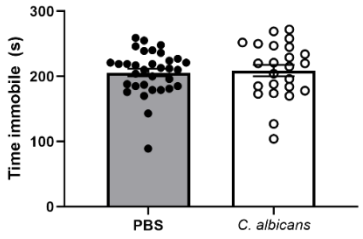

Fig. 2.4: *C. albicans* colonization had no effect on Forced Swim Test performance. Mice were mock-inoculated or inoculated with *C. albicans*. After two days of colonization, mice were placed in a beaker of water for a 6-minute trial in the Forced Swim Test. Figure shows a measure of behavioral despair, total time spent immobile. Gray bar represents mock-colonized mice and white bar represents *C. albicans*-colonized mice. Symbols represent mice and bars indicate average and SEM. PBS N=33, *C. albicans* N=24. Welch's t-test, $p<0.05$

There was no difference in the time spent immobile between the *C. albicans*-colonized mice and the mock-colonized mice (Fig 2.4, mock-colonized mice represented by black bar and *C. albicans*-colonized mice represented by open bar), indicating that *C. albicans* colonization did not affect depression-like behavior. Previous models of microbiota perturbation affected both depression-like and anxiety-like behavior, however, *C. albicans*-colonization specifically affected anxiety-like behavior.

2.3.3 *C. albicans* colonization increases basal CORT and alters post-stress CORT regulation

Anxiety disorder in humans, and anxiety-like behavior in mouse models is complex and multifaceted.[161,183–185] One neuroendocrine pathway that has been shown to be dysregulated in human patients with anxiety is the hypothalamus-pituitary-adrenal (HPA) axis.[116,117,186] Disruption of the HPA axis in a mouse model results in analogous neuroendocrine changes including an increase in anxiety-like behavior.[187–189] We observed increased anxiety-like behavior in the *C. albicans*-colonized mice, a phenotype that could indicate dysregulation of the HPA axis.

To determine whether *C. albicans* colonization affected the HPA axis, we sacrificed mice after three days of *C. albicans* colonization and measured circulating serum CORT, the output of the HPA axis under basal conditions and in response to acute psychological stress.*C. albicans*-colonized and mock-colonized mice were anesthetized in their home cages and sacrificed unstressed. *C. albicans*-colonized mice had significantly higher unstressed basal CORT (Fig 2.5A, Student's t-test, p=0.0012). Further analysis of unstressed serum CORT data demonstrated a distinct effect of the circadian rhythm on serum CORT, as basal CORT in both groups increased over time when mice were

sacrificed at various times throughout the afternoon (Fig. 2.5B). Basal CORT in *C. albicans*-colonized mice began to rise sooner than that of the mock-colonized mice and thus was significantly higher in mice sacrificed from 14:00-16:00 (four-to-five hours prior to lights out), consistent with a circadian advance phenotype.

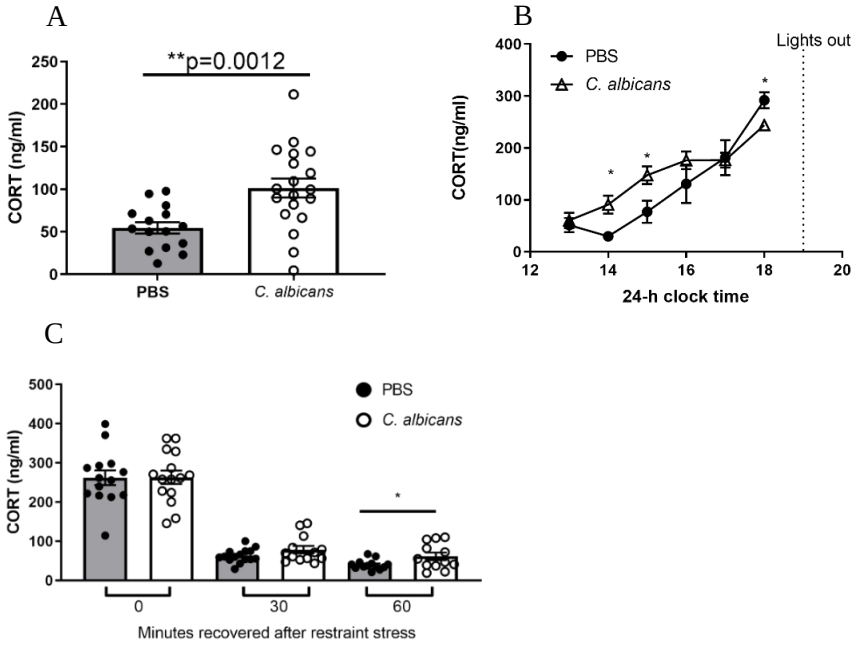

Figure 2.5: *C. albicans* colonization increased basal CORT via circadian advance and disrupted CORT regulation after stress Mice were mock-inoculated or inoculated with *C. albicans* and then sacrificed on day three. Trunk blood was collected after sacrifice and used to measure serum CORT. A) Mice were sacrificed without stress from 14:00-17:00 and serum CORT averaged. Mock-colonized mice N=15 and *C. albicans*-colonized mice N=19 Symbols indicate individual mice and bars indicate average and SEM. B) Mice were sacrificed without stress during various time windows as shown on x-axis. Symbols indicate average and bars SEM. Black circles represent mock-colonized mice and white triangles *C. albicans*-colonized mice. (13:00 PBS N=5, Ca N=6; 14:00 PBS N=9, Ca N=13; 15:00 PBS N=11, Ca N=10; 16:00 PBS N=8, Ca N=11; 17:00 PBS N=9, Ca=8; 18:00 PBS N=5, Ca=9). C) Mice were subjected to 30m of restraint stress, then immediately sacrificed (0m recovered) or allowed to recover in their home cage for 30m or 60m prior to sacrifice (0: PBS N=14 Ca N=15; 30: PBS N=15, Ca N=13; 60 PBS N=13, Ca N=12). All figures, Student's t-test $p<0.05$

After this timepoint, basal CORT in the mock-colonized mice rose sufficiently that CORT was comparable between the two groups. In mice sacrificed one hour prior to

lights out (6pm-7pm), basal CORT was at its highest point detected for both groups, and this peak CORT was significantly higher in the mock-colonized mice compared to the *C. albicans*-colonized mice. These results indicate that *C. albicans* colonization dysregulates the circadian regulation of the HPA axis. In order to investigate the mechanism by which *C. albicans* interacts with the HPA axis, the experiments that follow were designed such that mice were sacrificed during the time window in which CORT was significantly different, four-to-five hours prior to lights out.

To determine whether the changes to basal CORT regulation affected the stress-responsive function of the HPA axis, mice were subjected to 30 minutes of restraint stress and then sacrificed immediately or after 30 minutes or 60 minutes of recovery in their home cage. *C. albicans*-colonized mice and mock-colonized had comparable peak CORT immediately after stress (Fig 2.5B, 0 minutes recovered) but *C. albicans*-colonized mice failed to recover from stress to the same extent as the uncolonized mice after 60 minutes of recovery time (Fig 2.5B; Student's t-test, $p=0.04$). Thus, similar to the mice sacrificed under basal conditions, *C. albicans*-colonized mice had increased CORT after 60 minutes of recovery from stress while mock-colonized mice had low CORT comparable to that of unstressed mice. These results indicated that *C. albicans* colonization alone stimulated the HPA axis and increased basal CORT. After stress and recovery, CORT in the *C. albicans*-colonized mice returned to the elevated baseline observed under basal conditions, indicating that the negative feedback of CORT production induced by stress was not sufficient to override the *C. albicans* stimulation of the HPA axis.

2.3.4 *C. albicans* colonization did not increase basal or stress-induced activity of the hypothalamus

Stimulation of the HPA axis begins in the brain, through excitation of the CRH-producing neurons of the hypothalamus. Because we found that C. albicans colonization affected the final output of the HPA axis, CORT, we examined whether C. albicans colonization altered the activity of the hypothalamus, the top of the HPA axis. cFos is a protooncogene expressed in neurons in response to activation and depolarization,

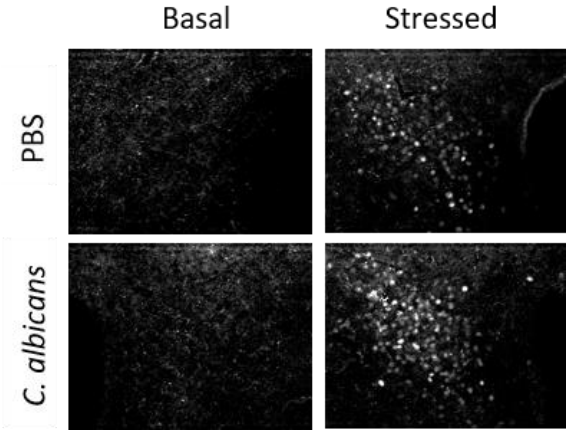

Fig. 2.6: *C. albicans* colonization did not change PVN cFos protein expression. Mice were sacrificed three days after mock-inoculation or inoculation with *C. albicans.* 40µM slices of the brain containing the PVN were collected by cryostat and immunostained with α-cFos antibody. Representative images are shown. The brains of mice sacrificed under unstressed basal conditions are on the left (mock-colonized, top; *C. albicans*-colonized, bottom) and brains of mice subjected to 30m of restraint stress and 30m of recovery prior to sacrifice are shown on the right.

therefore an increase in cFos expression in the hypothalamus indicates an increase in hypothalamus activity. We quantified cFos protein expression in the paraventricular nucleus of the hypothalamus using immunohistochemistry and fluorescence microscopy. No nuclear cFos protein was detected in brain slices from unstressed mock-colonized or *C. albicans*-colonized mice (Fig. 2.6, left), indicating that the degree of HPA axis activation evident in the *C. albicans*-colonized mice at baseline is not reflected in PVN

activation. In mice subjected to 30 minutes of stress and 30 minutes of recovery, nuclear cFos protein was measured in both mock-colonized and *C. albicans*-colonized mice (Fig. 2.6, right) and was comparable between groups, in agreement with the observed comparable peak serum CORT (Fig 2.5B). The PVN remains stress-responsive in the *C. albicans*-colonized mice, and was not sufficiently stimulated at baseline to be detected by this method.

We observed similar results when we compared mRNA cFos levels in mock-colonized and *C. albicans*-colonized mice, with and without stress. RNA was isolated from the hypothalamus of mice sacrificed without stress and after 30 minutes of restraint stress and qRT-RT PCR was performed to measure cFos mRNA expression levels. cFos gene expression was detected in both stressed and unstressed mice.

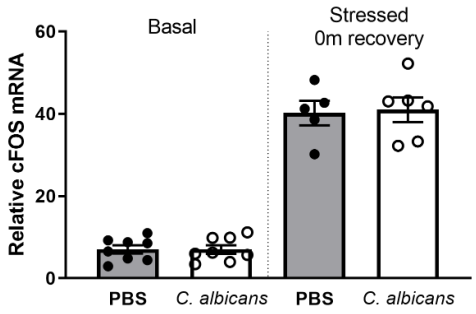

Figure 2.7: *C. albicans*-colonization did not alter cFos mRNA in the hypothalamus under basal or stressed conditions. Mice were sacrificed unstressed (left) or subjected to 30m of restraint stress and immediately sacrificed (right). qPCR was used to quantify cFos levels in the hypothalamus (Basal PBS N=8, Ca N=8; stressed PBS N=5 and Ca N=6). Symbols represent individual mice and bars indicate average and SEM. Mock-colonized mice are solid bars/symbols and *C. albicans*-colonized mice open bars/symbols.

There was no difference in cFos mRNA expression levels between mock-colonized and *C. albicans*-colonized mice when sacrificed under basal conditions or after 30 minutes of restraint stress (Fig 2.7, PBS=solid bars, *C. albicans*-colonized mice=open bars). Thus

the difference in basal CORT production was not reflected in the cFos mRNA or protein in the hypothalamus in mice sacrificed under basal conditions.

To summarize, *C. albicans* colonization alters basal homeostatic CORT production but the stress-responsive HPA axis remains intact and can be activated during psychological stress. Although *C. albicans*-colonized mice achieved a comparable increase in CORT in response to stress, they failed to downregulate CORT production to the same degree after 60 minutes of recovery from stress. Together these results demonstrate that *C. albicans* colonization significantly impacts the gut-brain axis by changing CORT production and anxiety-like behavior.

2.3.5 Gastrointestinal *C. albicans* colonization alters the gut endocannabinoidome

Previous studies have demonstrated that one mechanism by which changes in the microbiota impact the gut-brain axis is through changes to the host metabolome.[74,78] To determine whether *C. albicans* colonization had a significant impact on the metabolite composition of the GI tract, untargeted metabolomic analysis of the cecum contents of mice was performed. The vast majority of metabolites measured were not affected by *C. albicans* (Fig. 6.4). Of the 788 compounds measured, 16 were significantly more abundant in the *C. albicans*-colonized mice and 5 were significantly less abundant in the *C. albicans*-colonized mice (Student's t-test $p<0.05$). The significance threshold of $p=0.05$ would predict a false discovery rate of 39.4 compounds out of the 788 measured; therefore additional analysis was required to investigate the relevance of the 21 metabolites identified as significantly altered by *C. albicans* colonization We used the pathway enrichment tool and compound database provided by Metabolon to determine whether the 21 compounds identified as differentially abundant as a result of *C. albicans*

colonization had a significant impact on a biological pathway. Of the five subpathways with >1 significantly altered metabolite, two were significantly enriched in *C. albicans*-dependent metabolic changes (Table 2.1, Fisher's exact test, Holm correction for multiple comparison $p<0.05$): sterols and endocannabinoids.

Metabolite subpathway	Enrichment	p-value
Sterols	16.67724868	0
Tocopherol Metabolism	9.380952381	0.0688
Glycolipid Metabolism	7.504761905	0.0536
Endocannabinoids	6.822510823	0.0322
Lysophospholipids	4.894409938	0.0615

Table 2.1: Pathway enrichment analysis of untargeted metabolomic screen of GI tract contents. Abundance of metabolites (788 total) was compared in cecum contents of mock-colonized and *C. albicans*-colonized mice. Pathway analysis using Metabolon database of the 21 metabolites identified as significantly different is summarized above (only pathways with >1 significant metabolite shown). Enrichment value is the following ratio: (significant metabolites in pathway/total metabolites detected in pathway)/(total significant metabolites/total metabolites detected in study). P-value was calculated using Fisher's exact test and corrected for multiple comparisons (5 subpathways analyzed) using the Holm-Bonferroni method.

Based on this enrichment analysis, we went back to the original metabolomics analysis to compare the abundance of compounds in those two enriched metabolite families. The sterols significantly altered by *C. albicans* colonization include three phytosterols and cholesterol (Supplemental Figure 5), all of which are increased in abundance in the *C. albicans*-colonized mice. Although interesting, the relevance of this metabolic change to the neuroendocrine phenotypes of interest is unclear.

Endocannabinoids, by contrast, are highly relevant to the phenotypes of interest, as they are lipid signaling molecules that regulate basal CORT production[190,191] and can affect anxiety-like behavior[151,154,192,193]. The endocannabinoids significantly altered by *C. albicans*-colonization include linoleoyl ethanolamide and linolenoyl ethanolamide (Fig

2.8A and B, Student's t-test, p=0.01). Two additional endocannabinoid compounds (Fig. 2.8C, oleoyl ethanolamide and Fig. 2.8D, N-linoleoyltaurine) detected in the cecum contents were elevated in the *C. albicans*-colonized mice but did not reach statistical significance. Linoleoyl-, linolenoyl- and oleoyl-ethanolamide are all N-acylethanolamide (NAEs) compounds, with a common structure and synthetic pathway that differ in the degree of unsaturation of their common 18-carbon acyl chain.

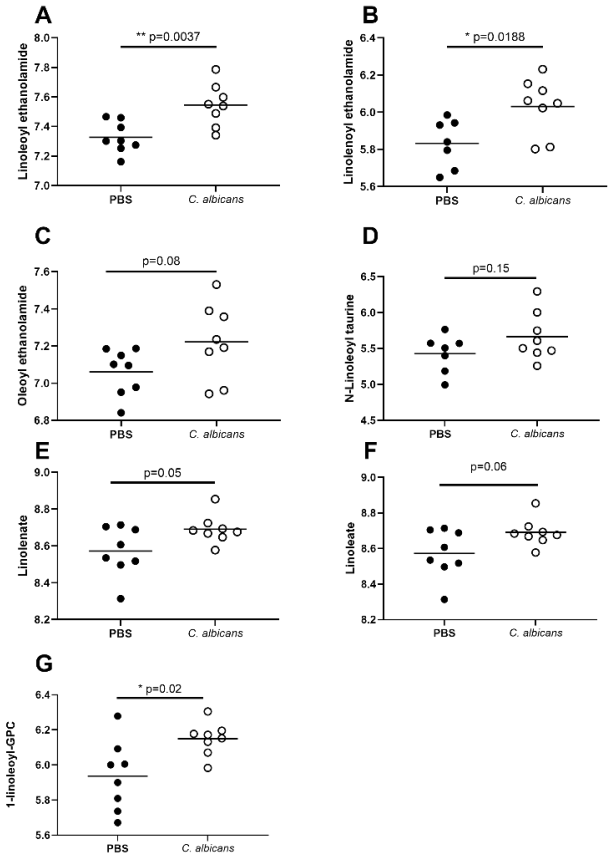

Figure 2.8: 18-C N-acylethanolamides are increased in the *C. albicans*-colonized mice. Untargeted metabolomics analysis of the GI tract contents was performed. Of the 752 compounds detected, four endocannabinoid compounds and their fatty acid and lysophospholipid precursors are shown in figure 8. Relative mass spec data was log-transformed and plotted on arbitrary scale. Each symbol represents an individual mouse. Black circles represent mock-colonized mice, white circles represent *C. albicans*-colonized. Glycerophosphatidic acid (GPA); glycerophosphocholine (GPC); glycerophosphoethanolamine (GPE); glycerophosphoglycerol (GPG) Lines indicate the average. Welch's t-test, $p<0.05$

Both free fatty acids and membrane phospholipid acyl chains can act as a substrate for the production of NAEs. We measured a trend towards an increase in the 18-C free fatty acids linolenate (Fig. 2.8E, Welch's t-test, p=0.05) and linoleate (Fig. 2.8F, Welch's t-test, p=0.06) as well as a significant increase in the lysophospholipid containing linolenate, 1-linoleoyl-glycerophosphocholine (Fig. 2.8G, Welch's t-test, p=0.02) in the GI tract of *C. albicans*-colonized mice. We hypothesized that this increase in 18-C acyl group substrates could increase the synthesis of 18-C NAEs. NAEs are synthesized on demand and the identity of the NAE produced is partially regulated by fatty acid acyl group availability. Therefore increasing the abundance of 18-C unsaturated acyl groups in general could increase 18-C NAE production, in the GI tract (where the metabolomics analysis was performed) and throughout the host in general.

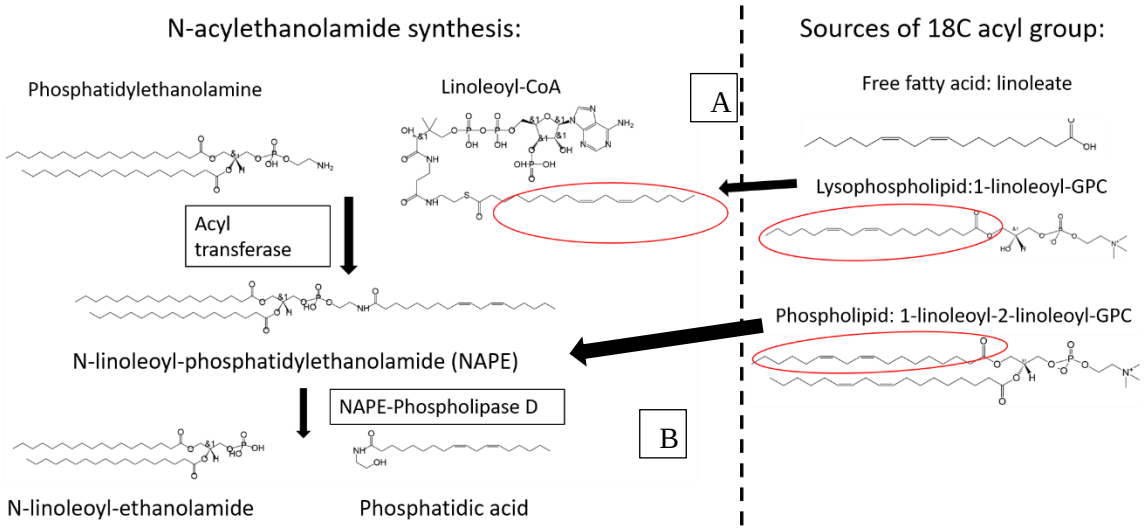

Fig. 2.9: NAEs are synthesized through a common pathway. A synthetic pathway of NAEs, including AEA is shown here. Fatty acids are imported into the cell (A) and transferred to CoA, or a transferase enzyme acts on membrane phospholipids (B) directly to transfer the acyl group to phosphatidylethanolamine. This NAPE is then cleaved to form the signaling lipid, N-acyl-ethanolamide and phosphatidic acid.

A well-characterized NAE, N-arachidonoylethanolamide (AEA), was not detected in the GI contents of mock-colonized or *C. albicans*-colonized mice. AEA is a canonical

endocannabinoid whose physiological regulatory role has been extensively characterized. AEA binds to the receptor CB1 and has been shown to regulate the HPA axis and emotional behavior as a negative regulator of neurotransmitter release[151,194]. The circadian advance in basal CORT and anxiety-like behavior observed in the *C. albicans*-colonized mice are consistent with decreased AEA signaling and resemble the phenotype of the CB1 knock-out mouse[143]. We hypothesized that the increase in free fatty acids and lysophospholipids containing 18-C unsaturated acyl chains (linoleate and linolenate) could reduce synthesis of AEA, as all NAEs share common synthetic pathways (Fig. 2.9) and determination of which NAE is produced is partly regulated by fatty acid precursor availability[140,195–197]. By increasing the abundance of 18C fatty acid precursors, the metabolite changes observed in the *C. albicans*-colonized mice could increase production of 18C NAE and limit production of AEA, resulting in an AEA deficit and possibly contributing to the observed neuroendocrine changes.

2.3.6 Altered hepatic lipid metabolism in *C. albicans*-colonized mice reflects gut metabolite changes

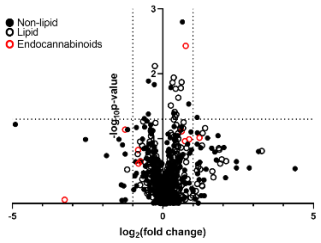

Fig. 2.10: *C. albicans*-colonization increased lipid abundance. Untargeted metabolomic analysis of the cecum contents of mock-colonized and *C. albicans*-colonized mice is shown. 788 total compounds were detected (each symbol represents a compound). Solid circles indicate non-lipid compounds; open circles indicate lipids and red open circles represent endocannabinoids (neuroactive lipids). Dotted line on the y-axis (y=1.3) indicates p=0.05, a threshold for statistical significance. The dotted lines on the x-axis indicate a 2-fold change in abundance.

In addition to the specific elevation of 18-carbon NAEs identified in the *C. albicans*-colonized mice, we also detected a general increase in lipid compounds containing long-chain polyunsaturated fatty acids (PUFAs) in the *C. albicans*-colonized mice. Of the 21 differentially abundant compounds identified in the screen, 12/21 (57%) were lipids, indicating a specific effect of *C. albicans* colonization on lipid metabolism (Fig. 2.10). These lipids included the essential PUFA linolenate and five other compounds with 18-carbon polyunsaturated acyl chains as well as the long-chain PUFA heptadecatrienoate. Thus *C. albicans* colonization increased the availability of PUFAs from gut contents, both free (Fig. 2.8E and F) and incorporated into the lysophospholipid glycerophosphocholine (Fig. 2.8B) and into NAEs (Fig. 2.8B and C).

These increased lipid levels in the GI tract could affect lipid metabolism in the mouse host liver. Mice were sacrificed after three days of *C. albicans* colonization and qRT-PCR was used with RNA extracted from the liver to measure the expression of lipid metabolism genes known to be regulated by dietary fatty acid levels in general and by long-chain and polyunsaturated fatty acids specifically. A decrease in expression of the enzyme stearoyl-coA desaturase (SCD1) was detected in the *C. albicans*-colonized mice compared to the mock-colonized mice (Fig. 2.11A, Student's t-test, $p=0.006$), consistent with the liver sensing an increase in PUFAs from the GI tract[198,199]. Additional genes expected to be upregulated by a general increase in lipid abundance (desaturase enzymes acyl-CoA 8-3 desaturase (FADS1) and acyl-CoA 6 desaturase (FADS2), lipid metabolism transcription factor sterol regulatory element-binding protein 1 (SREBP1c), and fatty acid synthase (FASN))[200] were not significantly changed by *C. albicans*

colonization (Fig. 2.10B), consistent with a specific increase in PUFAs in the gut of *C. albicans*-colonized mice rather than a general increase in lipids.

Additionally, expression of two enzymes that regulate rate-limiting steps of hepatic gluconeogenesis, phosphoenoylpyruvate carboxykinase (PEPCK-C) and glucose-6-phosphatase (G6Pase) were measured. These genes are highly regulated by endocrine mediators including CORT, insulin and glucagon, as well as the nutritional status of the host. Previous researchers have shown that both PEPCK-C and G6Pase are upregulated in response to fatty acid sensing in the liver[201–203]. We observed an increase in PEPCK-C (Fig. 2.11C) and G6Pase (Fig. 2.11D) expression in the *C. albicans*-colonized mice, consistent with a transcriptional response to sensing increased long-chain PUFAs. CORT is a positive regulator of gluconeogenesis in the liver and it is possible that the elevated

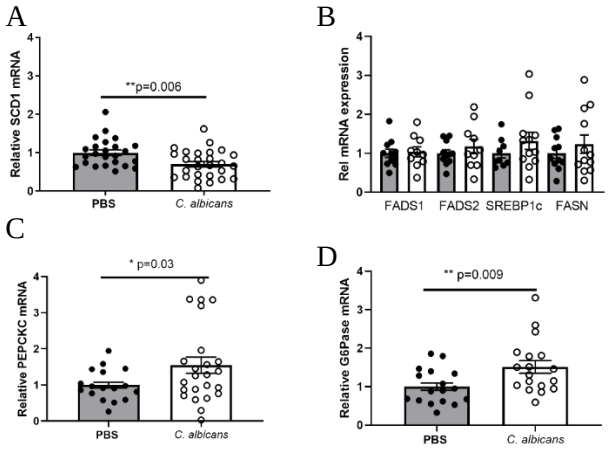

Fig. 2.11: Increased PUFAs in *C. albicans*-colonized mice alter hepatic gene expression. Mice were sacrificed after three days of C. albicans-colonization or mock-colonization. RNA was isolated from livers and qRT-PCR used to measure mRNA expression. A) SCD1 expression relative to GAPDH, normalized to the experimental mean of the mock-colonized mice. B) mRNA expression of genes known to be regulated by lipid abundance. C) PEPCK-C expression relative to GAPDH normalized to the experimental mean and D) G6Pase expression relative to GAPDH, normalized to experimental mean. In all figures, solid symbols/bars represent mock-colonized mice and open symbols/bars *C. albicans*-colonized mice. Student's t-test, $p<0.05$. Symbols indicate individual mice and bars average and SEM.

CORT observed in the *C. albicans*-colonized mice also contributes to the increased liver expression of GFPase and PEPCK-C. SCD1 is also positively regulated by CORT. However, we observed decreased SCD1 expression in the *C. albicans*-colonized mice, consistent with a predominance of negative regulation by increased PUFA abundance rather than positive regulation due to elevated basal CORT. The observed changes in lipid-responsive gene expression in the liver supports the conclusion that the increase in lipid compounds detected in the untargeted metabolomics screen are not false positives, and are physiologically significant *C. albicans*-dependent changes

Gene	Primer sequence	Reference
SCD1, stearoyl-CoA desaturase	F- AGCTCAGTCTCACTCCTTCCCTTA R- CAGCCAGCCTCTTGACTATTCC	Kajikawa et al, 2009[204]
FADS1, acyl-CoA 8-3 desaturase	F- CCAGCTTTGAACCCACCAA R- CATGAGGCCCATTCGCTCTA	Su et al, 2016[205]
FADS2, acyl-CoA 6 desaturase	F-TCAAAACCAACCACCTGTTCTTC R-GATGAACCAGGCAAGGCTTTC	Rosenblat et al, 2010[206]
SREBP1c, sterol regulatory element binding-protein 1	F- CGGCGCGGAAGCTGT R- TGCAATCCATGGCTCCGT	Kajikawa et al, 2009[204]
FASN, fatty acid synthase	F- TACCAGTGCCACAGGAGTCTCA R- TAAACACCTCGTCGATTTCGTTC	Osei-Hyiaman et al, 2005[207]
PEPCK-C, phosphoenoylpyruvate carboxykinase	F- GTGCTGGAGTGGATGTTCGG R- CTGGCTGATTCTCTGTTTCAGG	Volat et al, 2012[208]
G6PAse, glucose-6-phosphatase	F- ACTGTGGGCATCAATCTCCTC R- CGGGACAGACAGACGTTCAGC	Volat et al, 2012[208]
GAPDH, glyceraldehyde-3-phosphate dehydrogenase	F- TGTAGACCATGTAGTTGAGGTCA R- AGGTCGGTGTGAACGGATTTG	Overbergh et al, 1999[209]

Table 2.2: Primer sequences. qRT-PCR was performed using a Roche LightCycler480 and SYBR mastermix as per manufacturer's protocol. Expression of genes of interest was normalized to expression of GAPDH.

2.3.7 Treatment with FAAH inhibitors is sufficient to alleviate elevated CORT and decrease anxiety-like behavior in the *C. albicans*-colonized mice

Based on the observed neuroendocrine phenotypes of CORT circadian advance and increased anxiety-like behavior, and the altered endocannabinoid abundance measured in the GI tract of the *C. albicans*-colonized mice, we hypothesized that these phenotypes reflected insufficient endocannabinoid CB1 signaling. To probe this hypothesis, we treated mice with the fatty acid amide hydrolase (FAAH) inhibitor URB597, a well-

characterized drug that irreversibly inhibits the AEA degradative enzyme FAAH and therefore increases AEA-CB1 signaling[133,150,210,211].

Mice were given an intraperitoneal injection of either vehicle or URB597 (1mg/kg bodyweight) four hours prior to sacrifice under unstressed conditions, to assess the effect of increased CB1 signaling on basal CORT production. Vehicle injection did not have a significant effect on basal CORT in the mock-colonized or *C. albicans*-colonized mice, and as expected CORT was significantly higher in *C. albicans*-colonized mice. Although basal CORT trended higher in mock-colonized mice treated with URB597, this increase was not statistically significant.

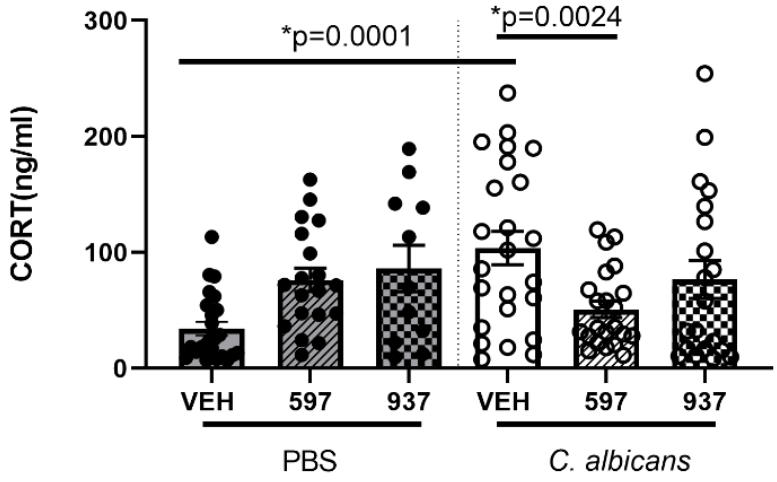

Figure 2.12: FAAH inhibition normalizes basal CORT in *C. albicans*-colonized mice. Mice were given an intraperitoneal injection of vehicle, URB597 (1mg/kg) or URB937 (1mg/kg), then sacrificed four hours later under unstressed conditions and trunk blood collected. CORT was measured in serum. Symbols indicate mice and bars indicate average and SEM. Symbols on the left represent mock-colonized mice and on the right *C. albicans*-colonized mice. PBS: Veh N=15, 597 N=19, 937 N=6; *C. albicans*: Veh N=16, 597 N=19, 937 N=8. Welch's t-test, corrected for multiple comparisons $p<0.02$

Administration of 1mg/kg URB597 was sufficient to decrease basal CORT in the *C. albicans*-colonized mice to the level observed in the vehicle-treated mock-colonized mice

(Fig 2.12, Student's t-test with Bonferroni correction $p<0.05$). This result is consistent with *C. albicans* colonization raising basal serum CORT through changes in endocannabinoid metabolism leading to an anandamide deficit. Therefore, the metabolic changes in the GI tract as a result of *C. albicans* colonization had a significant impact on the gut-brain axis.

In addition to URB597 we also tested the ability of the peripherally restricted FAAH inhibitor URB937 to affect the elevated basal CORT of the *C. albicans*-colonized mice. URB937 has been shown to have minimal effect on FAAH activity in the brain but inhibit >90% of FAAH activity in the periphery[134,135,212].

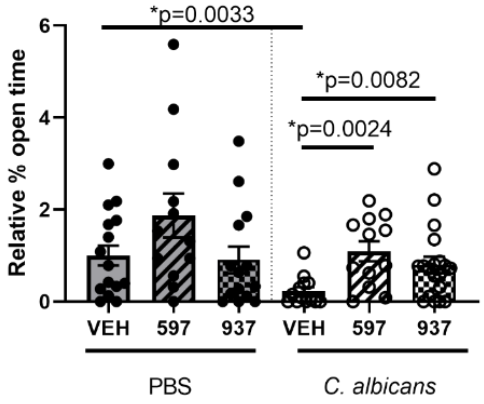

Figure 2.13: FAAH inhibitors improve anxiety-like behavior in the *C. albicans*-colonized mice. Mice were given an IP injection of vehicle, URB597 (0.15mg/kg) or URB937 (0.15mg/kg) four-six hours prior to testing in the EPM. One metric to assess behavior in the EPM is shown, % time spent in open arms (comparable to Fig 2.3A). Symbols indicate mice and bars indicate average and SEM. Symbols on the left represent mock-colonized mice and on the right represent *C. albicans*-colonized mice. Welch's t-test, $p<0.02$ PBS: Veh N=17, 597 N=8, 937 N=10; *C. albicans* Veh N=16, 597 N=8, 937 N=16

We found that unlike URB597, administration of URB937 (1mg/kg) did not significantly decrease the elevated CORT of the *C. albicans*-colonized mice (Fig. 2.12). However, CORT was also elevated in the mock-colonized mice treated with URB937 such that *C.*

albicans-colonized and mock-colonized mice treated with URB937 had comparable basal CORT. This result means we cannot conclude whether or not URB937 alleviated the *C. albicans*-induced increase in basal CORT, because URB937 alone elevates basal CORT.

Increased AEA levels have been shown to have a biphasic effect on anxiety-like behavior, such that low doses of FAAH inhibitors or direct administration of AEA has an anxiolytic effect while high doses of the same drugs have an anxiogenic effect[213]. At sufficiently high doses, AEA interacts with the transient receptor potential vanilloid (TRPV1) channel and increases anxiety-like behavior, a phenotype that dominates the anxiolytic interaction of AEA with CB1[214,215]. There is no such biphasic effect observed in AEA-CB1 regulation of CORT production and TRPV1 signaling is not thought to be involved in HPA axis regulation. Treatment with the 1mg/kg dose of URB597 used to alleviate CORT was anxiogenic in our model (data not shown) therefore we administered a lower dose (0.15mg/kg) of URB597 and URB937 four hours prior to testing in the EPM, to determine whether increasing AEA-CB1 signaling was sufficient to alleviate anxiety-like behavior in the *C. albicans*-colonized mice. Due to significant variability in the activity level of mice in different cohorts used in this experiment, we expressed the data as the percentage of time spent in the open arm (open arm time/total arm time) normalized to the experimental mean of the mock-colonized vehicle control. *C. albicans*-colonized mice treated with the vehicle control had increased anxiety-like behavior compared to the mock-colonized mice (Fig. 2.13, Welch's t-test, $p<0.05$). Neither URB597 nor URB937 had a statistically significant effect on behavior of the mock-colonized mice. Open arm time increased in *C. albicans*-colonized mice treated with either URB597 or URB937, such that these groups were not significantly different from

the mock-colonized vehicle control mice. Although in some models, FAAH inhibitors have been shown to decrease locomotor activity, we did not observe a difference in closed arm entries or in total arm entries in either mock-colonized or *C. albicans*-colonized mice treated with the FAAH inhibitors (data not shown). These results indicate that increasing AEA signaling decreased anxiety-like behavior in the *C. albicans*-colonized mice. Therefore, one way in which *C. albicans* alters anxiety-like behavior is through changes to the endocannabinoid system. Interestingly, the peripherally-restricted FAAH inhibitor URB937 was as effective as the systemic FAAH inhibitor URB597, implying that AEA signaling in the periphery contributes to the regulation of anxiety-like behavior in this model.

2.3.8 Colonization of adult mice with *C. albicans* does not affect the gut-brain axis

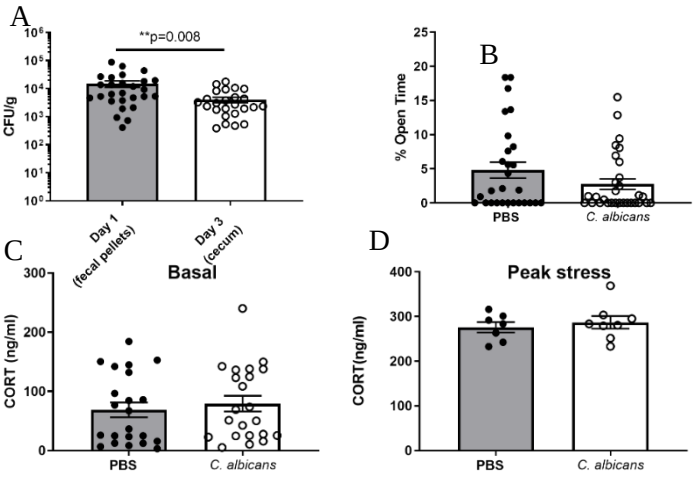

Fig. 2.14: *C. albicans* colonization does not affect neuroendocrine phenotypes of 9-week-old mice. Adult 9-week old female mice were mock-inoculated or inoculated with *C. albicans*. A) GI tract colonization was assessed by plating fecal pellets on day 1 post-inoculation and cecum contents after sacrifice on day 3. B) Behavior in the EPM was assessed on day 2 post-inoculation C) CORT was measured in serum from trunk blood of mice sacrificed unstressed or D) mice subjected to 30m of restraint stress and sacrificed immediately. Symbols indicate individual mice and bars indicate average and SEM. Welch's t-test, $p<0.05$

The experiments described above used 5-week-old (mid-adolescent) C57BL/6 female mice to model early acquisition of *C. albicans* as has been observed in humans. Adult (9-week-old) C57BL/6 female mice were also studied to determine whether acquisition of *C. albicans* as an adult would affect the host gut-brain axis. 9-week-old mice were housed and inoculated with *C. albicans* as described above and *C. albicans* was recovered in fecal pellets and from the GI tract after sacrifice (Fig. 2.14A), demonstrating that this acute colonization model is also effective in adult mice. There was a significant decrease in *C. albicans* colonization between one day and three days post-inoculated in the 9-week-old mice (Fig. 2.14 A, Welch's t-test, $p=0.008$), which was not observed in the 5-week-old mice (Fig. 2.1A), indicating that *C. albicans* did not colonize the adult mouse GI tract as effectively as the adolescent mouse GI tract.

Anxiety-like behavior was evaluated in the EPM after two days of colonization. A trend towards increased anxiety-like behavior in the adult *C. albicans*-colonized mice was observed but the difference was not statistically significant (Fig. 2.14B, Welch's t-test, $p=0.14$). To determine the effect of *C. albicans* on regulation of the HPA axis in adult mice, mice were sacrificed on day three of colonization as above, during the time window (2-4h prior to lights out) in which basal CORT was significantly different in the five-week-old mice. *C. albicans* colonization did not significantly increase unstressed basal CORT production in nine-week-old mice (Fig 2.14B, Welch's t-test, $p<0.05$). Mice were also subjected to 30 minutes of restraint stress, then immediately anesthetized and sacrificed to measure stress-responsive CORT production. There was no difference in peak stress-induced CORT between the mock-colonized and *C. albicans*-colonized mice.

Together these results indicate that 9-week-old adult mice show decreased sensitivity to the neuroendocrine influence of *C. albicans*-colonization.

To summarize, we demonstrated that colonization of adolescent mice with the commensal fungus *C. albicans* results in significant changes to the gut-brain axis including increased anxiety-like behavior and activity of the HPA axis. An untargeted metabolomic screen revealed an increase in PUFAs in the GI tract of *C. albicans*-colonized mice which was sufficient to alter hepatic regulation of lipid metabolism and gluconeogenesis. We identified altered endocannabinoid levels in the GI tract of the *C. albicans*-colonized mice and demonstrated that increasing levels of the endocannabinoid AEA through administration of FAAH inhibitors was sufficient to reverse the *C. albicans*-induced increase in CORT production and decrease anxiety-like behavior.

2.4 Discussion

C. albicans is the most common fungal member of the human gut microbiota and is also the most common fungal pathogen of humans. In order to better understand this complex relationship between *C. albicans* and the human host, we investigated the effect of *C. albicans* colonization on the gut-brain axis. *C. albicans* had a small but significant effect on the gut metabolome that translated into a significant change in multiple neuroendocrine phenotypes. Previous investigations of the gut-microbiota-brain axis have shown that colonization with commensal bacterial species decreased CORT produced in response to stress and decreased depression-like or anxiety-like behaviors[85,87,165]. In contrast to these commensal bacteria, *C. albicans* increased basal CORT (while peak stress-responsive CORT was unchanged) and increased anxiety-like behavior. In this way, *C. albicans* behaved more like a pathogen, comparable to infection

models with the parasite *Trichuris muris*[87] or the mouse gastrointestinal pathogen *Citrobacter rodentium*[216]. Researchers demonstrated that infection with these organisms increased local and systemic inflammation and resulted in increased anxiety-like behavior. *C. albicans* in contrast, did not induce significant systemic inflammation. Our work showed that *C. albicans*-colonization did not significantly alter the immune response, but rather changed the gut metabolome and altered endocannabinoid system signaling to produce the observed increase in basal CORT and anxiety-like behavior. To our knowledge, this is the first communication to report that a commensal fungus, *C. albicans,* affects neuroendocrine host phenotypes and that microbiota-induced changes to the endocannabinoid system affect CORT regulation and anxiety-like behavior.

We found that treatment with the systemic FAAH inhibitor URB597 was sufficient to decrease basal CORT and anxiety-like behavior in *C. albicans*-colonized mice, indicating that *C. albicans*-colonization affects the gut-brain axis through the disruption of endocannabinoid metabolism. Addition of *C. albicans* to the gut microbiota might result in alteration of the brain or changes could be confined to the gut and communicated to the brain, resulting in the observed neuroendocrine changes. Due to the increased basal CORT observed in mock-colonized mice treated with URB937, we could not distinguish the effect of peripherally-restricted versus systemic FAAH inhibition on basal CORT regulation in the *C. albicans*-colonized mice. URB937 did not have such a confounding effect on anxiety-like behavior. Surprisingly, we observed that both the systemic FAAH inhibitor URB597 and the peripherally restricted drug URB937 decreased anxiety-like behavior in the EPM in *C. albicans*-colonized mice, suggesting that AEA signaling in the periphery alone can affect a centrally-regulated process like

anxiety-like behavior. There is precedent for the conclusion that peripheral AEA signaling is involved in regulating emotional behavior. Bellochio *et al* similarly found that the peripheral endocannabinoid system regulates anxiety-like behavior, as the anxiogenic effects of the CB1 antagonist rimonabant were blocked by pretreatment with the peripherally restricted β-blocker sotalol[217]. *C. albicans*-colonized mice treated with URB937 have elevated basal CORT, yet these mice no longer showed increased anxiety-like behavior. This result indicates that although increased basal CORT (regulated centrally) in the *C. albicans*-colonized mice likely contributes to the increased anxiety-like behavior, a deficit of AEA signaling in the periphery may also directly increase anxiety-like behavior.

We repeated these experiments using nine-week-old adult female mice, and found that *C. albicans* colonization did not affect basal CORT of the adult mice. We did observe a consistent trend towards increased anxiety-like behavior in the adult *C. albicans*-colonized mice despite the lack of CORT phenotype, which also implies that elevated basal CORT is not the exclusive mechanism by which *C. albicans* colonization affects anxiety-like behavior. Our results indicate that the HPA axis of adolescent five-week-old mice can be dysregulated by GI tract colonization with *C. albicans*, while the HPA axis of adult mice is not so disrupted. Such age-dependent sensitivity of the HPA axis to microbiota manipulation is consistent with work by Sudo *et al* that identified a key developmental window during which the bacterial gut microbiota could affect the HPA axis. In this model, the abnormal HPA axis response of germ-free mice could be normalized by fecal microbiota transfer from specific-pathogen-free mice if the transfer was performed in six-week-old mice, but not in eight-week-old mice, indicating a

developmental window in which the HPA axis was more sensitive to changes to the gut microbiota[85]. Similarly, we showed that five-week-old mice colonized with *C. albicans* exhibited significant changes in HPA axis regulation and behavior in the EPM while nine-week-old mice colonized with *C. albicans* did not have the same neuroendocrine response.

We would hypothesize that regardless of host age, *C. albicans* colonizing the GI tract produces lipases and phospholipases which could alter lipid abundance in the GI tract and affect endocannabinoid substrate availability. However, the HPA axis of the nine-week-old mice is no longer sensitive to these proposed changes in endocannabinoid levels. Using a rodent model, Lee et al showed that AEA levels in the brain increased significantly between adolescence and adulthood[218], thus it is possible that a decrease in AEA caused by *C. albicans* colonization is physiologically significant in adolescent mice, but is not sufficient to limit AEA-CB1 signaling in adult mice. Previous researchers have also demonstrated significant developmental differences in HPA axis regulation and response[219,220] using both rodent models[221] and human studies[222,223]. Thus, differences in the endocannabinoid signaling system as well as decreased sensitivity of the HPA axis itself likely contribute to the lack of phenotype observed in the adult *C. albicans*-colonized mice. Because in humans *C. albicans* is acquired prior to adulthood, the neuroendocrine changes observed in the adolescent mice remain relevant to our understanding of neuroendocrine health and development of the gut-brain axis.

In addition to the specific effect of *C. albicans* colonization on endocannabinoid metabolism, the untargeted metabolomics analysis also highlighted the effect of *C. albicans* on gut lipid homeostasis in general. *C. albicans* encodes several lipases and

phospholipases,[224–226] some of which are secreted and which could cleave lipids from various sources (plant cell walls, bacterial cell walls, *C. albicans* cells) in the GI tract environment, increasing availability for host uptake and incorporation into membranes. This increase in PUFAs could result in broad changes in energy metabolism in the *C. albicans*-colonized mouse as processes such as glucose and lipid metabolism in the liver are highly responsive to dietary PUFAs[198,199,204,227]. As an example, we observed a decrease in expression of the fatty acid desaturase SCD1 and an increase in expression of enzymes involved in gluconeogenesis. Changes to hepatic metabolism could lead to changes in energy usage and storage throughout the host, and thus *C. albicans* colonization could contribute to metabolic disorders such as obesity and diabetes.

Outside of the context of *C. albicans* colonization, these results imply that enrichment of PUFAs in the GI tract, such as through a high-fat diet or a specific PUFA-rich diet, could have similar metabolic and neuroendocrine effects on the host. Indeed, researchers have shown that long-term (four-to-six weeks) supplementation of diet with PUFAs can significantly impact host metabolism[228,229], and emotional behaviors[230,231], including anxiety-like behavior[231,232]. Our results demonstrate that even short-term changes to GI tract PUFA abundance can affect these same host systems. Altogether this work demonstrates the ability of limited changes to the gut metabolome to have a significant impact on the brain and behavior, and illustrates the ability of the common gut commensal fungus *C. albicans* to affect the host beyond the GI tract.

2.5 Chapter 2 contributions

I performed mouse experiments with assistance from Carol Kumamoto. Untargeted mass spec analysis (and preceding HPLC extraction) was performed by

outside company Metabolon. All other data included in figures in Chapter 2 was produced and analyzed by me.

Chapter 3 Pre-colonization with the commensal fungus *Candida albicans* reduces murine susceptibility to *Clostridium difficile* infection[2]

[2] Markey, Laura, Lamyaa Shaban, Erin Green, Katherine Lemon, Joan Mecsas and Carol Kumamoto. "Pre-colonization with the commensal fungus *Candida albicans* reduces murine susceptibility to *Clostridium difficile* infection." Gut Microbes, 2018 Nov 9 (6): 497-509

3.1 Introduction

In recent years, the bacterium *Clostridium difficile* has become an increasingly significant cause of human morbidity and mortality[233]. The major risk factor for infection is the use of broad-spectrum antibiotics, with elderly and immunocompromised individuals at particularly high risk for disease[234–236]. Antibiotic treatment disrupts the normally protective, resident bacterial community in the gut and leads to susceptibility to *Clostridium difficile* infection (CDI). This debilitating infection is treated with other antibiotics, all of which continue to disrupt the gut microbiota to some degree, and recurrence occurs in up to 25% of cases[235,236].

An alternative approach to CDI, fecal microbiota transplantation (FMT), relies on restoring a normal gut microbial community in a CDI patient who has experienced more than one recurrence. A randomized-controlled clinical trial and other smaller studies show success rates of 80-90% for FMT in treatment of recurrent CDI[42,237,238]. This approach is thus extremely promising but there is currently no consensus on the optimal source or makeup of donor microbiota. In addition, there have been instances of unintended consequences following FMT, including exacerbation of inflammatory bowel disease[239,240]and unexplained weight gain[241]. A deeper understanding of the effects of commensal organisms on CDI would contribute to identification of an optimal donor microbiota composition.

The study described in this communication focuses on the effects of the commensal fungus *Candida albicans* on the outcome of CDI. *C. albicans* colonizes the gut of most humans as a benign commensal. Huffnagle and co-workers demonstrated that, in mice, gut colonization by *C. albicans* influences the recovery of the bacterial gut

community after antibiotic disruption[180]. Therefore, *C. albicans* gut colonization might affect the susceptibility of a host to CDI following antibiotic treatment. In addition, *C. albicans* affects the immunological milieu. Gut colonization by *C. albicans* promotes accumulation of regulatory T cell populations[9]. Cytokines such as IL-17 and IL-22 are up-regulated in the gut in response to *C. albicans* colonization[12,242–244]. Monocytes exposed to *C. albicans* are reprogrammed to confer nonspecific protection from secondary infections, a process termed trained immunity[245]. These properties of *C. albicans* led us to hypothesize that the presence of the fungus in the gut microbiota would protect an antibiotic-treated host from a *C. difficile* challenge.

The data described here show that mice pre-colonized with *C. albicans* exhibit an increased ability to survive a lethal challenge with *C. difficile.* These results highlight a new aspect of *C. albicans* biology and show that under some circumstances, the effects of *C. albicans* colonization are beneficial for the host.

3.2 Methods

3.2.1 Strains and growth conditions

C. albicans strain CKY101[171], a virulent strain derived from the sequenced strain SC5314, was used for all studies. For mouse inoculations, cells were grown at 37°C in YPD (1% yeast extract (BD 212750), 2% peptone (Difco 0118-17-0), 2% glucose (Sigma G8270))[246] for 21-24 hrs.

C. difficile strain UK1, a NAP1/027/BI human epidemic strain[247] was used for all studies. Spores were isolated as previously described[248] except that gradient purification was omitted. For enumeration of *C. difficile* spores in extracts from mice, samples were plated on pre-reduced TCCFA plates (Taurocholate (Calbiochem 580217), cycloserine

(Sigma C6880), cefoxitin (Sigma C4786), fructose (Macron Fine Chemicals 7756-12))[249] and incubated at 35°C for 2 days in an anaerobic chamber.

3.2.2 GI colonization in mice

Five-week-old female C57BL/6 mice (Jackson Laboratory) were co-housed in a large cage (24" x 17"). Mice were treated with antibiotic (cefoperazone (Sigma C4292), 0.5 gm/L) in drinking water for 10 days. All mice were treated with cefoperazone for 10 days, except for the no antibiotics, no *C. difficile* mice used in Figs. 4D and S4.

Prior to inoculation with *C. albicans*, mice were tested and shown to be negative for cultivable fungi on YPD-SA agar medium [YPD agar plus 100 μg/ml streptomycin (Sigma S6501) and 50 μg/ml ampicillin (Sigma A9518)] incubated for 2 days at 37°C. On the 10th day of antibiotic exposure, some mice were inoculated orally with 5 x 10^7 *C. albicans* cells in 25 μl (n=10 mice). All of the inoculated mice described in this study became colonized with *C. albicans* following a single inoculation.

All mice were transferred from the large cage to standard sized cages, housed 2 mice per cage and switched to water without cefoperazone. *C. albicans* colonization was measured over time by collecting fresh fecal pellets and plating homogenates on YPD-SA agar. Mice that were not inoculated with *C. albicans* (n=10 mice), but had been treated with cefoperazone in the same large cage as the *C. albicans*-inoculated mice, were housed in the same room as the *C. albicans*-inoculated mice.

After 3 weeks of *C. albicans* colonization, mice were orally inoculated with *C. difficile* spores (~3-8 x 10^5 spores per mouse). On the day before inoculation with *C. difficile*, mice were inoculated intraperitoneally with clindamycin (Sigma C5269) (10

mg/kg). Some mice were inoculated intraperitoneally with IL-17A (R&D Systems 421-ML-025, 1 μg in 100 μl PBS) or with PBS on the day before and the day after *C. difficile* inoculation. All mice used in these experiments were shown to be negative for *C. difficile* colonization prior to inoculation with *C. difficile* spores by collecting fecal pellets and plating on pre-reduced TCCFA.

Mice were weighed daily and sacrificed 5 days post-inoculation or when moribund. Mice exhibiting severe signs of illness (extreme inactivity, hunched posture, ruffled fur) were considered moribund and were sacrificed. Mice were also sacrificed if their weight loss exceeded 20%. Within one experiment (i.e., one batch of mice), some of the mice were sacrificed on day 1 or 2 post-inoculation for the various analyses while other mice were monitored for survival over 5 days. The survival data show combined results of mice from 3-4 experiments.

Relative weights were compared using the *t* test. Survival was compared using the log rank test. The cecum was dissected for further studies. Samples of cecum contents were plated on both YPD-SA to detect *C. albicans* and on pre-reduced TCCFA after heating at 60^{o}C for 10 min. to detect *C. difficile*.

All experiments were done in compliance with Tufts University IACUC guidelines. *C. difficile* susceptibility experiments were performed during the winter months to avoid the occasional presence of cultivable fungi in the GI tracts prior to inoculation with *C. albicans*.

3.2.3 Microbiota analysis

The distal portion of the cecum, including contents, was dissected from mice two days post-inoculation with *C. difficile*. For comparison, ceca from control, untreated mice that did not receive antibiotic treatment and were not inoculated with microbes were collected. Mice from 4-5 different experiments were analyzed. The mucosa was scraped using a glass slide and the scraped material plus the luminal contents were combined in PBS. The sample was centrifuged at 16,100 rcf in a refrigerated Eppendorf microcentrifuge for 5 min. and the pellet was weighed and frozen at -80^{o}C. Microbial DNA was extracted using the QIAamp DNA Stool Mini Kit (Qiagen 51504) with an additional beadbeating step. Briefly, cecum samples were lysed by beadbeating in Qiagen lysis buffer ASL, and the lysate was treated with InhibitEX tablets followed by enzymatic digestion with proteinase K (20mg/ml) and RNaseA (1mg/ml) and column DNA purification.

Libraries were prepared from each sample and sequenced as described[250]. Briefly, PCR amplification of the V4 region of the 16S rRNA gene was performed with primers that included adapters for Illumina sequencing and twelve base barcodes. Two hundred fifty bp paired-end sequencing was performed using an Illumina MiSeq. Base calling was performed using CASAVA 1.8 and the resulting fastq files were used as input for downstream analysis using QIIME (1.8.0)[175]. Briefly, the paired-end reads from the fastq files were joined, barcodes extracted and then demultiplexed. The operational taxonomic units (OTUs) were determined using a closed reference approach by aligning reads to the Greengenes Database (version 13_8) at 99% identity. The Greengenes phylogenetic tree was used to define the phylogenetic relationship between OTUs. The resultant OTU

tables contained the relative abundance of bacterial taxa in each sample. These tables were used to calculate overall diversity within each sample. To compare the composition and diversity of samples to each other taking into account phylogenetic relatedness, the OTU tables were used to calculate the weighted UniFrac distance matrix, which was summarized with Principal Coordinate Analysis. Permanova analysis was performed using Qiime.

Total levels of bacteria per cecal tip sample were measured by qPCR using eubacterial primers. qPCR reactions were conducted using SYBR Green PCR Master Mix (Applied Biosystems 4364346) and a LightCycler 480 II (Roche) instrument. Normalized abundance of bacterial genera was calculated by multiplying the fraction of total reads for a genus by the total level of bacteria per mg of cecum sample (in arbitrary units).

3.2.4 Histology

Cecum tissue was dissected from mice sacrificed prior to or two days post-inoculation with *C. difficile.* Tissue was fixed in buffered formalin and processed for staining with Hematoxylin and Eosin (H & E) by the Tufts Animal Histology Core facility (http://sites.tufts.edu/histopath/animal-histology-core/).

3.2.5 *C. difficile* toxin assay

Cecum contents from mice sacrificed one or two days post-inoculation with *C. difficile* or fecal pellets collected one day post-inoculation were weighed and diluted with 10 times the volume of PBS. Serial three-fold dilutions were made in DMEM (Corning Cell Gro MT10-013CV) and samples were applied to monolayers of mouse embryonic fibroblast cells (MEF) cells grown in DMEM with 10% heat-inactivated Fetal Bovine

Serum (Atlanta Biologicals S11150). Cells were incubated for 24 hours at 37°C and 5% CO_2 and scored visually at 10X magnification for cell rounding. Toxin titer is defined as the inverse of the greatest dilution that resulted in 100% cell rounding.

3.2.6 Cytokine gene expression

For measurement of cytokine gene expression, mice were sacrificed prior to or two days post-inoculation with *C. difficile* and colon tissue was frozen in RNALater (Invitrogen AM7021) at -80ºC. RNA was purified with Trizol (Invitrogen 15596026) extraction and column purification, using the Ambion Purelink RNA mini kit (Invitrogen 12183018A). DNA was eliminated with on-column DNase treatment. cDNA preparation with Superscript III (Invitrogen 18080051) was performed using manufacturer's protocol. qRT-PCR reactions were performed as described above for qPCR. Triplicate samples were measured; controls lacking template did not yield products. Standard curves were generated and all results normalized to the level of GAPDH expression in each sample.

3.3 Results

3.3.1 Prior colonization of mice with *C. albicans* reduces susceptibility to lethal challenge with *C. difficile*

We conducted a direct test of the central hypothesis that *C. albicans* pre-colonization would attenuate lethal CDI. Antibiotic treatment was used to increase the susceptibility of mice to lethal CDI using a modification of the model established by Young and co-workers (Fig. 3.1A)[251]. These investigators demonstrated that cefoperazone-treated mice remained susceptible to CDI for up to 6 weeks after cessation

of cefoperazone treatment if given clindamycin on the day before spore challenge.

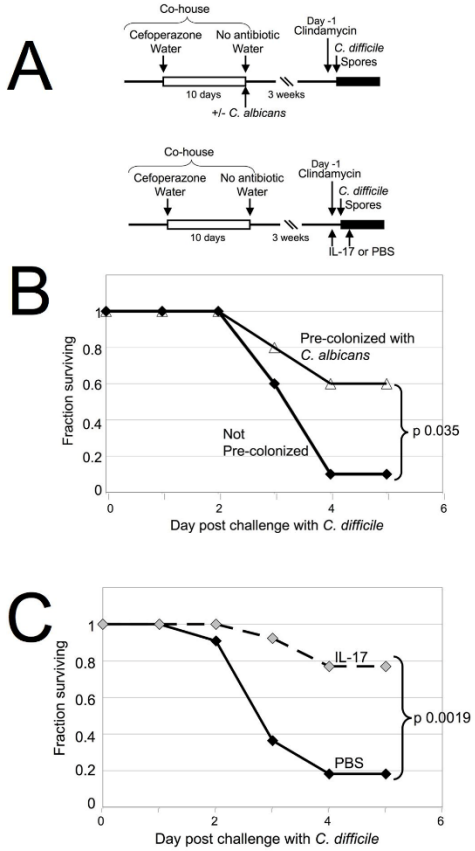

Figure 3.1. Enhanced survival of Cd-challenged mice that were pre-colonized with *C. albicans*. (**A**) Timeline of the experiments. All mice used in one experiment were co-housed in a large cage as shown. Mice were given cefoperazone in drinking water, shown as a white box. Mice were then split into smaller groups, given standard water and some mice were orally inoculated with *C. albicans.* Mice were housed for 3 weeks and then injected with clindamycin intraperitoneally (Day -1). *C. difficile* challenge was initiated by oral inoculation with *C. difficile* UK1 spores on the following day. Survival and weight loss were monitored for 5 days following inoculation, shown as a black box. In some experiments, mice treated as above were not colonized with *C. albicans* and instead received recombinant IL-17A or PBS by intraperitoneal injection on the day before and the day after *C. difficile* challenge. (**B**) The fraction of mice surviving on each day after challenge with *C. difficile* is plotted as a function of day post-challenge. Combined results are from 4 different experiments. Black diamonds, without *C. albicans*, n=10; open triangles, pre-colonized with *C. albicans*, n=10; *p* value, log rank test. (**C**) The fraction of mice surviving on each day after challenge with *C. difficile* is plotted as a function of day post-challenge. Combined results are from 3 different experiments. Black diamonds, treated with PBS, n=11; grey diamonds, treated with IL-17A, n=13. *p* value, log rank test.

Building on these key observations, we modified the procedure of Reeves, et al. to establish *C. albicans* colonization in mice prior to challenge with *C. difficile* spores. Briefly, C57BL/6 mice received cefoperazone in drinking water for 10 days. This antibiotic regimen was used for all mice except certain control mice, as described in Materials and Methods. On the tenth day, some mice were orally inoculated with *C. albicans.* All mice were then switched to standard water without antibiotics to permit the gut microbiota to recover from the antibiotic treatment for 3 weeks, in the presence or absence of *C. albicans*. *C. albicans* colonization over this time period was shown by plating homogenized fecal pellets collected at various times post-inoculation (Fig. 6.5). All mice were successfully colonized with *C. albicans* following a single inoculation.

After 3 weeks, mice received a single dose of clindamycin by intraperitoneal injection and, on the following day, were orally inoculated with approximately 4 x 10^5 *C. difficile* spores. *C. difficile* strain UK1, a NAP1/027/BI human epidemic strain[247] was used for all studies. The response of inoculated mice to the *C. difficile* challenge was monitored over 5 days. Weight loss was often evident at day 2 post-inoculation and some mice died or became moribund by day 3. There were slight differences in the timing and synchrony of deaths between experiments and more deaths were observed when higher numbers of spores were used.

In the absence of *C. albicans* pre-colonization, only 1 of 10 mice with CDI survived to day 5 (Fig. 3.1B), consistent with previous results[251]. Of the 9 who succumbed to severe CDI within 5 days, 5 died, 2 became moribund and were sacrificed and 2 were sacrificed due to weight loss. The average relative weight of surviving mice on day 2 post-inoculation was 0.92$\pm$0.06 and on day 3 post-inoculation was 0.84$\pm$0.03 of

each mouse's pre-inoculation weight (p <0.00004; paired t test, day 3 versus day of inoculation), demonstrating weight loss due to CDI. Mice injected intraperitoneally with PBS on the day before and the day after *C. difficile* challenge (as a control for cytokine treatment, see below) were also highly susceptible to lethal CDI (Fig. 3.1C). Only 2 of the 11 mice in this group survived to day 5 and of the other 9, 7 died, 1 was sacrificed when moribund and1 was sacrificed due to weight loss. The relative weight of these surviving mice on day 3 post-inoculation was 0.84$\pm$0.05 (p<0.00098; paired t test), demonstrating weight loss due to CDI.

In contrast, the majority of mice pre-colonized with *C. albicans* survived challenge with *C. difficile* as compared to those not pre-colonized (Fig.3.1B; p=0.035; log rank test). Six of the 10 mice pre-colonized with *C. albicans* survived to day 5, while only 1 died, 1 was sacrificed when moribund and 2 were sacrificed due to weight loss. Mice pre-colonized with *C. albicans* thus showed increased survival of CDI compared to mice without *C. albicans* pre-colonization.

There was no statistically significant difference in weight loss due to CDI with or without *C. albicans* pre-colonization. For *C. albicans* pre-colonized mice infected with *C. difficile*, average relative weight was 0.91$\pm$0.05 of their starting weight on day 2 post-*C. difficile* inoculation and 0.84$\pm$0.06 on day 3 post-*C. difficile*-inoculation, a statistically significant difference (p<0.00003; paired t test, day 3 vs day of inoculation) indicating weight loss. Relative weights for surviving mice generally increased at the end of the experiment. The average relative weight at day 5 post-inoculation was 0.96$\pm$0.07 (p<0.003, t test, relative weight on day 3 vs. day 5) consistent with recovery from infection.

Histological analysis of cecum and colon tissues demonstrated that *C. difficile*-challenged (Cd-challenged) mice exhibited histological features of murine CDI, regardless of the presence of *C. albicans.* Regions exhibiting edema with leukocyte influx into the lamina propria (Fig. 6.6, panel E,F) had a patchy distribution. Eighteen sections of cecal tissue from 7 Cd-challenged mice without *C. albicans* at day 2 post-infection (with or without PBS) were examined. Each cecum section exhibited multiple regions showing edema and leukocyte influx (Fig. 6.6, panel E; 125 10x microscope fields examined). Ten cecal sections from 5 Cd-challenged mice with *C. albicans* pre-colonization (with or without PBS) at day 2 post-infection revealed multiple regions with

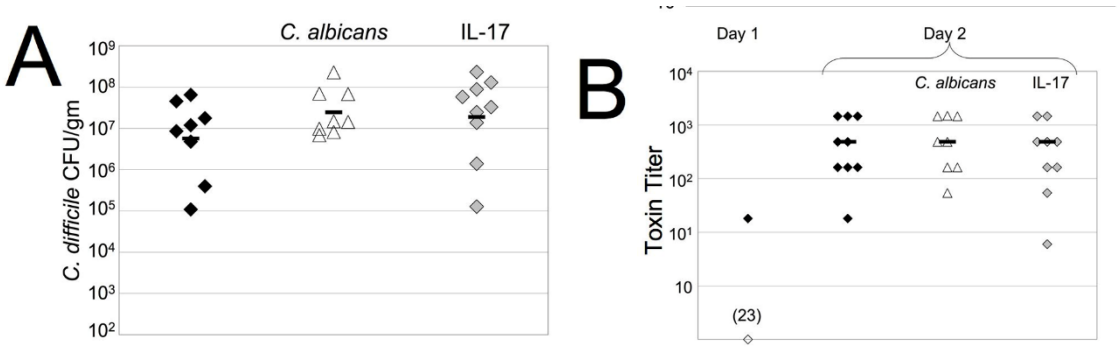

Fig. 3.2: *C. difficile* spore levels and toxin production are unaffected in pre-colonized or IL-17A-treated mice. (**A**) Mice were treated as described in Fig. 1A. Mice were euthanized 2 days post-*C. difficile* inoculation and cecal contents were collected. Samples were heated at 60ºC for 10 min and *C. difficile* spores were enumerated by plating on TCCFA. Black diamonds, received PBS and *C. difficile;* open triangles, received *C. albicans*, PBS and *C. difficile;* grey diamonds, received IL-17 and *C. difficile.* Each symbol shows CFU/gm from an individual mouse; the bar shows the geometric mean. (**B**) *C. difficile* toxin titer in fecal or cecal extracts was measured by a cell-rounding assay. Fecal pellets were collected 1 day post-inoculation. Cecal contents were collected after mice were sacrificed on day 1 or 2 post-inoculation. Toxin titer is defined as the inverse of the greatest dilution that produced 100% cell rounding. Black diamonds, received PBS and *C. difficile;* open diamond, samples that yielded no detectable toxin activity (23 indicates that 23 of the 24 samples yielded undetectable toxin levels); open triangles, received *C. albicans*, PBS and *C. difficile;* grey diamonds, received IL-17 and *C. difficile.* Each sample shows results from an individual mouse and the bar shows the median.

edema and leukocyte influx (Fig. 6.6, panel F; 74 10x microscope fields examined).

Eleven cecal sections from 6 control mice that were antibiotic treated but not challenged with *C. difficile*, either with or without *C. albicans* did not exhibit these features (Fig. 6.6, panel A,B).

Additional parameters of CDI were similar in mice with or without *C. albicans* even though *C. albicans* pre-colonized mice had increased survival of CDI. For example, the levels of *C. difficile* spores detected in the GI tracts of mice at day 2 post-*C. difficile* inoculation were similar in mice with or without pre-colonization with *C. albicans* (Fig. 3.2A; p=0.76, *t* test with log transformed data). For this and subsequent experiments, mice were injected intraperitoneally with PBS on the day before and the day after *C. difficile* challenge. Regardless of pre-colonization with *C. albicans*, spore levels were lower on day 1 (Fig. 6.7) than on day 2 (Fig. 3.2A; median 5,000-fold lower on day 1 than on day 2), showing that spores detected on day 2 reflected growth and new spore production within the GI tract of the host and were not solely the spores fed to the mice.

C. difficile toxin levels were also similar in infected mice with or without *C. albicans* pre-colonization. *C. difficile* produces glucosylating toxins that act on small G-proteins of the host, such as Rho and Rac, during growth in the GI tract[252]. Toxin activity was measured in extracts of the cecum or fecal pellets from mice using a mammalian cell-rounding assay[253]. Toxin titer was defined as the inverse of the greatest dilution that produced 100% cell rounding. The results showed that toxin levels in cecum contents of infected mice sacrificed 1 day post-*C. difficile* inoculation or in fecal pellets collected on the same day were mostly undetectable (Fig. 3.2B). Higher levels of toxin activity were present in cecum contents of infected mice sacrificed 2 days post-*C. difficile* inoculation (Fig. 3.2B). Levels of toxin were comparable in mice with or without *C. albicans* pre-

colonization (p=0.91; Mann Whitney test). Toxin activity was not detected in samples from mice that were not inoculated with *C. difficile.* Therefore, pre-colonization with *C. albicans* did not reduce the ability of *C. difficile* to grow and produce toxins in the mouse GI tract. Thus, the presence of *C. albicans* did not increase the colonization resistance of the host.

Combined, our observations indicate that mice pre-colonized with *C. albicans* were better able to resist lethal disease due to *C. difficile* despite the growth of *C. difficile* in the GI tract, the production of *C. difficile* toxin and the presence of inflammation and tissue damage.

3.3.2 Altered host response to *C. difficile* challenge in pre-colonized mice.

A significant fraction of hospitalized patients colonized with *C. difficile* do not develop symptomatic CDI. Host factors such as immunological status are therefore thought to affect the risk of CDI[235]. Based on this and on the increased survival of the *C. albicans* pre-colonized mice, we hypothesized that *C. albicans* altered the immune response to *C. difficile* challenge, which contributed to resistance to lethal CDI.

We therefore measured the expression of genes encoding IL-17A, IL-22, TNF-α and IFN-γ in colonic tissue of Cd-challenged mice with or without *C. albicans* pre-colonization. Results showed that two days post challenge with *C. difficile,* mice pre-colonized with *C. albicans* expressed higher levels of *Il17a* mRNA than mice without *C. albicans* (Fig. 3.3B). In contrast, expression of the other cytokines was not significantly altered by pre-colonization with *C. albicans*. The genes encoding IL-17A and IFN-γ were also expressed at higher levels in *C. albicans* pre-colonized mice prior to inoculation with *C. difficile* (Fig.3.3A). These results demonstrated that the presence of *C. albicans* altered

the host response both before and after the initiation of *C. difficile* infection. These results raised the possibility that higher levels of IL-17 are protective against lethal CDI. We therefore hypothesized that administration of IL-17A, in the absence of C. albicans pre-colonization, would protect mice from lethal CDI. To test this hypothesis, mice were given cefoperazone antibiotic treatment for 10 days and then standard water for 20 days,

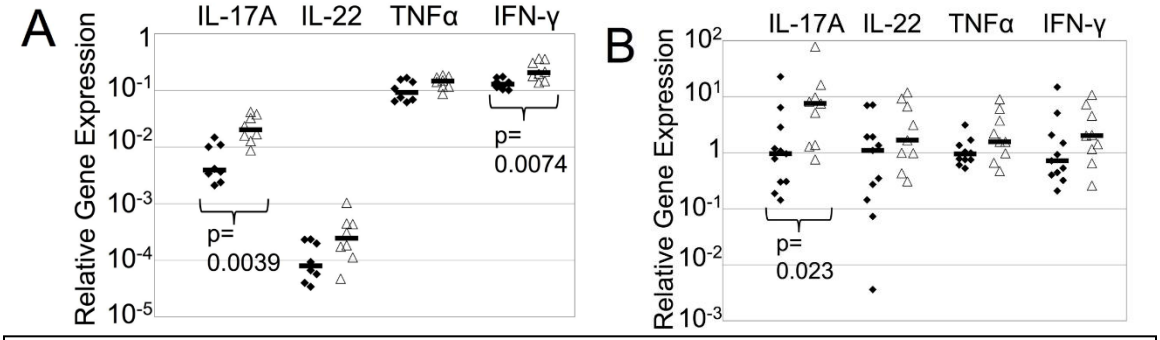

Figure 3.3. Increased expression of *Il17a* in the colon of *C. albicans*-precolonized, Cd-challenged mice. All mice were treated with cefoperazone for 10 days and received clindamycin. Mice were euthanized on the day of challenge before receiving spores (**A**) or 2 days post challenge with *C. difficile* (**B**). RNA was extracted from colon tissue, converted to cDNA and expression of transcripts was measured in cDNA by qRT-PCR and was expressed in arbitrary units using GAPDH for normalization. The average for Cd-challenged mice was set to 1 for each experiment and samples were expressed relative to this value. Combined results of two experiments are shown. Each symbol represents a sample from an individual mouse and the bar indicates the geometric mean. Black diamond, received PBS but no *C. albicans*; open triangle, received PBS and *C. albican*s. *p* values, Mann Whitney test.

as shown in Fig. 1A. The day before *C. difficile* challenge, mice were injected intraperitoneally with recombinant IL-17A (or PBS) and clindamycin. Mice were orally inoculated with *C. difficile* UK1 spores and one day later injected intraperitoneally again with IL-17A (or PBS). Survival and weight loss were monitored for up to 5 days post-*C. difficile* infection (Fig. 3.1C). Only 2 of the 11 mice that were injected with PBS survived, while 7 died, 1 was sacrificed when moribund and 1 was sacrificed due to weight loss, as noted above. In contrast, 10 of the 13 mice that were injected with IL-17A survived, while 2 died and 1 was sacrificed due to weight loss. IL-17A treated mice thus

showed a significant and striking improved survival of CDI in comparison to mice that were not treated (Fig. 3.1C, p=0.0019; log rank test). Average relative weight of surviving IL-17A-treated mice on day 3 post-inoculation was 0.85±0.04, significantly different from the starting weight ($p<0.000009$; paired t test). Also, IL-17A treatment did not significantly alter the levels of spores or *C. difficile* toxin in the infected mice (Fig. 3.2). Histological analysis of 9 cecal sections from 4 IL-17A treated, Cd-challenged mice showed multiple regions exhibiting edema with leukocyte influx (Fig. 6.6, panel H; 80 10x microscope fields examined) but not in uninfected mice (Fig. 6.6, panel D). These results demonstrated that higher levels of IL-17A enhanced survival following challenge with *C. difficile* spores although IL17A-treated mice had similar levels of weight loss, spore counts and inflammation due to CDI when compared to mice not treated with IL-17A.

3.3.3 Effects of pre-treatments on microbiota composition.

In humans, susceptibility to CDI is strongly affected by the state of the gut bacterial microbiota and antibiotic treatment is a major risk factor for infection[234–236]. Therefore, we analyzed the composition of the cecal bacterial microbiota in Cd-challenged mice with or without *C. albicans* pre-colonization and with or without additional IL-17A treatment. We did not detect a statistically significant difference in the overall microbiota composition between groups; however, there were some differences between groups for specific genera.

The cecal microbiota of mice treated with cefoperazone, colonized (or not) with *C. albicans* and then given clindamycin, PBS or IL-17A, and finally, *C. difficile* spores was analyzed. Bacterial community composition was characterized by sequencing the V4

region of the 16S rRNA gene and analyzed using QIIME[175]. Principal Coordinate Analysis (PCoA) of weighted UniFrac distance for the bacterial communities in Cd-challenged mice with or without *C. albicans* and with or without additional IL-17A is shown in Fig. 3.4A. Permanova analysis of these results did not detect a statistically significant difference between the treatment groups (p=0.148).

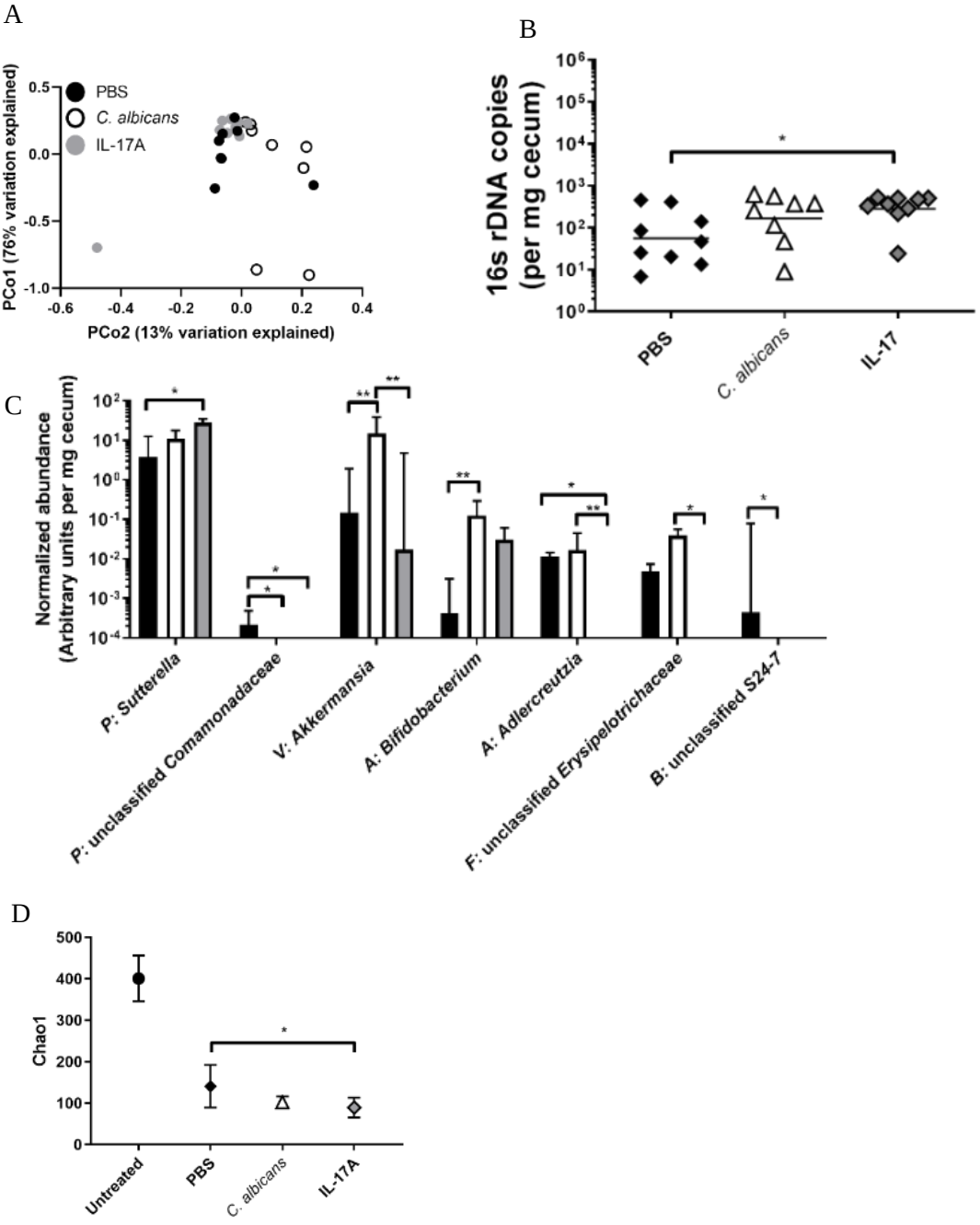

Figure 3.4 Bacterial microbiota of Cd-challenged mice with or without *C. albicans* pre-colonization or IL-17A treatment. Cecal bacterial microbiota composition from mice euthanized on day 2 post-*C. difficile* challenge was analyzed by Illumina sequencing of the V4 region of bacterial 16S rRNA gene. Relative abundance of bacterial taxa was determined using QIIME. (**A**) Results were analyzed by determining weighted UniFrac distances and performing Principal Coordinate Analysis using QIIME. Black Diamond, PBS-treated, Cd-challenged mice without *C. albicans;* white triangle, PBS-treated, Cd-challenged mice pre-colonized with *C. albicans*; grey diamond, IL-17A-treated, Cd-challenged mice without *C. albicans*. (**B**) Total levels of bacteria per cecal tip sample were measured by qPCR using eubacterial primers and normalized to milligrams of cecum sample used for DNA extraction. Symbols, as in (A); bar indicates the geometric mean. (**C**) Normalized abundance per mg of cecum sample (arbitrary units) for bacterial genera in the cecal microbiota of mice treated with PBS and *C. difficile* (black bars; n=9); with PBS, *C. albicans* and *C. difficile* (white bars; n=8); or with IL-17A and *C. difficile* (grey bars; n=9). All genera with a statistically significant difference between at least two groups are shown. Phyla are indicated with a one letter abbreviation as follows: P=Proteobacteria, V=Verrucomicrobia, A=Actinobacteria, F=Firmicutes, B=Bacteroidetes. Column indicates the median value, bar indicates the upper quartile, brackets indicate statistically significant comparisons (*p<0.05 **p<0.01, Kruskal Wallis Test followed by Dunn's multiple comparisons test) **D**) Chao1 rarefaction analysis indicates that gut microbial community diversity for *C. difficile*-inoculated mice is low. Diversity of each sample was calculated by averaging 10 rarefactions taken at a depth of 11,500 sequences. For comparison, community diversity in untreated mice (no antibiotics and not inoculated with *C. albicans* or *C. difficile*) is shown (Grey squares). Black diamonds, PBS and *C. difficile*; open triangles, PBS, *C. albicans* and *C. difficile*; grey diamonds, IL-17A and *C. difficile.* Symbol indicates mean for mice in each group, with standard error of the mean.

Total levels of bacteria were measured using qPCR and universal 16s rRNA primers. The total number of bacteria detected per milligram of cecum sample was not significantly different between mice that received PBS versus mice that were pre-colonized with *C. albicans* (Fig. 3.4B). Cecum samples from mice that received IL-17A contained higher numbers of bacteria per milligram of cecum sample in comparison to mice receiving only PBS (Fig. 3.4B; geometric mean for IL-17A treated mice 5-fold higher than PBS-treated mice; p=0.0385, ANOVA with Tukey's multiple comparisons test, using log transformed data).

To test for possible differences in specific genera within the microbiota between groups, we compared the relative abundance of bacterial genera, normalized to the total level of bacteria per milligram of cecum sample. Normalization was used to account for differences in the total levels of bacteria per mg of sample. All bacterial genera with a median fraction greater than 0 in at least one of the three groups were included in order to identify the consistently observed genera. These mice had received multiple antibiotic treatments and were infected with *C. difficile*, and they were colonized with relatively few genera. We detected a total of 67 genera and 28 exhibited a median greater than 0 in at least one group.

The normalized abundance of the 28 genera was compared between Cd-challenged mice with or without *C. albicans* or IL-17A using the Kruskal-Wallis nonparametric test followed by Dunn's multiple comparisons test. Of the 28 genera that met the criterion for analysis, 7 exhibited a statistically significant difference between at least two of the three experimental groups (Fig. 4.4C). These included the abundant genera *Akkermansia sp.* (phylum *Verrucomicrobia*) and *Sutterella sp.* (phylum *Proteobacteria*) and the relatively rare genera *Bifidobacterium sp.* (phylum *Actinobacteria*), *Adlercreutzia sp.* (phylum *Actinobacteria*), and unidentified genera within the family *Comamonadaceae* (phylum *Proteobacteria*), the family *Erysipelotrichaceae* (phylum *Firmicutes*) and the family *S24-7* (phylum *Bacteroidetes*).

To detect a possible effect of *C. albicans* or IL-17A on the relative abundance of rare taxa, we measured community diversity using the Chao1 estimator (Fig. 4.4D). The microbiota of Cd-challenged mice exhibited relatively low diversity in comparison to mice not treated with antibiotics or microbes, consistent with previous results[254–256], and

this decrease was statistically significant. However, the microbiota of mice that were more likely to survive *C. difficile* challenge (*C. albicans* precolonized or IL-17A treated) did not exhibit increased diversity in comparison to the highly susceptible, antibiotic-treated infected mice using the Chao1 or other measures (Fig. 4.4D; Simpson index and Shannon index shown in Fig. 6.8). The above results showed that the communities present in *C. difficile*-challenged mice with or without *C. albicans* or IL-17A exhibited some differences in composition and overall low diversity.

To summarize, the results of this study demonstrate that increased levels of IL-17A were protective against CDI and that *C. albicans* pre-colonization enhanced expression of IL-17A following *C. difficile* challenge. Differences in microbiota composition or amounts were detected in association with *C. albicans* colonization or IL-17A administration and might also play a role in protection. Thus, *C. albicans* pre-colonization altered the GI tract ecosystem, leading to reduced susceptibility to *C. difficile* challenge.

3.4 Discussion

The results of this study demonstrated significant attenuation of lethal murine CDI conferred by pre-colonization with the commensal fungus *C. albicans*. Previous studies have shown that bacterial microbiota influence susceptibility to CDI by affecting the metabolism of bile acids that serve as spore germinants[234] and by increasing colonization resistance[38,257]. By contrast, the protective effect of *C. albicans* did not alter growth of *C. difficile* in the GI tract or the production of *C. difficile* toxin. Thus, *C. albicans* protects against lethal murine CDI through a mechanism other than colonization resistance.

The results reported here used an experimental mouse model to demonstrate protection against lethal CDI due to *C. albicans* colonization. Some evidence suggestive of a protective effect of *Candida* colonization against CDI has been observed in humans. Manian and Bryant found that only 10 of 60 patients with CDI (16.7%) were colonized with high levels of *Candida* spp., statistically significantly different from the rate in patients who tested negative for CDI (30.5%)[50]. Similarly low frequencies of *Candida* colonization in CDI patients were observed by Nerandzic et al. (16%) [258]and Blanco et al. (18%)[51]. Interestingly, Blanco et al. observed that CDI patients who carried the hypervirulent *C. difficile* 027 ribotype were more likely than patients carrying other ribotypes to exhibit high level *C. albicans* colonization[51]. This observation may reflect the association between high level *Candida* colonization and situations that produce higher levels of inflammation[21]. In another study, recent antifungal use (within 6 weeks) was found to be a risk factor for CDI[259]. Perhaps related, administration of the probiotic yeast, *Saccharomyces boulardii,* to human patients has also shown some efficacy in ameliorating symptoms of CDI[260–262]. Combined, the observations from these studies are consistent with fungal colonization being protective against CDI. However, one investigation of CDI and *Candida* colonization contradicts this showing a significant correlation between CDI and *Candida* colonization[52]. Since the histories of the patients in the various studies are not identical, other variables may have contributed to the finding of a correlation between CDI and *Candida* colonization in the latter study. Our results are consistent with those human studies in which fungal colonization appears to protect against symptomatic CDI and support a role for *C. albicans* in altering the intestinal environment and preventing the most serious consequences of *C. difficile* infection.

Pre-colonization with *C. albicans* had multiple effects on the GI tract ecosystem. Pre-colonized mice exhibited higher IL-17A expression in the colon both before and after challenge with *C. difficile,* demonstrating that the activities of the host were altered. Further, we demonstrated that direct administration of IL-17A resulted in reduced lethality following challenge with *C. difficile* spores. Despite the strong effect of IL-17A administration seen in these studies, loss of IL-17 does not exacerbate CDI; an IL-17A IL-17F double null mutant mouse exhibits normal (or even slightly reduced) susceptibility to CDI[263]. These results suggest that high levels of IL-17A as a result of administration can improve host resistance but that basal levels of IL-17A are dispensable.

In contrast, cytokine IL-22 is necessary for normal susceptibility to CDI; IL-22-deficient mice are highly susceptible to lethal infection by *C. difficile*[264]. IL-27 receptor deficient mice also exhibit high susceptibility to CDI[265]. Further, administration of either IL-27 or IL-25 increases resistance of mice to lethal CDI[265,266]. These cytokines likely have related but not identical effects. In the absence of IL-17, the functions of other cytokines may compensate for the lack of IL-17.

IL-17 has a well-known role in promoting inflammation. IL-17 stimulates the recruitment of neutrophils to the site of inflammation[267] and is involved in neutrophil recruitment during CDI[263]. In addition, IL-17 plays a role in promoting the repair of epithelia. IL-17A deficient mice exhibit enhanced intestinal permeability and mislocalization of the tight junction protein occludin after treatment with dextran sodium sulfate (DSS)[268]. Either or both of these effects, enhancing neutrophil recruitment or repair processes, might contribute to attenuation of *C. difficile* infection.

We explored potential differences in the bacterial microbiota in the different groups of mice because alterations in bacterial microbiota increase susceptibility to CDI. Our results do not exclude a role for the bacterial microbiota in the protection from lethal CDI seen with *C. albicans* pre-colonization. However, we did not observe a major shift in gut bacterial microbiota in the different groups of mice. Pre-colonized mice did exhibit statistically significantly increased abundance of two bacterial genera, *Bifidobacterium* and *Akkermansia,* both of which are associated with beneficial effects on mammalian host health. Probiotic strains of *Bifidobacterium sp.* have been shown to decrease inflammation, protect against infection by intestinal pathogens and improve gut mucosa integrity in various mouse models[269–273]. *Akkermansia sp.* are mucin-degrading bacteria and a member of the normal human gut microbiota[274]. Gastrointestinal pre-colonization with *Akkermansia sp*. can decrease colonic inflammation and tissue damage[275], improve gut barrier function[276] and promote immune tolerance[277]. It is possible that the increased abundance of these two bacterial genera in the *C. albicans*-pre-colonized mice might contribute to the protective effects of *C. albicans* pre-colonization against *C. difficile* infection. These genera did not exhibit increased abundance in IL-17A-treated mice; *Bifidobacterium* and *Akkermansia* may be less important for protection when IL-17A is administered.

Finally, *C. albicans* promotes the ability of *C. difficile* to grow in aerobic conditions in the laboratory[278]. Thus, there may be direct effects of *C. albicans* on the growth of *C. difficile* in the GI tract. Attenuation of disease likely resulted from these multiple effects of *C. albicans* colonization on the GI tract ecosystem. Taken together, the results of this study establish a new facet of *C. albicans*-host interaction,

demonstrating that this fungal organism, a common colonizer of humans, can have a beneficial effect on the host through increased survival of CDI.

3.5 Chapter 3 contributions

Mouse experiments were carried out by Carol Kumamoto (survival data shown in Figure 3.1). Other authors performed toxin assay and measured CFU (data shown in Figure 3.2). I isolated RNA from colon tissue samples collected from those experiments and used qPCR to measure gene expression (Figure 3.3). The Phoenix Lab (Tufts Medical Center) extracted DNA and generated Illumina library to sequence the microbiota. I analyzed 16s rRNA DNA microbiota data used for analysis shown in Figure 3.4.

Chapter 4 Characterization of microbiome stability and resilience using composition-independent analyses demonstrated the ability of the fungus Candida albicans to alter the bacterial microbiota ecosystem[3]

[3] Markey, Laura, Richard Lavin, Antonia Pugliese, Theresa Tian, Carolina Chung, Kyongbum Lee and Carol Kumamoto. "Characterization of microbiome stability and resilience using composition-independent analyses demonstrated the ability of the fungus *Candida albicans* to alter the bacterial microbiota ecosystem" To be submitted to mBio

4.1 Introduction

The bacterial gut microbiota is a complex microbial community made up of hundreds of bacterial species. Studies have found that the composition of the gut microbiota can vary widely from person to person but generally fulfills similar key metabolic functions regardless of the identity of the species present[53]. Humans are colonized shortly after birth with a simple community, which then develops into the mature gut microbiota of adults by age one or two. During this period of acquisition, the community shifts in response to exposure to additional microbes with the introduction of solid foods as well as illness and exposure to antibiotics[54]. Once matured, the gut microbiota of an adult is generally stable[55], although its composition can still be shifted by radical changes in diet or exposure to antibiotics[56]. The process of acquisition, as well as the stability and diversity of the mature community, are likely regulated by interactions between bacterial species as well as collective interactions with the host. These interactions, during acquisition as well as during apparent equilibrium, remain largely uncharacterized and could be key to our understanding of what makes a "normal" microbiota beneficial to the host.

Although the role of individual bacterial species in affecting host health is largely unknown, overall diversity of the community is associated with improved human health[57,58] and with protection from severe gastrointestinal pathogens such as *C. difficile*[59]. Diversity is thus an important emergent property of the microbiota. The goal of this study was to define another characteristic of the microbiota by measuring the overall response of the microbiota to perturbation with antibiotics, as a functional readout of microbiota "health"; i.e. how well is the community able to withstand and recover

from disruption? These qualities fit the ecological definition of resilience, the ability of a system to persist in the face of changes in the environment and stability, the ability of a disrupted system to return to an equilibrium state[60].

The effect of the common commensal fungus, *Candida albicans*, on the bacterial gut microbiota and on host health in general remains largely unknown. Previous studies have demonstrated both beneficial immune priming that protects the murine host from infectious disease[18,19], and detrimental immune stimulation in rodent models of inflammatory bowel disease[23–25]. Other researchers have also demonstrated that *C. albicans* can alter the composition and diversity of the gut microbiota. They demonstrated separation between gut microbiota populations in mice colonized and not colonized with *C. albicans* (beta diversity) and specifically found that colonization with *C. albicans* inhibited recovery of *Lactobacillus sp.* and promoted recovery of *Enterococcus sp.*[64] These results indicated that *C. albicans* can affect how the gut microbiota recovers from antibiotic treatment. In order to determine the role *C. albicans* could play in modulating emergent properties of the gut microbiota we compared the gut microbiota community response to clindamycin challenge with or without *C. albicans* present in the gut and quantified microbiota resilience and stability.

4.2 Methods

4.2.1 Animal housing and antibiotic treatment

Five-week-old female C57BL/6 mice (Jackson Laboratory) were cohoused in a large cage (24”x17”) to standardize gut microbiota by coprophagy for nine days. Mice were then treated with cefoperazone (Sigma Aldrich, 0.5g/L) in drinking water for ten days to reduce the gut microbiota, then were switched to sterile water to allow the

microbiota to recover for three weeks. All mice were confirmed negative for cultivable fungi at this point by plating fecal pellet homogenates in PBS on YPD-SA agar ((YPD agar plus 100 μg/ml streptomycin (Sigma S6501) and 50 μg/ml ampicillin (Sigma A9518)) and incubating plates at 37C. After recovery from cefoperazone, mice were split into standard cages and given a single intraperitoneal injection of clindamycin (Sigma Aldrich, 1.11mg/kg, 3.33 mg/kg or 10mg/kg). In some cohorts, mice were sacrificed one day after clindamycin challenge. In other experimental cohorts, mice were then maintained on sterile food/water for up to 7 days. Fecal pellets were collected three days and one day prior to clindamycin injection as well as periodically after clindamycin injection (Day 1, 3, 5) and the bacterial microbiota was sequenced from fecal pellet samples.

All experiments were done in compliance with Tufts University IACUC guidelines.

4.2.2 Strains and growth conditions

C. albicans strain CKY101, a derivative of the sequenced strain SC5314, was used for all experiments. For preparation of mouse inoculum, cells were grown at 37°C in YPD (1% yeast extract (BD), 2% peptone (Difco) 2% glucose (Sigma Aldrich)) for 24 hours. They were then washed twice with sterile PBS (phosphate-buffered saline) and resuspended in 2% sucrose solution at a concentration of $2x10^9$ cells/ml. 25μl ($5x10^7$ cells) of this cell suspension was fed to mice for gastrointestinal colonization.

4.2.3 GI colonization with *C. albicans*

In two experiments, after the ten days of cefoperazone treatment, half of the mice were given a single oral inoculation of *C. albicans* ($5x10^7$ CFUS in 25ul) or were not inoculated, and then switched to sterile drinking water. C. albicans-colonized mice were

cohoused in one large cage and uncolonized mice were cohoused in a second large cage. Over the following three weeks, the gut microbiota recovered from cefoperazone treatment. *C. albicans* colonization was measured over time by sterilely collecting fecal pellets in PBS and plating homogenates on YPD-SA. Clindamycin was administered and fecal pellets collected as above.

4.2.4 Microbiota analysis

Microbial DNA was extracted using the QIAamp DNA Stool Mini Kit (Qiagen) with an additional beadbeating step. Briefly, cecum samples were lysed by beadbeating in Qiagen lysis buffer ASL, and the lysate was treated with InhibitEX tablets followed by enzymatic digestion with proteinase K (20mg/ml) and RNaseA (1mg/ml) and column DNA purification.

Libraries were prepared from each sample and sequenced as described[174]. Briefly, PCR amplification of the V4 region of the 16S rRNA gene was performed with primers that included adapters for Illumina sequencing and twelve base barcodes. Two hundred fifty bp paired-end sequencing was performed using an Illumina MiSeq. Base calling was performed using CASAVA 1.8 and the resulting fastq files were used as input for downstream analysis using QIIME (1.8.0)[175]. Briefly, the paired-end reads from the fastq files were joined, barcodes extracted and then demultiplexed. The operational taxonomic units (OTUs) were determined using a closed reference approach by aligning reads to the Greengenes Database (version 13_8) at 99% identity. The Greengenes phylogenetic tree was used to define the phylogenetic relationship between OTUs. The resultant OTU tables contained the relative abundance of bacterial taxa in each sample. These tables were used to calculate overall (alpha) diversity within each sample. To

compare the composition and diversity of samples to each other taking into account phylogenetic relatedness, the OTU tables were used to calculate the unweighted UniFrac distance matrix, which was summarized with Principal Coordinate Analysis.

Total amount of bacterial DNA per sample was measured by qPCR using eubacterial primers. qPCR reactions were conducted using SYBR Green PCR Master Mix (Applied Biosystems) and a LightCycler 480 II (Roche) instrument. Normalized abundance of bacterial genera was calculated by multiplying the fraction of total reads for a genus by the total level of bacteria per mg of fecal pellet sample (in arbitrary units). Fold change in absolute abundance was calculated by comparing the absolute abundance on day 1 after clindamycin treatment to the absolute abundance on day -1 prior to treatment. Genera that were detected on day -1 but not on day 1 were included as a genus that decreased by >10-fold. The percentage of genera decreased by 10-fold or more was calculated by dividing the number of genera whose absolute abundance decreased by 10-fold or more by the total number of genera present prior to clindamycin treatment, multiplied by 100. Genera with a median absolute abundance <0 in the pre-clindamycin microbiota samples were not included in the analysis.

4.3 Results

4.3.1 Gut microbiota response to clindamycin treatment revealed resilience threshold

One goal of this work was to determine the effect of *C. albicans* colonization on resilience and stability. We used an antibiotic pre-treatment model that reduces the gut microbiota sufficiently to allow *C. albicans* to stably colonize for several weeks. To this end, mice were given cefoperazone in drinking water for ten days and then the bacterial community allowed to recover for three weeks in the absence of antibiotics either with or

without *C. albicans*. We collected fecal pellets three days and one day prior to clindamycin treatment and sequenced the microbiota and found that after the three-week recovery period the microbiota is no longer changing significantly from day to day. We used standard alpha diversity metrics to quantify the average diversity of the microbiota one day and three days prior to clindamycin treatment, and noted very little change in diversity or composition (Fig. 6.9) between these two timepoints, indicating a stable community. This temporal stability was not affected by *C. albicans* colonization.

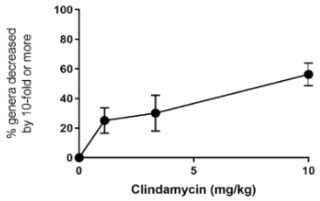

Figure 4.1: Percent of genera decreased after clindamycin demonstrate resilience threshold. The fecal pellet microbiota of mice was sequenced before and after treatment with clindamycin. Mice received either vehicle, low (1.11mg/kg), intermediate (3.33mg/kg) or a high (10mg/kg) dose of clindamycin by intraperitoneal injection. The fold change in absolute abundance was calculated for each mouse microbiota and averaged per clindamycin treatment group. Figure shows the average number of genera that decreased by 10-fold or more in mice treated with each dose of clindamycin. Symbols indicate the average of an experimental group in all cohorts, error bars indicate the standard deviation.

We then administered a single intraperitoneal dose of the antibiotic clindamycin (at high, intermediate and low concentrations) to these mice to assess the ability of this microbial community to resist acute antibiotic disruption. The highest concentration, 10mg/kg, was chosen because this dose of clindamycin renders mice susceptible to *C. difficile* infection, indicating that the microbiota loses one of its functional properties. Two lower doses were used to determine whether any amount of clindamycin was sufficient for disruption, or whether the microbiota would respond differentially to different degrees of challenge.

The response of the microbiota in the absence of *C. albicans* was analyzed first. We used absolute abundance rather than relative abundance to report change in each individual genus in response to clindamycin, rather than the response of the individual genus relative to the microbiota as a whole. We calculated fold change individually, by comparing the absolute abundance of a genus in the microbiota of a mouse before and after clindamycin treatment. We then averaged the fold-change of each genus in each clindamycin concentration treatment group within a cohort, then calculated the percentage of genera that decreased 10-fold or more for each treatment group per cohort. The figure displays the average and standard deviation percent genera decreased 10-fold or more of five cohorts. We observed a dose-dependent response in the percent genera that decreased by 10-fold or more after clindamycin treatment, and noted that this dose-dependency revealed a threshold for disruption (Fig. 4.1). In mice subjected to the low (1.11mg/kg) or intermediate (3.33mg/kg) doses of clindamycin, approximately a third of the genera decreased by 10-fold or more, compared to the 60% of genera that decreased by 10-fold or more in mice given the high (10mg/kg) dose. These results indicate that the gut microbiota was able to withstand up to the intermediate dose of clindamycin with minimal disruption, but once the dose of antibiotic reaches a threshold level the majority of the community members were substantially affected and decreased in absolute abundance by 10-fold or more.

The average results reported above reflect a common dose-dependent threshold response to clindamycin observed individually in each of the five cohorts. These

experiments took place across several years and seasons and have distinctly different starting compositions.

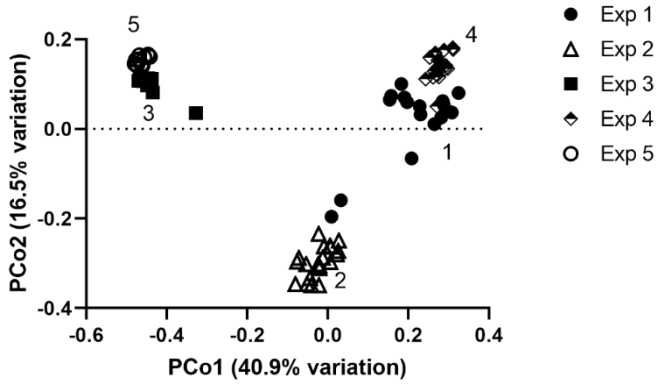

Figure 4.2: Beta diversity of pre-clindamycin microbiota for all experimental cohorts. This figure displays principal coordinates analysis of unweighted UniFrac scores of the pre-clindamycin (day -1) microbiota of mice from the five cohorts included in these experiments. All mice received the antibiotic cefoperazone in drinking water for ten days, then the antiobiotic was removed and the microbiota recovered for three weeks. Each symbol represents the microbiota of a mouse, and shapes indicate experimental cohort. Exp 1 N=12; Exp 2 N=15; Exp 3 N=9; Exp 4 N=23; Exp 5 N=11

We performed principal coordinates analysis using the unweighted UniFrac metric of the day -1 microbiota composition and observed significant separation between some of the populations based on experimental cohort (Fig. 4.2). Despite these differences in starting composition, the dose-dependent response to clindamycin in percent genera decreased by 10-fold or more is consistent across cohorts (Fig. 4.1), suggesting that this is a composition-independent property of the gut microbiota.

4.3.2 *C. albicans* colonization decreased diversity and stability of the gut microbiota

Previous studies have demonstrated that ten days of cefoperazone treatment are sufficient to decrease the bacterial microbiota and allow *C. albicans* to stably colonize for several weeks[18,64]. We performed two experiments to investigate the effect of *C.*

albicans colonization of bacterial microbiota sensitivity of clindamycin. After cefoperazone treatment, half of the mice in a cohort were inoculated with *C. albicans* and half of the mice remained uncolonized. In order to limit cage effects on bacterial microbiota composition, we continued to cohouse all of the uncolonized mice in one large cage and all of the *C. albicans*-colonized mice in a cohort in a second large cage. Throughout the three weeks of recovery from cefoperazone and *C. albicans* colonization, we collected fecal pellets from both groups of mice and plated homogenates on YPD-SA. Uncolonized mice did not have any culturable fungi recovered in their fecal pellets and *C. albicans*-colonized mice remained colonized throughout the experiment. As above, at the end of three weeks fecal pellets were collected one day prior to clindamycin treatment and one day after clindamycin (various concentrations) treatment and the bacterial microbiota of these samples was sequenced.

Prior to clindamycin treatment, *C. albicans* colonization did not have a significant effect on the abundance of any single bacteria genus (Fig. 6.13) Prior to clindamycin treatment (day -1), the *C. albicans*-containing microbiota had significantly decreased alpha diversity compared to the microbiota of the uncolonized mice (Fig 4.3). One measure of alpha diversity, the total number of different OTUs detected per sample (Fig. 4.3A) is a measure of species richness, but that does not take into account relative abundance or phylogenetic relatedness. The average total OTUS was decreased in the bacterial microbiota of *C. albicans*-colonized mice. The Simpson index (Fig. 4.3B) measures both richness (number of species) and evenness (abundance of each species compared to total abundance) and the Simpson index of diversity was also significantly decreased in the *C. albicans*-colonized mice. Finally, Faith's Phylogenetic Diversity

(Fig. 4.3C) accounts for both the number of species and their phylogenetic relatedness, such that the addition of a genetically disparate species contributes more to the overall diversity score than would the addition of a highly related species. This metric was also decreased in the *C. albicans*-colonized mice. Together these results demonstrate that the *C. albicans*-containing gut microbiota had significantly reduced richness and phylogenetic diversity, prior to clindamycin disruption.

We then measured the response of the microbiota to perturbation with high, intermediate and low doses of clindamycin as described above. The microbiota of mice carrying the less diverse *C. albicans*-containing community demonstrated a decrease in resilience threshold.

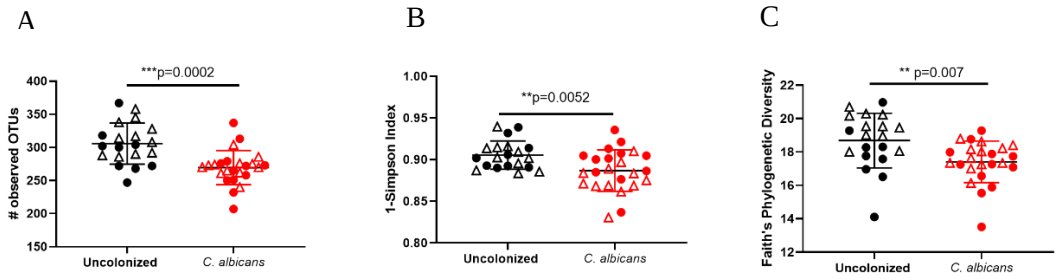

Figure 4.3: Three weeks of *C. albicans* colonization decreased microbiota alpha diversity. Mice were given cefoperazone in drinking water for ten days, then half of the cohort was colonized with C. albicans and the other half remained uncolonized. The microbiota then recovered for three weeks. The microbiota was sequenced from fecal pellet samples collected one day prior to clindamycin treatment. Three different metrics were used to quantify diversity (A, total number of OTUS per sample; B, the inverse of the Simpson Index score for each sample and C, Faith's phylogenetic diversity score for each sample) and each symbol represents a mouse microbiota pre-clindamycin treatment. Different shapes indicate different experimental cohorts, later referred to as Exp 3 and Exp 5. Red symbols indicate *C. albicans*-colonization. Mean and standard deviation are displayed as line and error bars. Welch's t-test to correct for different distributions was used, with $p<0.05$ considered significant. Uncolonized N=20, *C. albicans*-colonized N=24

Unlike the uncolonized mice (Fig. 4.4, black circles) the microbiota of mice colonized with C. albicans (Fig. 4.4, red triangles) was maximally disrupted following

administration of the intermediate dose of clindamycin. We observed a 10-fold or greater decrease in the majority of genera present in the *C. albicans* -colonized mice, compared

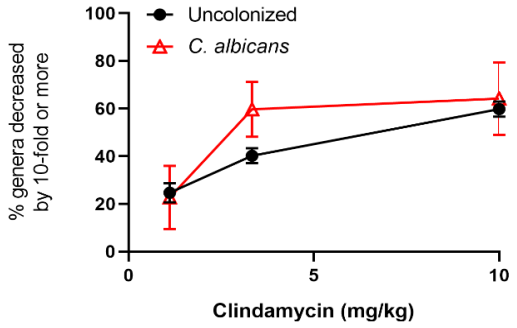

Figure 4.4: *C. albicans* colonization for three weeks decreases the clindamycin dose threshold for disruption. The absolute abundance of genera was compared before and after clindamycin treatment to calculate fold change in each microbiota. The percentage of genera that decreased by 10-fold or more in each experimental group was averaged. Symbols indicate the average of two cohorts, bars indicate standard deviation. Uncolonized: 1.11mg/kg N=6; 3.33mg/kg N=7; 10mg/kg N=7. *C. albicans* N=8 for all groups.

to the uncolonized mice in which we observed this decrease in less than 40% of their genera. These results demonstrate that changing the starting microbiota with the addition of the commensal fungus *C. albicans* altered a functional property of the community and resulted in decreased ability to resist antibiotic disruption.

4.3.3 Post-clindamycin microbiota response demonstrates community stability

One aspect of stability is the ability of a community to recover from perturbation and return to the pre-perturbation stable state. The metric described above allowed us to quantify the immediate response of the microbiota to clindamycin perturbation by sequencing the fecal pellet microbiota one day after clindamycin treatment. To characterize the kinetics of recovery from clindamycin disruption, we collected fecal

pellets from mice one, three and five days after administration of high, intermediate and low doses of clindamycin and sequenced the microbiota from these samples. We could then investigate whether there was a dose-dependent effect of clindamycin on the speed and completeness of recovery of microbiota diversity, and whether *C. albicans* colonization affected the kinetics of bacterial microbiota recovery. We used standard alpha diversity metrics to measure overall diversity of the microbiota of mice after one, three and five days of recovery from clindamycin treatment. Although there were differences in the degree of microbiota change over time depending on the metric chosen, the following patterns held true for all three metrics. Results shown below demonstrate the ability of the bacterial microbiota (mice not colonized with *C. albicans*) to rebound in diversity after perturbation.

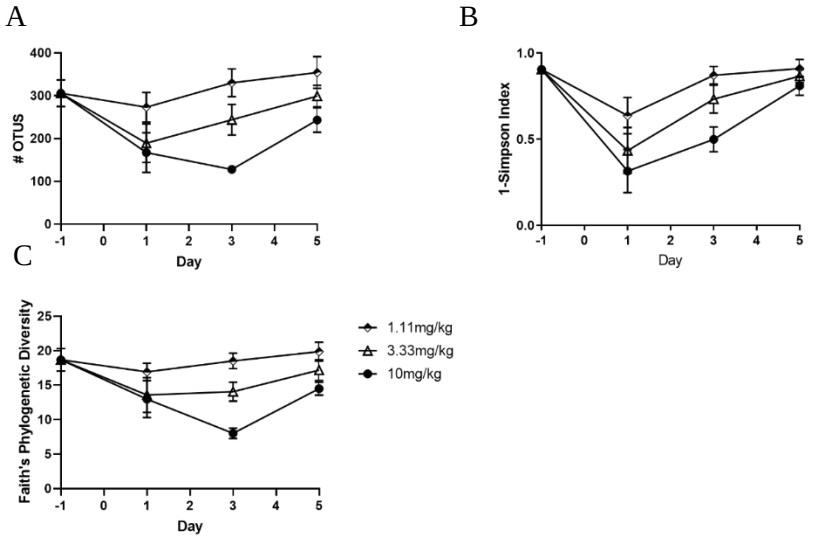

Figure 4.5: Gut microbiota rapidly recovers from clindamycin disruption. The microbiota of mice was sequenced prior to clindamycin treatment (day-1) and at three timepoints after clindamycin treatment. At each timepoint we assessed the diversity of the microbiota using three indices (A, B, C) of alpha diversity. Symbols indicate the average diversity of the experimental group (dose/day), error bars indicate the standard deviation. N=22 for all dosage groups, from five experimental cohorts.

On day one post-clindamycin administration, there was a dose-dependent decrease in diversity (Fig. 4.5) as we would expect based on the percentage genera lost (Fig 4.1). On day three post-clindamycin we observed that microbiota diversity of mice given the low dose of clindamycin recovered significantly while microbiota diversity of mice given the intermediate or high doses of clindamycin remained lower than their starting point in a dose-dependent manner.

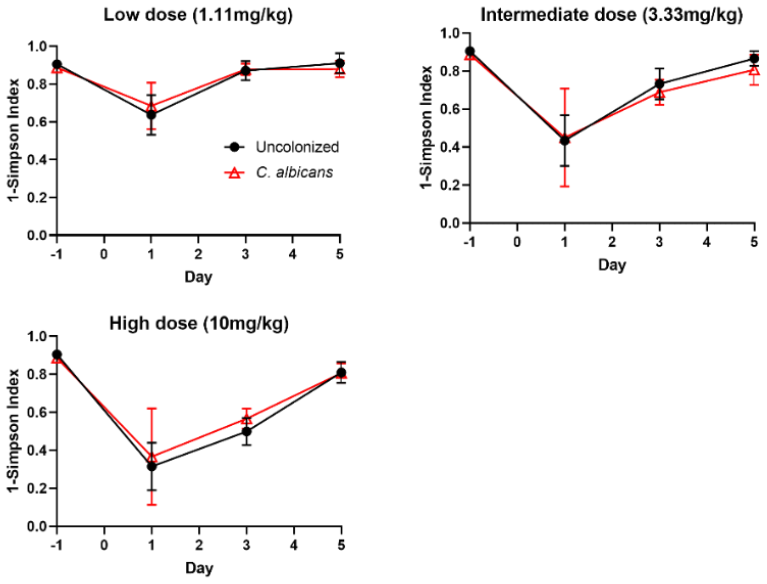

Figure 4.6: *C. albicans* colonization does not alter the diversity after clindamycin disruption. This figure shows the inverse Simpson index, separated by concentration of clindamycin given, of the microbiota of uncolonized and *C. albicans*-colonized mice over time. The symbols indicate average diversity, error bars show the standard deviation. Uncolonized: 1.11mg/kg N=6; 3.33mg/kg N=7; 10mg/kg N=7. *C. albicans* N=8 for all groups.

Microbiota diversity as measured by Simpson Index was indistinguishable from that prior to clindamycin treatment by day five from all experimental groups indicating that the starting gut microbiota is exhibits ecological stability (Fig 4.5). Other metrics showed significant rebound in intermediate and high doses and by day five post-clindamcyin

were not statistically significantly different from the starting microbiota diversity. These results indicate that the concentration of clindamycin given and thus degree of perturbation affects the time-scale of microbiota rebound in a dose-dependent fashion , but ultimately even the maximally disrupted microbiota of the high dose mice was still able to recover fully from disruption. Despite the decreased alpha diversity of the pre-clindamycin *C. albicans*-containing microbiota (Fig 4.3), alpha diversity after clindamycin treatment was comparable in the *C. albicans*-colonized and uncolonized mice. We observed a dose-dependent decrease in diversity followed by rebound on days one and three post-clindamcyin administration and complete recovery of diversity by day

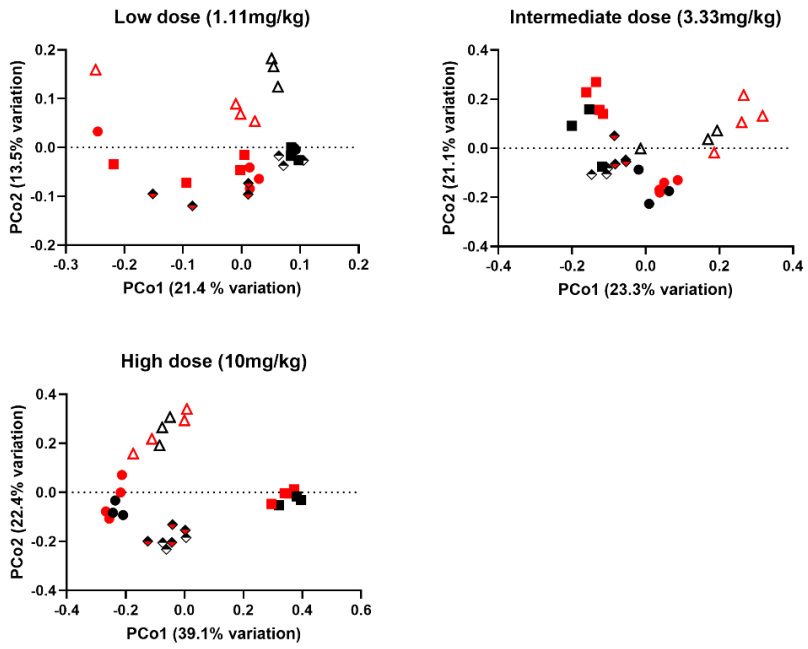

Figure 4.7: Both uncolonized and *C. albicans*-colonized microbiota exhibit stability and resilience in response to clindamycin. The microbiota of uncolonized and *C. albicans*-colonized mice was sequenced one, three and five days after clindamycin disruption. Beta diversity analysis using unweighted UniFrac as a metric for phylogenetic distance was used to analyze change in microbiota composition and beta diversity over time. Symbol shape indicates days post-clindamycin; black symbols represent uncolonized mice, red symbols represent *C. albicans*-colonized mice.

five (Fig. 4.6, Simpson Index, Fig. 6.10 additional metrics). These results indicate that although *C. albicans* decreased the diversity of the microbiota after three weeks of recovery from cefoperazone with *C. albicans* present, it did not affect the acute recovery of the microbiota from clindamycin disruption.

In addition to measuring alpha diversity and percentage genera decreased, we also used unweighted UniFrac distance and principal coordinates analysis to assess the effect of *C. albicans* colonization and clindamycin disruption on beta diversity, the phylogenetic distance between different groups. Prior to clindamycin treatment, we found that in one cohort *C. albicans* colonization had a strong effect on beta diversity, leading to significant separation between the communities while in another cohort *C. albicans* colonization had minimal impact on beta diversity (Fig. 6.11). Despite this variability in the effect of *C. albicans* on the pre-clindamycin composition, changes in beta diversity in response to clindamycin disruption were consistent between both cohorts and demonstrate similar recovery and resilience observed in the alpha diversity metrics. For clarity, only one experiment is shown in Fig. 4.7; additional beta diversity analysis is included in the supplement (Fig. 6.12).

At all doses, we observed separation between the starting microbiota (circles) and the day one post-clindamycin microbiota (triangles) (Fig. 4.7). The microbiota of mice given the lowest dose of clindamycin recovered fully by day three, such that the day three community (squares) overlaps with the starting community, as does the day five community (diamonds). The microbiota disrupted with the intermediate dose is still separate on day three, but largely returned to the pre-clindamycin state by day five. The microbiota disrupted with the high dose did not return to the pre-clindamycin state

although there is less separation on day five than on day three. These results suggest that there may be a threshold dose of clindamycin for microbiota stability, such that at the lowest dose the microbiota can rebound fully to the pre-clindamycin state, but higher doses of clindamycin disrupt the community sufficiently to prevent it from reaching the same starting state, although the community does reach an alternate state with comparable diversity.

C. albicans colonization did not have a strong effect on stability as quantified by beta diversity. There was some separation between populations based on the presence of *C. albicans* (red symbols), but the degree of separation based on dosage and day of recovery was unchanged. As seen in the uncolonized mice, the *C. albicans*-containing microbiota was stable at the low dose, and less stable at the intermediate and high doses.

4.4 Discussion

The model used in this study allowed us to examine the effect of long-term *C. albicans* colonization on the composition and diversity of the bacterial gut microbiota, as well as assess its effect on a functional property of the microbiota: the ability to respond to antibiotic disruption. Our initial studies in the absence of C. *albicans* colonization were used to characterize the bacterial microbiota ecosystem in our experimental model. We demonstrated that the response to clindamycin fits a discontinuous threshold model in which the majority of genera are maintained at low and intermediate doses of clindamycin, but decrease substantially when exposed to a high dose of clindamycin. We also showed that the bacterial microbiota in our system demonstrated community stability and could recover rapidly after the disruptive pressure of clindamycin was relieved (five day wash-out period) although it was unclear as to whether the community that recovers

from intermediate and high doses of clindamycin has returned to the starting state or has achieved an alternate yet equally diverse state.

Previous studies that analyzed the ability of the bacterial microbiota to recover from antibiotic treatment found that the microbiota remained significantly different from the starting community in diversity and composition three months after disruption, implying that disruption of the microbiota can prevent the community from returning to its baseline structure. The incomplete resilience of the microbiota in response to clindamycin in our study similarly demonstrated that it is possible to disrupt the microbial community to the point that it cannot rebound to the previous state, but instead finds a new, equally diverse, set-point. In a clinical setting, the human gut microbiota has been largely stable, whether healthy or dysbiotic, which limits the ability to improve health by changing the gut microbiota. This study implies that a sufficient degree of disruption, or perhaps disruption of specific groups, can result in the community being unable to return to baseline, healthy or otherwise. Additional work to define the stability threshold and identify aspects of the community that are lost above that threshold, but maintained below it would provide insight into requirements for microbiota stability.

Although *C. albicans* colonization did not have a strong effect on the abundance of any single genus of bacteria (Fig. 6.13), *C. albicans* colonization affected some of these properties of the microbiota. *C. albicans* reproducibly decreased overall diversity of the bacterial microbiota. In some mice, the presence of *C. albicans* also substantially changed community composition and phylogenetic diversity, such that substantial separation was observed between the pre-disruption populations as a consequence of *C. albicans* colonization. *C. albicans* also affected the threshold stability of the bacterial

microbiota, as this less diverse community was more susceptible to disruption at the intermediate dose of clindamycin. Colonization with *C. albicans* thus had a significant impact on these emergent properties of the microbiota.

The ability of *C. albicans* to stably alter the gut microbiota and affect its response to antibiotic perturbation demonstrates that long-term change of the microbial community as a whole through the addition of a commensal microbe is possible. Previous studies have characterized direct antagonistic interactions between *Lactobacillus sp*. and *C. albicans* in the GI tract, as well as observed correlations between the abundance of *C. albicans* and the abundance of bacterial families *Enterococcaceae* and *Lachnospiraceae*. In our study, *C. albicans* did not significantly alter the abundance of any particular bacterial species or taxonomic group but did impact properties of the community as a whole. It is possible that *C. albicans* altered the bacterial microbiota indirectly by stimulating the host local immune environment which could then shape the bacterial microbiota. *C. albicans* could also have changed the metabolites available to the bacterial microbiota, by adding nutrients to the gut milieu such as yeast cell wall-derived glucans, or by limiting nutrients available to bacteria due to *C. albicans* consumption. Additional studies to characterize *C. albicans*-bacteria interactions in the context of the host GI tract would improve our understanding of this complex ecosystem, especially now that we have identified *C. albicans* as a factor that can alter bacterial microbiota stability.

The bacterial microbiota is a complex ecosystem integral to human health. We have demonstrated the sensitivity and stability of this system and shown that one emergent quality of it can be changed through the addition of a single commensal

microbe, *C. albicans*. By better understanding the factors that drive diversity, stability, resilience and define the shape of the microbiota, we can better manipulate it to achieve long-lasting improvement in host health.

4.5 Chapter 4 contributions

Richard Lavin, Antonia Pugliese, Carolina Chung and Theresa Tian each performed a mouse experiment in which they collected fecal pellet samples and sacrificed mice. Fecal pellet samples were processed by the Phoenix Lab which extracted DNA and prepared Illumina libraries for sequencing. I performed all analysis of 16s rRNA DNA microbiota data (using standard QIIME analysis pipeline) which was used to generate the figures included in this manuscript.

Chapter 5 Discussion

5.1 *C. albicans* modulation of endocannabinoid system is a novel way for the microbiota to affect neuroendocrine health

We demonstrated that the *C. albicans*-colonized mice have increased anxiety-like behavior and increased basal CORT. These neuroendocrine phenotypes are both regulated by signaling through the endocannabinoid system (ECS), as signaling through CB1 via AEA or 2-AG limits neurotransmitter release within neurons that have been shown to regulate both CRH release (upstream of basal CORT) and anxiety-like behavior. We showed that increasing CB1 signaling by elevating AEA levels throughout the host through treatment with the FAAH inhibitor URB597 was sufficient to decrease basal CORT to normal levels in the *C. albicans*-colonized mice. Treatment with the peripherally-restricted FAAH inhibitor URB937 did not decrease basal CORT significantly in the *C. albicans*-colonized mice, indicating that an increase in brain AEA levels was required to normalize CORT regulation. Interestingly, low concentrations of both URB597 and URB937 decreased anxiety-like behavior in the *C. albicans*-colonized mice. This result indicates that peripheral CB1 signaling can affect anxiety-like behavior, which is surprising as this behavior is largely thought to involve signaling within the brain. However, another group has shown that the peripherally-restricted β-blocker sotalol is sufficient to block the increased anxiety-like behavior observed in mice treated with the CB1 antagonist rimonabant[217] and concluded that peripheral endocannabinoid signaling is involved in regulating anxiety-like behavior, consistent with the trends observed with URB937 in our study. They suggest that peripheral activation of the sympathetic nervous system (which then signals to the various brain structures previously identified as involved in anxiety-like behavior) is a key regulator of anxiety.

One reason it may be difficult to completely restore normal behavior in the *C. albicans*-colonized mice, is that other endocannabinoid compounds including oleoylethanolamide (OEA), linolenoylethanolamide (LnEA) and linoleoylethanolamide (LEA) are increased in abundance in the *C. albicans*-colonized mice, as shown in our untargeted metabolomic analysis. These compounds could increase anxiogenic endocannabinoid signaling. One aspect of the biphasic effect of pharmacological treatment with CB1 agonists such as AEA is that at high doses AEA interacts with the anxiogenic ion channel, transient receptor potential vanilloid one (TRPV1)[157,213–215] as well as with the anxiolytic CB1 receptor. At low doses, AEA largely interacts with the CB1 receptor (anxiolytic effects) but at high doses it interacts with both the CB1 and TRPV1 receptors, leading to increased anxiety at sufficiently high doses[213]. Previous *in vitro* studies have shown that the endocannabinoid compounds elevated in the *C. albicans*-colonized mice, OEA, LEA and LnEA are agonists for TRPV1 but not for CB1[155], which could alter the balance between CB1 and TRPV1 signaling in the *C. albicans*-colonized mice and contribute to the increased anxiety-like behavior observed in these mice. FAAH also degrades OEA, LnEA, and LEA, so treatment with FAAH inhibitors would be expected to increase both AEA and these other possibly anxiogenic TRPV1 agonists, which would limit the ability of FAAH inhibitors to fully normalize anxiety-like behavior.

TRPV1 signaling has also been shown to contribute to GI tract inflammation in models of DSS colitis[279,280], indicating that the increase in endocannabinoid TRPV1 agonists observed in our study in *C. albicans*-colonized mice could contribute to the exacerbated inflammation previous researchers have observed when mice with

chemically-induced colitis were colonized with *C. albicans*[25]. Gastrointestinal endocannabinoid signaling by AEA and 2-AG signaling through the receptors CB1 and CB2 has been shown to regulate multiple aspects of GI tract function, including barrier permeability, gut motility and inflammation[281–284]. Some studies have also demonstrated that the gut microbiota can modulate GI tract endocannabinoid signaling and therefore affect host health. AEA-CB1 signaling in the intestine increases permeability *in vitro*[284] and in mouse models[285] and can be modulated through changes to the gut microbiota such as antibiotic treatment[285]. A study using genetically obese mice (ob/ob) found that prebiotic diet supplementation which increased abundance of the commensal bacteria, *Akkermansia muciniphila*, decreased CB1 mRNA expression in both the colon and surrounding adipose tissue, decreased AEA levels in the adipose tissue and that these changes in the ECS correlated with decreased adipose tissue mass[72]. Our study implies that such changes of the gut endocannabinoid system can have an impact beyond the GI tract. Although these studies of the bacterial microbiota and the endocannabinoid system did not characterize the neuroendocrine implications of their microbiota and/or endocannabinoid system manipulation, based on our findings we would hypothesize that the decreased CB1 signaling in mice given the prebiotic diet would also affect host anxiety-like behavior or other emotional behaviors. Indeed, the first drug that targeted the endocannabinoid system in humans to regulate obesity, the CB1 antagonist rimonabant, was withdrawn from the market after it became clear that CB1 antagonism had severe psychiatric side-effects including increased depression[286].

The endocannabinoid 2-AG is also an agonist for CB1 but through its action at the CB2 receptor it has an opposing role to AEA in regulating intestinal permeability. The

CB2 receptor is expressed at low levels in epithelial tissue and is widely expressed on immune cells distributed through the GI tract[287]. 2-AG/CB2 signaling decreases the inflammatory state of the gut environment in various models of intestinal disease[288–290] and limits intestinal permeability[291]. As would be expected therefore, manipulations of the bacterial microbiota that increased intestinal 2-AG also improved barrier function and metabolic health. Prolonged (4 week) treatment with the commensal bacteria *Akkermansia muciniphila* increased intestinal 2-AG levels and normalized metabolic function in a mouse model for diet-induced obesity[72]. A study of the probiotic bacteria *Lactobacillus acidophilus* did not examine its effect on host metabolic health but did demonstrate that 15 days of treatment with *L. acidophilus* increased CB2 expression in the colonic epithelium[292], additional evidence that a bacterial species thought of as a beneficial for host health interacts with the ECS.

In contrast to the studies described above, we did not identify a significant effect of *C. albicans* colonization on inflammatory state or permeability of the GI tract based on qPCR analysis of large and small intestine tissues to quantify expression of inflammatory cytokines and tight junction proteins. Our results indicate that *C. albicans* does not alter host ECS gene expression in the GI tract. There was no significant effect of *C. albicans* on CB1 or CB2 gene expression in the GI tract, or on the expression of the ECS synthetic and degradative enzymes DAGL, MAGL and FAAH. We did measure significant differences in transcription in the liver, indicating that the metabolic changes we measured in the GI tract are sensed by the host and are physiologically relevant. We did not detect any significant differences in ECS genes in the liver, but did measure increased transcription of enzymes in the gluconeogenesis pathway (PEPCK-C and G6Pase) as well

as decreased transcription of the fatty acid desaturase SCD1. These transcriptional changes are consistent with the increased host absorption of lipids from the GI tract and liver sensing of such a metabolic change. We did not perform metabolomics analysis of the liver, but it is possible that the changes in endocannabinoid abundance observed in the GI tract are also present in the liver, and could affect a range of metabolic pathways. The ECS is a major regulator of energy metabolism in the liver, including processes such as gluconeogenesis, insulin production and lipid beta-oxidation. Gastrointestinal *C. albicans* colonization could affect host metabolism by increasing dietary fatty acids available to the host and through the modulation of the endocannabinoid system.

Brain endocannabinoid signaling is also an important regulator of metabolism. Because the increased CORT observed in *C. albicans*-colonized mice was only alleviated when treated with the FAAH inhibitor URB597 with activity in the brain, we conclude that *C. albicans* colonization affects brain endocannabinoid signaling. AEA is an orexigenic molecule that increases appetite through CB1 signaling when elevated in the brain[293]. In contrast, the endocannabinoid OEA which was elevated in the gut contents of *C. albicans*-colonized mice, is an anorexigenic molecule that produces satiety and decreases food intake in mice[294,295]. By disrupting the balance between OEA and AEA/2-AG, *C. albicans*-colonization could affect central energy metabolism. In peripheral organs such as the liver[296] and adipose tissue[297], AEA and 2-AG signaling through CB1 result in increased fatty acid biosynthesis and lipogenesis. Dysregulation of peripheral endocannabinoid signaling has been shown to contribute to diet-induced obesity models[285,298,299] in mice and has been correlated with metabolic disorders including liver disease[300,301] and obesity[302,303] in humans. The decreased CB1 signaling observed in the

C. albicans-colonized mice could result in protection against these metabolic disorders. By altering the abundance of multiple endocannabinoid molecules, *C. albicans* could have a broad effect on the metabolic state of the host.

Given the wide range of regulatory targets of the endocannabinoid system, future studies of *C. albicans* could focus on multiple host systems. Although we did not detect a change in tight junction gene expression in the large or small intestine, we could investigate more closely the effect of *C. albicans* colonization on the permeability of the GI tract. We could also quantify GI tract motility in the *C. albicans*-colonized mice, to determine whether this endocannabinoid and microbiota-regulated process is altered by the addition of *C. albicans*. Endocannabinoid signaling in both the GI tract and the brain has been shown to regulate appetite and food consumption. We could determine whether *C. albicans*-colonization is affecting this aspect of endocannabinoid signaling using a fasting and refeeding model for overall change in consumption, or look for altered consumption of foods high in fat or sugar defined as "high reward" foods. More broadly, we could investigate whether the changes in liver lipid metabolism in the *C. albicans*-colonized mice altered host risk for metabolic disorders like diabetes, by testing whether the metabolic changes in the *C. albicans*-colonized mice alter host glucose and insulin tolerance.

5.2 *C. albicans* encodes multiple enzymes that could affect lipid abundance in the GI tract

The untargeted metabolomic screen of cecum contents revealed that *C. albicans*-colonized mice had significant changes in lipid metabolism. We found an increase in abundance of multiple metabolites containing polyunsaturated fatty acids such as

membrane phospholipids, lysophospholipids, and signaling lipids like the endocannabinoids. There was also an increase in several phytosterols, lipid components of plant cell walls with a similar structure to cholesterol. Host sensing of a significant change in lipid abundance could alter global regulation of lipogenesis and closely linked glucose energy metabolism and indeed we measured decreased expression of the desaturase enzyme SCD1 and increased expression of gluconeogenesis enzymes G6Pase and PEPCK-C in the liver of *C. albicans*-colonized mice.

One way in which *C. albicans* could influence the abundance of lipids in the GI tract is through the expression and secretion of lipases. Previous researchers have characterized a family of lipases in *C. albicans* with lipolytic activity against mammalian cells including macrophages and epithelial cells[224]. These lipases were expressed by non-invasive *C. albicans* cells colonizing the mouse GI tract as well as by *C. albicans* cells invading tissue in an oral infection model[304] and by *C. albicans* cells infecting the liver in a bloodstream infection model[305]. *C. albicans* can use lipids as an exclusive carbon source, demonstrating that one role for these secreted lipases *in vivo* is to provide nutrients in an at times nutrient-limited environment. The family of lipases were defined as such due to their ability to cleave triglycerides and release the acyl groups as free fatty acids. Additional investigation into one member of the family, Lip4, showed that this secreted lipase preferentially freed long-chain unsaturated fatty acids, although it did still have activity against long-chain unsaturated fatty acid esters[306]. Our metabolomic analysis specifically showed an increase in long-chain unsaturated and polyunsaturated fatty acids in the *C. albicans*-colonized mice, consistent with such lipase preference.

C. albicans also secretes several phospholipases which can cleave membrane phospholipids and produce free fatty acids. *C. albicans* encodes phospholipases belonging to every major class of phospholipase: A (releases a single acyl chain as a free fatty acid), B (cleaves and releases both acyl chains from the phospholipid as free fatty acids), C (releases diacylglycerol and a phosphate-containing headgroup) and D (releases phosphatidic acid and an alcohol)[307]. Researchers have shown that the *C. albicans* phospholipase B (PLB1) is expressed both when *C. albicans* is present as a commensal colonizer and during infection of human patients[308]. *In vitro* analysis of clinical isolates from human patients demonstrated a correlation between strain phospholipase B activity and pathogenicity in mice[308,309] and genetic deletion studies have demonstrated that PLB1 is an important virulence factor in mouse infection models[310,311]. These studies suggest a physiologically significant amount of secreted PLB1 activity occurs during *C. albicans* colonization of the host, such that the action of this secreted phospholipase could contribute to the overall increase in fatty acids observed in the GI tract in our untargeted metabolomic screen. This change in fatty acid abundance in the GI tract could lead to changes throughout the host, as lipids are absorbed by the host, circulate through the blood stream and are taken up by cells throughout the body and incorporated into complex lipids.

Changes we observed in the GI tract could affect endocannabinoid metabolism throughout the host as researchers have shown that changes to the GI tract fatty acid substrate pools (through feeding defined diets) alters levels of N-acylethanolamides produced systemically[139,140,312]. Before lipids absorbed from the GI tract circulate through the body, they pass through the liver, a major regulator of lipid metabolism. The

majority of arachidonic acid incorporated into phospholipids in the brain is produced in the liver from precursor fatty acids and reaches the brain through the blood[313]. Although the brain can synthesize some arachidonic acid *de novo*, the balance in the liver between arachidonic acid uptake and release has been shown to regulate brain arachidonic acid availability and AEA levels[314]. The changes we observed in liver gene expression imply that the liver of *C. albicans*-colonized mice is sensing and responding to changes in lipid levels in the GI tract, which could therefore change the production and release of arachidonic acid in the liver and alter overall arachidonic acid availability. We hypothesized that the increase in long-chain PUFAs in the GI tract of *C. albicans*-colonized mice could alter the substrate pool for N-acylethanolamide metabolism and result in altered endocannabinoid abundance and the observed neuroendocrine changes.

Additionally, it is possible that *C. albicans* cells directly contribute to the altered N-acylethanolamide levels measured in the GI tract. Researchers identified homologues with a high degree of identity to the mammalian endocannabinoid degradative enzymes FAAH and MAGL in the yeast *Saccharomyces cerevisiae*[315]. Although functional studies were not done to demonstrate whether these homologous enzymes could degrade AEA, 2-AG or other endocannabinoids *in vitro*, it raises the possibility that yeast produce endocannabinoid compounds. *C. albicans* encodes a predicted amidase (orf19.5536) which aligns with the FAAH homologue identified in *S. cerevisiae*, although only with 31% identity, so it is possible that *C. albicans* could affect host endocannabinoid signaling through direct degradation of endocannabinoid molecules in the GI tract. Researchers did not identify a homologue with significant identity to the endocannabinoid synthetic enzymes NAPE-PLD or DAGL-α in *S. cerevisiae*. However,

a separate study demonstrated that *S. cerevisiae* cells contain the same N-acylethanolamide compounds found in mammalian cells and identified three type B phospholipases of *S. cerevisiae* that produced N-acylethanolamides *in vitro* from N-acyl-phosphotidylethanolamine precursors[316]. This synthetic pathway is analogous to alternate pathways for AEA synthesis identified in mammalian cells. Although comparable analysis has not been performed in *C. albicans, C. albicans* does encode several type B phospholipases and therefore could directly affect endocannabinoid signaling in the host GI tract through the synthesis of endocannabinoid molecules. Future studies could determine whether the *C. albicans* amidase or phospholipases are required for the observed neuroendocrine phenotypes in the *C. albicans*-colonized mice. We could determine whether *C. albicans* produces or degrades N-acylethanolamides *in vitro*, create mutant strains lacking these enzymes and colonize mice with them to determine whether this enzymatic activity of *C. albicans* is required for the endocannabinoid and neuroendocrine changes observed.

Other changes to the cell membrane composition could also affect endocannabinoid system signaling. The mammalian cell membrane is a highly dynamic environment in which lipid composition and organization have been shown to have a significant impact on cell signaling and function. The outer leaflet of the phospholipid bilayer is studded with distinct subdomains called lipid rafts largely made up of sphingolipids, cholesterol and proteins. These tightly packed subdomains play a functional role both in organizing proteins within the cell membrane and in interacting with the proteins to modulate their availability and activity[317]. G-protein coupled receptors, including the endocannabinoid receptor CB1, are targeted to lipid rafts, as are

their cognate GTP-binding proteins. *In vitro* studies that disrupted lipid rafts through cholesterol depletion demonstrated that intact lipid rafts are important for normal localization and activity of the CB1 receptor and uptake of the CB1 agonists AEA and 2-AG[318,319]and therefore lipid raft composition is a key regulator of endocannabinoid signaling. We observed an increase in phytosphingosine, cholesterol, and multiple phytosterols in the GI contents of the *C. albicans*-colonized mice, which could be absorbed, incorporated into cell membranes and affect lipid raft composition. Therefore, altered lipid raft composition is another mechanism by which the metabolic changes observed in the GI tract of *C. albicans*-colonized mice could affect endocannabinoid system signaling.

5.3 Long-term interactions between *C. albicans*, the bacterial microbiota and host systems are integrated into the host response to CDI challenge

C. albicans is thought to colonize humans over long periods of time, from weeks to months, throughout life. In order to investigate the long-term effects of *C. albicans* colonization, mice were treated with the antibiotic cefoperazone in drinking water for ten days to decrease the bacterial microbiota, then orally inoculated with *C. albicans*. Over the course of three weeks, *C. albicans* remained detectable in fecal pellets, indicating successful long-term colonization. Using this long-term colonization model, we no longer observed the same neuroendocrine phenotypes measured in the acute colonization model. Both the age of the host and antibiotic treatment were identified as confounding variables, as each had an effect separately on the neuroendocrine phenotype of the *C. albicans*-colonized mouse (Section 6.2). Therefore we cannot conclude that duration of colonization alone normalized host behavior and basal CORT production. However,

these results are consistent with a model in which the host is able to re-establish neuroendocrine homeostasis despite ongoing exposure to gastrointestinal *C. albicans*. In the human population, this could indicate that after being acquired for the first time soon after birth, ongoing *C. albicans* carriage may shape the developing neuroendocrine system through stimulation of the HPA axis and subsequent host compensatory changes to return to homeostasis.

While the host HPA axis and anxiety-like behavior were comparable to phenotypes of uncolonized mice in the long-term colonization model, we did detect significant changes to the host immune response and the bacterial gut microbiota after three-weeks of *C. albicans* colonization. We found that *C. albicans* affected both the host immune response and the bacterial microbiota, both components of host GI tract health that have been shown to be important in protecting the host from CDI. Disruption of the bacterial gut microbiota through antibiotic exposure is a major risk factor for the development of CDI[320,321]. Comprehensive studies in mouse models and in clinical trials of human patients have demonstrated that restoration of the healthy gut microbiota through either fecal microbiota transplant[42,43] or through targeted restoration of commensal bacteria[46,322] is sufficient to effectively treat CDI as well as prevent future relapse. The ability of the bacterial microbiota to resist disruption and maintain its structure and abundance in the face of antibiotic treatment is thus an important metric to assess the relative health of the microbiota and possibly predict its ability to predict the host from CDI. In our research we found that the addition of *C. albicans* to the bacterial microbiota during recovery from the antibiotic cefoperazone decreased bacterial microbiota diversity and rendered it more sensitive to disruption by the antibiotic

clindamycin. We described the *C. albicans*-containing microbiota as less stable due to increased loss of genera at the intermediate dose of clindamycin. At the high dose of clindamycin given to mice prior to challenge with *C. difficile* spores, uncolonized and *C. albicans*-colonized microbiotas were equally disrupted. However, it is possible that the difference in stability observed at the intermediate dose could translate into a functional difference in how the microbiota responds to clindamycin even at higher doses (at which the % genera lost is the same). We could predict that this would make the *C. albicans*-colonized microbiota less well-suited to defend the host from CDI.

Interestingly, we observed the opposite effect of *C. albicans* colonization on *C. difficile* challenge: mice pre-colonized with *C. albicans* were better protected from CDI than uncolonized mice. We showed that in these experiments, there was not a significant effect of *C. albicans* on the bacterial microbiota, but there was a significant IL-17 immune response both as a consequence of *C. albicans* colonization alone and an enhanced response to *C. difficile* challenge. Increased IL-17 was sufficient alone to protect the host from CDI, therefore we concluded that the *C. albicans*-induced IL-17 response was a key part of the protection against CDI observed in the *C. albicans*-colonized mice. These opposing results suggest that during the three-week colonization period, *C. albicans* interacts with both the host immune system and the bacterial microbiota. In the context of a severe perturbation like clindamycin treatment and *C. difficile* challenge, the immune effects dominate and the presence of *C. albicans* protects the host rather than making it more susceptible. Despite the decreased microbiota stability observed at the intermediate dose of clindamycin, the effect of *C. albicans* on the bacterial microbiota is not stronger than the beneficial impact of *C. albicans* on the host

immune system. Although small changes in bacterial microbiota such as the increased sensitivity to perturbation could be relevant to microbiota health in other contexts, in the context of a strong disruption such as clindamycin treatment followed by *C. difficile* challenge, they did not predict protective function of the microbiota.

Additional studies using the reduced microbiota model could better establish the effect of microbiota stability on susceptibility to CDI. We could give mice the low, intermediate and high doses of clindamycin and then challenge them with *C. difficile* spores, to determine whether the observed difference in degree of clindamycin disruption affects host response to *C. difficile*. We could also determine the effect of *C. albicans* pre-colonization on the response to *C. difficile* in low and intermediate clindamycin disruption models and see whether the IL-17 immune response induced during three weeks of *C. albicans* colonization remains more beneficial to the host than bacterial microbiota stability in mice given the intermediate dose of clindamycin.

Principles of ecological theory have been defined and applied to the gut microbiota and could further inform our understanding of bacteria-*C. albicans* interactions[323]. Correlation analysis to identify interactions between *C. albicans* and specific bacterial genera, or within different bacterial genera, in stable versus unstable ecosystems could reveal specific determinants of microbiota stability[324]. Deeper analysis of the composition of the bacterial microbiota utilizing transcriptomics to characterize the metabolic activity of the community, or metagenomics to define composition at the strain level could also reveal a more subtle effect of *C. albicans* on the bacterial gut microbiota that is lost in our limited 16s rRNA DNA sequencing analysis. It is likely that all three factors, the bacterial microbiota, the host immune response, and *C. albicans* itself

contribute to the integrated phenotypes (response to clindamycin disruption and protection from *C. difficile*) of the long-term *C. albicans* colonized mice.

Chapter 6 Appendix

6.1 Supplemental figures

6.1.1 Chapter 2 Supplemental Figures

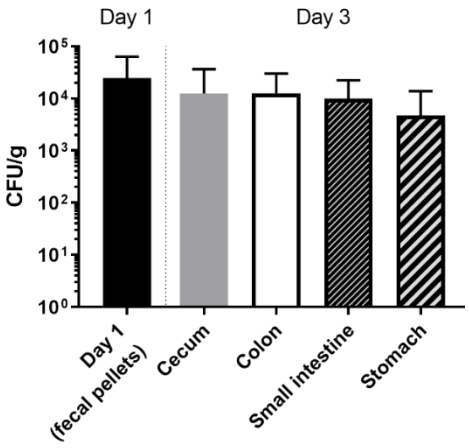

Fig. 6.1: *C. albicans* colonizes throughout the GI tract. On day 3, the contents of the cecum, colon, small intestine and stomach were each homogenized in 1ml PBS and plated on YPD-SA. Bars indicate average CFU/g and standard deviation. Day 1 N=98; Day 3 cecum N=77, colon N=35, small intestine N=19, stomach N=19

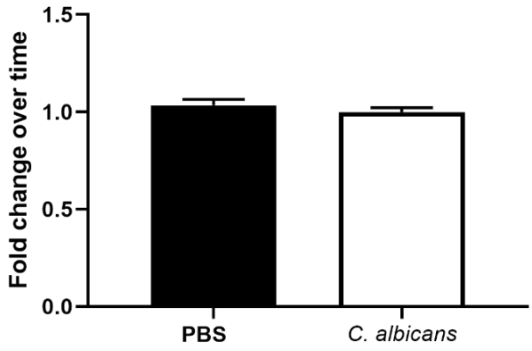

Fig. 6.2: *C. albicans* colonization does not result in significant weight loss. Mice were weighed prior to colonization and then the morning of sacrifice (four days later). Weight on day of sacrifice divided by weight prior to colonization is shown. Bars indicate average and standard deviation. N=8 for both groups.

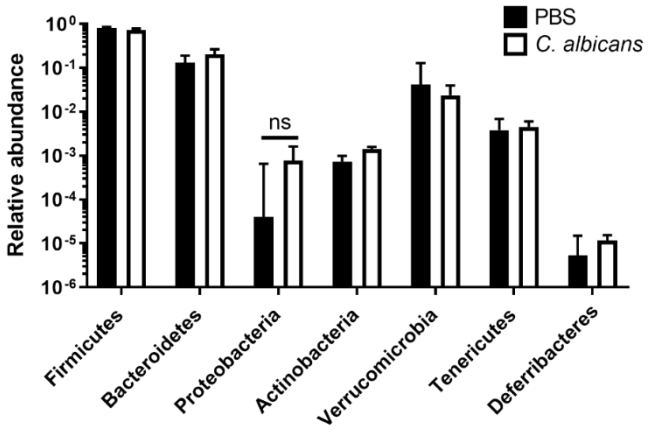

Fig. 6.3: *C. albicans* colonization did not significantly alter relative abundance of bacterial taxa at phylum level. Fraction of total reads shown, bars indicate average relative abundance and standard deviation. N=8 for both groups.

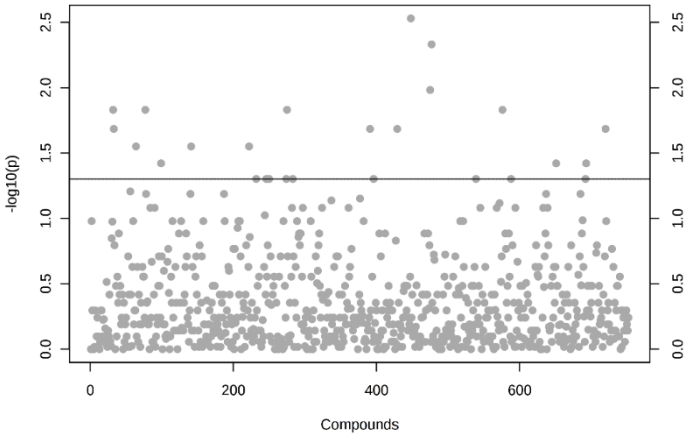

Fig. 6.4: Summary of all compounds measured in untargeted metabolomic screen. 752 compounds were detected in the cecum contents of mice. Each dot represents a compound, arrayed across the x-axis. Y-axis is the -log of the p-value of the t-test comparing the abundance of each compound in mock-colonized to *C. albicans*-colonized mice. Compounds above the line were significantly different.

6.1.2 Chapter 3 Supplemental Figures

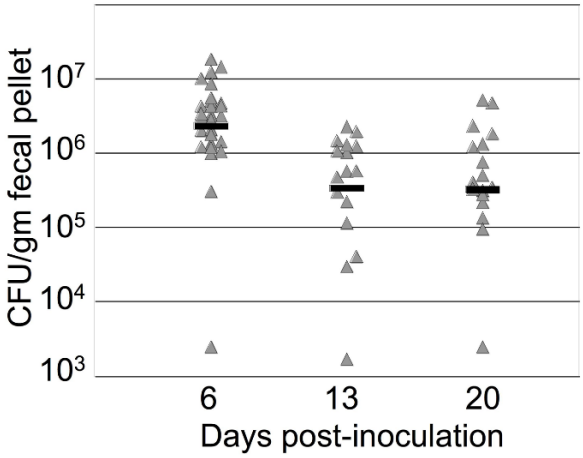

Fig. 6.5: C. albicans colonization of cefoperazone-treated mice. Mice were treated with cefoperazone in drinking water for 10 days and then orally inoculated with *C. albicans*. Fecal pellets were collected on days indicated on graph, homogenized and plated to measure *C. albicans* CFU/gm. Each symbol represents a sample from an individual mouse and the bar indicates the geometric mean.

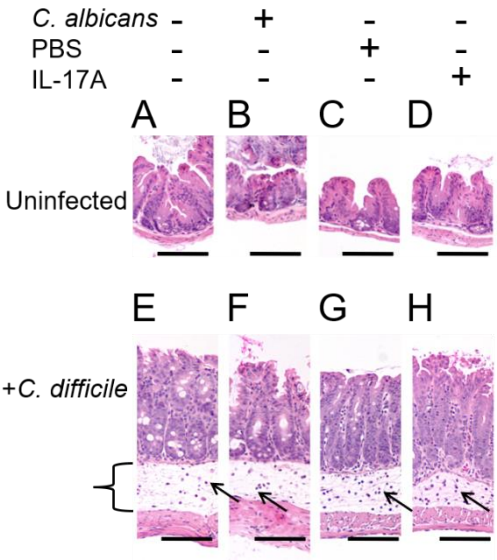

Fig. 6.6. Cecal histology of *C. difficile* infected mice with and without *C. albicans* or IL-17A. All mice were treated with cefoperazone for 10 days and received clindamycin. Some mice also received either *C. albicans* (B,F), PBS (C,G) or IL-17A (D,H). Mice were sacrificed two days post-inoculation with *C. difficile* (E-H) or prior to inoculation, for uninoculated (A-D). Histology of the cecum wall is shown after H & E staining. Ceca from *C. difficile* infected mice (E-H) showed regions of edema (brackets) and leukocyte influx (arrows) into the lamina propria. Scale bar, 100 um.

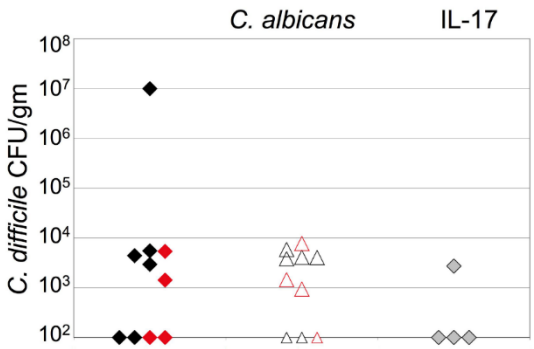

Fig. 6.7 Low levels of *C. difficile* spores in samples collected on day 1 post-inoculation from mice with and without *C. albicans*. Fecal pellets were collected from mice 1 day post-inoculation. Some mice were euthanized 1 day post-*C. difficile* inoculation and cecal contents were collected. *C. difficile* spores were enumerated in these samples by plating on pre-reduced TCCFA. Black diamonds, mice received PBS and *C. difficile;* triangles pre-colonized with *C. albicans* and given PBS and *C. difficile*; grey diamonds, mice given IL-17A and *C. difficile.* Red symbols, samples of cecum. Black/open symbols, fecal pellets. Each sample shows results from an individual mouse.

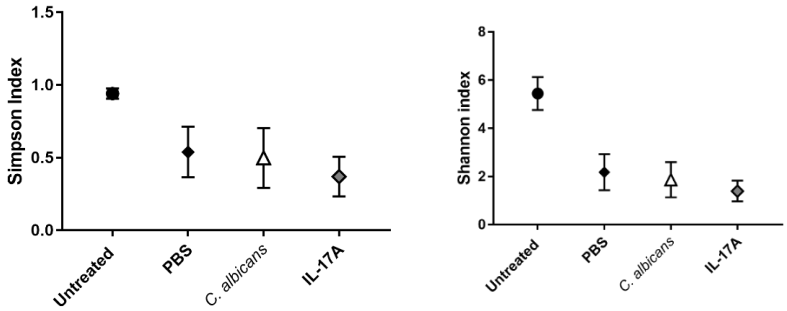

Fig. 6.8: Low community diversity of cecal microbiota from *C. difficile* inoculated mice. Diversity scores were calculated within QIIME 1.8. Each point represents the mean diversity score for all mice within a group. Diversity of each sample was calculated by averaging 10 rarefactions taken at a depth of 11,500 sequences. Black circles, untreated mice (no cefoperazone or clindamycin treatment, not inoculated with microbes); black bars indicate the standard error of the mean (SEM) throughout the figure. Black diamonds, given PBS and *C. difficile*; open triangles, given *C. albicans*, PBS and *C. difficile*; grey diamonds, given IL-17A and *C. difficile.*

6.1.3 Chapter 4 Supplemental Figures

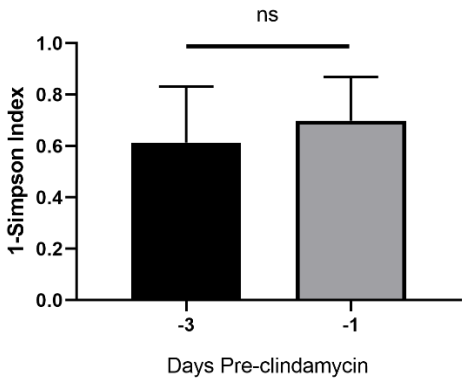

Fig. 6.9: Prior to clindamycin, post-cefoperazone microbiota is stable. The microbiota was sequenced from fecal pellets collected three days to clindamycin and one day prior to clindamycin. Bars are the average of two cohorts, error bars are standard deviation. Both groups N=29

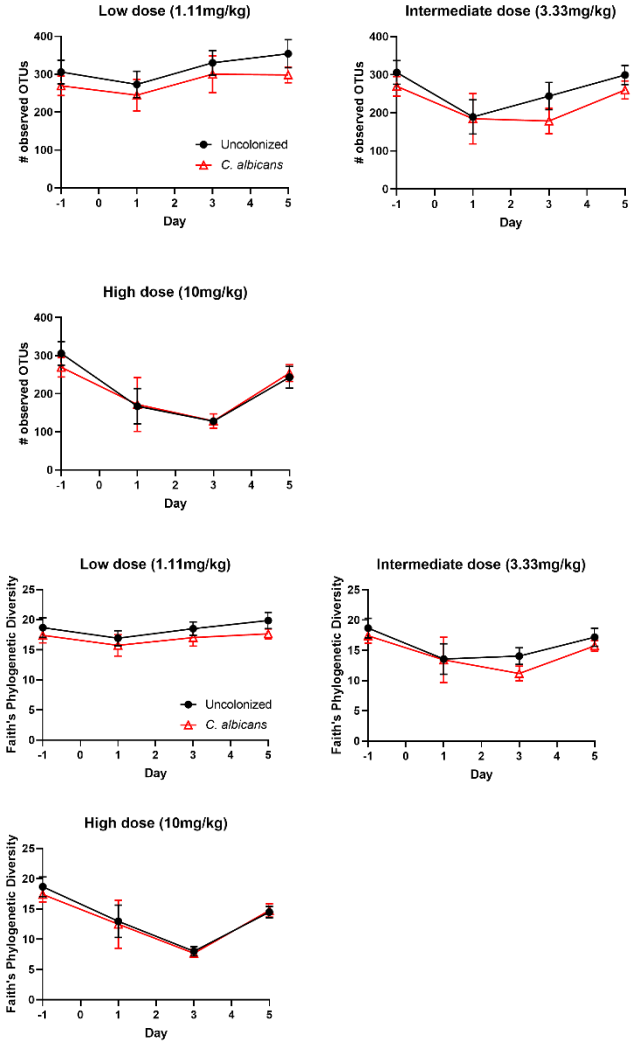

Fig. 6.10: Additional alpha diversity metrics demonstrate rebound in diversity after three to five days of recovery from clindamycin. Microbiota was sequenced from fecal pellets collected one, three and five days after clindamycin treatment. Various alpha diversity metrics were used to measure the change in diversity over time. Supplemental figure 2 displays the # observed OTUs over time in uncolonized mice and mice colonized with C. albicans. Supplemental figure 3 shows Faith's Phylogenetic Diversity index over time. One clindamycin treatment group per graph is shown. Symbols indicate the average diversity of that experimental group, bars indicate the standard deviation.

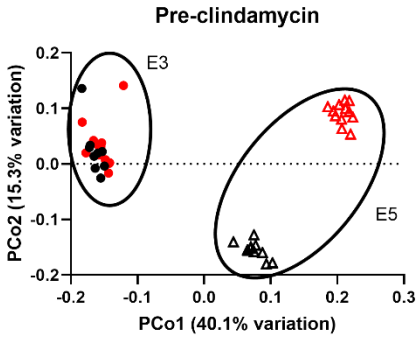

Fig. 6.11: Beta diversity of the post-cefoperazone recovery pre-clindamycin microbiota. Mice received the antibiotic cefoperazone in drinking water for ten days, then half of the mice were colonized with C. albicans and the other half was not. After three weeks, the microbiota was sequenced from fecal pellets. Principal coordinates analysis of unweighted UniFrac scores is shown. Each symbol represents a mouse gut microbiota, shape of the symbol indicates cohort, black symbols are uncolonized (N=20) and red symbols are *C. albicans*-colonized (N=24).

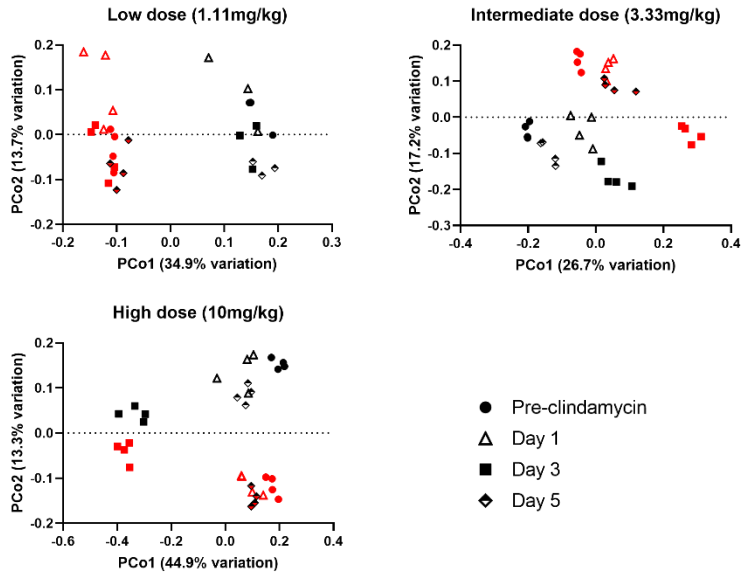

Fig. 6.12: Beta diversity of E5, a cohort with significant *C. albicans*-dependent separation. The microbiota of mice was sequenced from fecal pellets collected prior to clindamycin treatment and one, three and five days after clindamycin. Unweighted UniFrac scores were used to perform principal coordinates analysis to compare the microbiota of mice over time, in response to different doses of clindamycin, with and without *C. albicans* colonization. Each symbol represents the microbiota of a mouse; symbol shape indicates the timepoint, black symbols represent uncolonized mice and red symbols represent *C. albicans*-colonized mice.

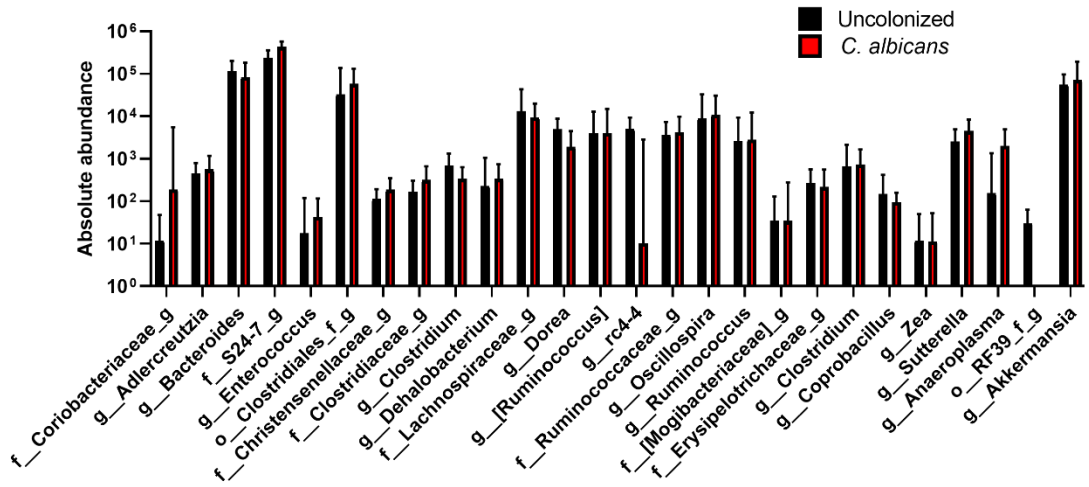

Fig. 6.13: *C. albicans* colonization did not significantly alter abundance of bacterial taxa at genus level. Mice were treated with the antibiotic cefoperazone for ten days in drinking water, then half of the mice were inoculated with *C. albicans*. Uncolonized and *C. albicans*-colonized mice recovered for three weeks without antibiotics present. Fecal pellets were collected at the end of this three-week period, one day prior to clindamycin treatment, and the microbiota sequenced. Average absolute abundance of genera is shown. Only genera that were present in both experimental cohorts that included *C. albicans*-colonized mice are shown here. Average abundance in uncolonized mice is represented by black bars and in *C. albicans*-colonized mice by red bars. Bars indicate the average and standard deviation.

6.2 Long-term effects of *C. albicans* colonization on the gut-brain axis

The research described in Chapter 2 demonstrated that upon initial colonization, *C. albicans* interacts with the host gut-brain axis resulting in dysregulation of the HPA axis and increased anxiety-like behavior. Humans are likely colonized for longer periods of time with *C. albicans*, therefore we wanted to investigate how *C. albicans* and the gut-brain axis interacted over a longer period of time. Researchers have shown that chronic activation of the HPA axis, as in a chronic restraint stress or chronic unpredictable stress model in rodents, changed the HPA response to acute stressors and increased anxiety-like

behavior[325–327]. Because acute *C. albicans* colonization dysregulated CORT production,

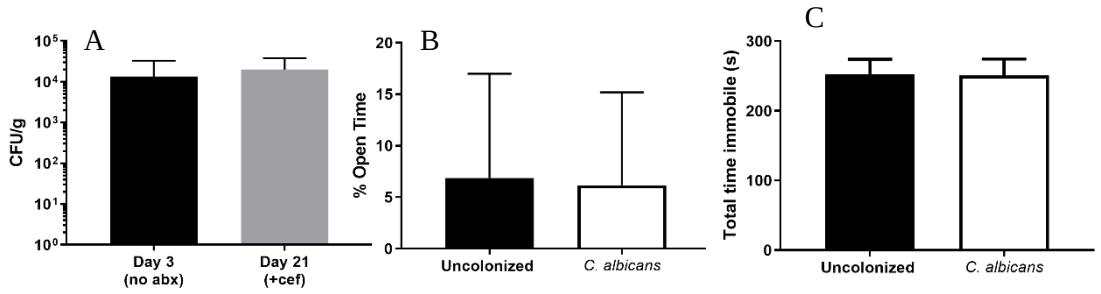

Figure 6.14: Mice colonized with *C. albicans* for three weeks no longer exhibit behavioral changes. Mice were colonized for three weeks. A) Cecum content homogenate was collected on day 3 (no abx, black bar) or day 21 (cefoperazone, gray bar) after sacrifice and plated on YPD-SA. B) % of time spent in open arms of the EPM (open arm time/total arm time*100). C) Total time immobile during a 6m trial in the FST. Black bars represent uncolonized mice, white bars represent *C. albicans*-colonized mice. Bars show the average and standard deviation

we hypothesized that similar to repeated stress exposre, three weeks of exposure to *C. albicans* could have differential effects on behavior and stress-induced CORT production. In order to stably colonize mice with *C. albicans* for multiple weeks, we used the long-term colonization model described in Chapters 3 and 4. Mice were given the antibiotic cefoperazone in drinking water for ten days, then half of each cohort were given a single oral inoculation of *C. albicans* ($5x10^7$CFUs). Colonization proceeded for three weeks, during which we periodically measured *C. albicans* colonization levels by sterilely collecting fecal pellets and plating fecal pellet homogenate on YPD-SA. On day 19 post-inoculation, mice were put through either the EPM test for anxiety-like behavior, or the FST for depression-like behavior.

In contrast to the mice colonized with *C. albicans* for three days, mice colonized with *C. albicans for* three weeks did not have increased anxiety-like behavior (Fig. 6.15 B). Behavior in the FST remained comparable between the uncolonized and *C. albicans*-colonized mice (Fig. 6.15 C). This result suggested that the effect of *C. albicans* on

behavior changed over time. The level of *C. albicans* measured in cecum contents after three days of colonization without antibiotic treatment (as in Chapter 2) and after three weeks of colonization with antibiotic pre-treatment is comparable (Fig. 6.15 A). This suggests that although the host is being exposed to the same level of *C. albicans* in the GI tract, it no longer triggers a change in anxiety-like behavior.

Mice were sacrificed on day 21, either under unstressed conditions to measure basal CORT production, or after 30 minutes of restraint stress and 0, 30 or 60 minutes of recovery to measure stress-responsive CORT production.

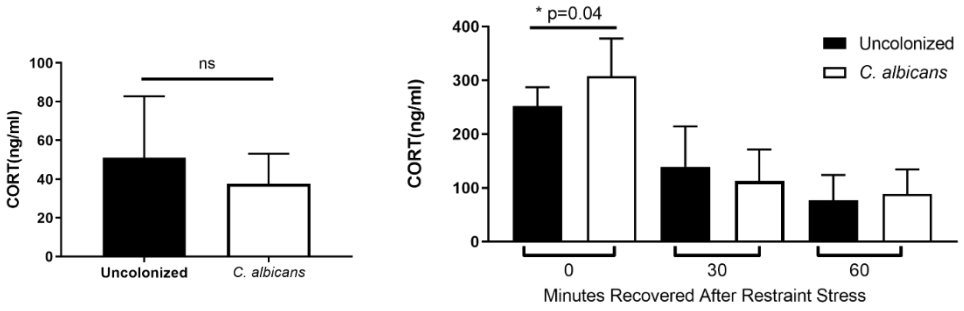

Figure 6.15: Stress-induced CORT is altered in long-term *C. albicans* colonization model. Mice were sacrificed without stress (top) and CORT measured in serum. Other mice were subjected to 30m of restraint stress and sacrificed immediately or after 30 or 60 minutes of recovery (bottom). Black bars represent uncolonized mice, white bars represent *C. albicans*-colonized mice. Student's t-test, p=0.04

Basal CORT production in the long-term *C. albicans*-colonized mice was comparable to that of the uncolonized mice (Fig. 6.16 left). After stress, CORT was significantly higher in the *C. albicans*-colonized mice (Fig. 6.16, right, t-test p=0.04) than in the uncolonized mice, indicating dysregulation of CORT produced in response to stress. After 30 or 60 minutes of recovery, CORT was comparable between the uncolonized and *C. albicans*-colonized mice. This result suggested that *C. albicans* colonization of the GI tract had both acute and chronic effects on HPA axis activity and regulation. In the acute

colonization model (Chapter 2) we demonstrated a circadian advance in HPA axis CORT production resulting in increased basal CORT and increased CORT after 60m of recovery from stress. In the long-term colonization model, we found that basal CORT was comparable, but that peak stress-responsive CORT was now altered. These results are consistent with a model in which the host HPA axis changes in response to the acute *C. albicans* stimulation, such that over time basal CORT is no longer affected by *C. albicans* colonization but these changes to the HPA axis result in a dysregulated stress response.

In addition to being colonized with *C. albicans* for longer, mice in the long-term colonization model were also treated with the antibiotic cefoperazone and were four weeks older (10 weeks old) at the time of sacrifice. Both antibiotic treatment and age of the host have also been shown to affect the HPA axis, therefore we performed additional experiments to determine whether these factors changed the phenotype of interest. We found that colonization of 9-week-old mice (10 weeks old when sacrificed) in the acute colonization model did not affect anxiety-like behavior or peak stress-responsive CORT (Fig. 2.13) Therefore, the lack of anxiety-like behavior in the long-term colonization model (Fig. 6.15) could represent decreased sensitivity of older mice to *C. albicans* colonization rather than habituation to *C. albicans* over the course of three weeks. Adult mice had no change in peak CORT in response to acute *C. albicans* colonization (Fig. 2.13), so it is possible that the increased peak CORT observed in the long-term model (Fig. 6.16) is a reflection of chronic *C. albicans* stimulation of the HPA axis over three weeks changing the way the host responds to subsequent stressors.

To investigate the effect of cefoperazone treatment on the neuroendocrine phenotypes of the *C. albicans*-colonized mice, 5-week-old mice were given cefoperazone

in drinking water for 10 days, then inoculated with *C. albicans* or mock-inoculated with PBS. Mice were tested in the EPM for anxiety-like behavior two days after inoculation and sacrificed without stress three days after inoculation.

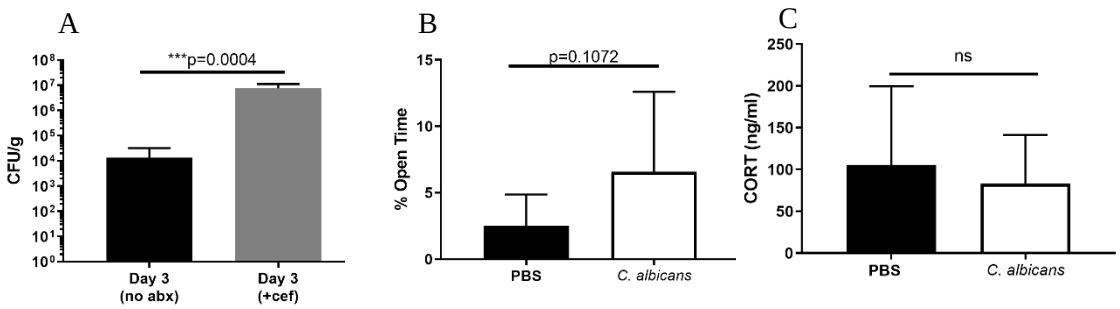

Figure 6.16: Effect of *C. albicans* in acute colonization model with cefoperazone pre-treatment. Mice were given cefoperazone in drinking water for ten days, then inoculated with *C. albicans* or mock-inoculated. Behavior in the EPM was assessed on day 2 post-inoculation and mice were sacrificed unstressed on day 3 post-inoculation. A) Cecum contents were collected from mice sacrificed after three days of *C. albicans* colonization and plated on YPD-SA. Black bar represents mice colonized without pretreatment and gray bar represents mice treated with 10d cefoperazone in drinking water. B) % open arm time in the EPM is shown (open arm time/total arm time*100). C) CORT was measured in mice sacrificed under basal unstressed conditions. For B and C, black bars represent mock-colonized mice and white bars represent *C. albicans*-colonized mice. Throughout bars indicate average and standard deviation. Welch's t-test, $p<0.05$.

C. albicans colonization measured in cecum contents after sacrifice on day 3 post-inoculation was significantly higher than that measured in mice colonized for 3 days without cefoperazone pre-treatment (Fig. 6.17A, Welch's t-test, p=0.0004). Behavior in the EPM was not significantly different between the *C. albicans*-colonized and mock-colonized mice, although we did observe a trend towards increased open arm time (Fig. 6.17B, Welch's t-test, p=0.1072) and therefore decreased anxiety-like behavior in the *C. albicans*-colonized mice. This would indicate that cefoperazone treatment actually reverses the effect of *C. albicans* colonization on anxiety-like behavior, as mice colonized with *C. albicans* in the acute model without antibiotic pretreatment had

increased anxiety-like behavior (Fig. 2.3). Mice in the antibiotic pre-treatment acute colonization model also had significantly more *C. albicans* present in the GI tract (Fig.6.17A), so it is unclear whether the altered behavior was due to the changes in bacterial microbiota or the significant increase in *C. albicans* load. There was no difference in basal CORT between the mock-colonized and *C. albicans*-colonized mice (Fig. 6.17C), indicating that cefoperazone pre-treatment resulted in mice that were insensitive to the effect of acute *C. albicans* colonization on basal CORT production.

In summary, we found that both age of the mouse and cefoperazone pre-treatment altered the neuroendocrine effect of *C. albicans* on the host gut-brain axis. Although the results of the long-term colonization model are interesting, there are likely multiple interacting variables changing the neuroendocrine response of the host, in addition to the *C. albicans* colonizing the GI tract. A different model that did not include antibiotic pre-treatment would eliminate one of those variables and perhaps be more informative.

Chapter 7 Bibliography

1. Kondori, N. *et al.* Candida species as commensal gut colonizers: A study of 133 longitudinally followed Swedish infants. *Med. Mycol.* (2019) doi:10.1093/mmy/myz091.
2. Arendorf, T. M. & Walker, D. M. The prevalence and intra-oral distribution of Candida albicans in man. *Arch. Oral Biol.* 25, 1–10 (1980).
3. Reef, S. E. *et al.* Nonperinatal nosocomial transmission of Candida albicans in a neonatal intensive care unit: prospective study. *J. Clin. Microbiol.* 36, 1255–1259 (1998).
4. Raimondi, S. *et al.* Longitudinal Survey of Fungi in the Human Gut: ITS Profiling, Phenotyping, and Colonization. *Front. Microbiol.* 10, 1575 (2019).
5. Mukaremera, L., Lee, K. K., Mora-Montes, H. M. & Gow, N. A. R. Candida albicans Yeast, Pseudohyphal, and Hyphal Morphogenesis Differentially Affects Immune Recognition. *Front. Immunol.* 8, (2017).
6. Soll, D. R. The role of phenotypic switching in the basic biology and pathogenesis of Candida albicans. *J. Oral Microbiol.* 6, (2014).
7. Pfaller, M. A. & Diekema, D. J. Epidemiology of Invasive Candidiasis: a Persistent Public Health Problem. *Clin. Microbiol. Rev.* 20, 133–163 (2007).
8. Wenzel, R. P. Nosocomial Candidemia: Risk Factors and Attributable Mortality. *Clin. Infect. Dis.* 20, 1531–1534 (1995).
9. Luca, A. D. *et al.* Functional yet Balanced Reactivity to Candida albicans Requires TRIF, MyD88, and IDO-Dependent Inhibition of Rorc. *J. Immunol.* 179, 5999–6008 (2007).
10. Bonifazi, P. *et al.* Balancing inflammation and tolerance in vivo through dendritic cells by the commensal Candida albicans. *Mucosal Immunol.* 2, 362–374 (2009).
11. Bellocchio, S. *et al.* The Contribution of the Toll-Like/IL-1 Receptor Superfamily to Innate and Adaptive Immunity to Fungal Pathogens In Vivo. *J. Immunol.* 172, 3059–3069 (2004).
12. Zelante, T. *et al.* IL-23 and the Th17 pathway promote inflammation and impair antifungal immune resistance. *Eur. J. Immunol.* 37, 2695–2706 (2007).
13. Cenci, E. *et al.* IFN-γ Is Required for IL-12 Responsiveness in Mice with Candida albicans Infection. *J. Immunol.* 161, 3543–3550 (1998).
14. Mencacci, A. *et al.* IL-10 Is Required for Development of Protective Th1 Responses in IL-12-Deficient Mice upon *Candida albicans* Infection. *J. Immunol.* 161, 6228–6237 (1998).
15. Huang, W., Na, L., Fidel, P. L. & Schwarzenberger, P. Requirement of Interleukin-17A for Systemic Anti-Candida albicans Host Defense in Mice. *J. Infect. Dis.* 190, 624–631 (2004).
16. Conti, H. R. *et al.* Th17 cells and IL-17 receptor signaling are essential for mucosal host defense against oral candidiasis. *J. Exp. Med.* 206, 299–311 (2009).
17. Romani, L. & Puccetti, P. Protective tolerance to fungi: the role of IL-10 and tryptophan catabolism. *Trends Microbiol.* 14, 183–189 (2006).
18. Markey, L. *et al.* Pre-colonization with the commensal fungus Candida albicans reduces murine susceptibility to Clostridium difficile infection. *Gut Microbes* 9, 497–509 (2018).

19. Shao, T.-Y. *et al.* Commensal Candida albicans Positively Calibrates Systemic Th17 Immunological Responses. *Cell Host Microbe* 25, 404-417.e6 (2019).
20. Standaert-Vitse, A. *et al.* Candida albicans Colonization and ASCA in Familial Crohn's Disease. *Am. J. Gastroenterol.* 104, 1745–1753 (2009).
21. Kumamoto, C. A. Inflammation and gastrointestinal Candida colonization. *Curr. Opin. Microbiol.* 14, 386–391 (2011).
22. Stamatiades, G. A., Ioannou, P., Petrikkos, G. & Tsioutis, C. Fungal infections in patients with inflammatory bowel disease: A systematic review. *Mycoses* 61, 366–376 (2018).
23. Zwolinska-Wcislo, M. *et al.* Effect of Candida colonization on human ulcerative colitis and the healing of inflammatory changes of the colon in the experimental model of colitis ulcerosa. *J. Physiol. Pharmacol. Off. J. Pol. Physiol. Soc.* 60, 107–118 (2009).
24. Bertolini, M. *et al.* Candida albicans induces mucosal bacterial dysbiosis that promotes invasive infection. *PLOS Pathog.* 15, e1007717 (2019).
25. Jawhara, S. *et al.* Colonization of mice by Candida albicans is promoted by chemically induced colitis and augments inflammatory responses through galectin-3. *J. Infect. Dis.* 197, 972–980 (2008).
26. Pierce, J. V., Dignard, D., Whiteway, M. & Kumamoto, C. A. Normal Adaptation of Candida albicans to the Murine Gastrointestinal Tract Requires Efg1p-Dependent Regulation of Metabolic and Host Defense Genes. *Eukaryot. Cell* 12, 37–49 (2013).
27. White, S. J. *et al.* Self-Regulation of Candida albicans Population Size during GI Colonization. *PLOS Pathog* 3, e184 (2007).
28. Doedt, T. *et al.* APSES proteins regulate morphogenesis and metabolism in Candida albicans. *Mol. Biol. Cell* 15, 3167–3180 (2004).
29. Pande, K., Chen, C. & Noble, S. M. Passage through the mammalian gut triggers a phenotypic switch that promotes Candida albicans commensalism. *Nat. Genet.* 45, 1088–1091 (2013).
30. Pierce, J. V. & Kumamoto, C. A. Variation in Candida albicans EFG1 Expression Enables Host-Dependent Changes in Colonizing Fungal Populations. *mBio* 3, e00117-12 (2012).
31. Tyc, K. M. *et al.* The game theory of Candida albicans colonization dynamics reveals host status-responsive gene expression. *BMC Syst. Biol.* 10, 20 (2016).
32. Ramírez, M. A. & Lorenz, M. C. The Transcription Factor Homolog CTF1 Regulates β-Oxidation in Candida albicans. *Eukaryot. Cell* 8, 1604–1614 (2009).
33. Carman, A. J., Vylkova, S. & Lorenz, M. C. Role of Acetyl Coenzyme A Synthesis and Breakdown in Alternative Carbon Source Utilization in Candida albicans. *Eukaryot. Cell* 7, 1733–1741 (2008).
34. Vargas, S. L., Patrick, C. C., Ayers, G. D. & Hughes, W. T. Modulating effect of dietary carbohydrate supplementation on Candida albicans colonization and invasion in a neutropenic mouse model. *Infect. Immun.* 61, 619–626 (1993).
35. Gunsalus, K. T. W., Tornberg-Belanger, S. N., Matthan, N. R., Lichtenstein, A. H. & Kumamoto, C. A. Manipulation of Host Diet To Reduce Gastrointestinal Colonization by the Opportunistic Pathogen Candida albicans. *mSphere* 1, e00020-15 (2016).

36. Guinea, J. Global trends in the distribution of Candida species causing candidemia. *Clin. Microbiol. Infect. Off. Publ. Eur. Soc. Clin. Microbiol. Infect. Dis.* 20 Suppl 6, 5–10 (2014).
37. Brown, G. D. *et al.* Hidden Killers: Human Fungal Infections. *Sci. Transl. Med.* 4, 165rv13-165rv13 (2012).
38. Buffie, C. G. *et al.* Precision microbiome reconstitution restores bile acid mediated resistance to *Clostridium difficile*. *Nature* 517, 205–208 (2015).
39. Wilson, K. H. Efficiency of various bile salt preparations for stimulation of Clostridium difficile spore germination. *J. Clin. Microbiol.* 18, 1017–1019 (1983).
40. Drasar, B. S., Hill, M. J. & Shiner, M. THE DECONJUGATION OF BILE SALTS BY HUMAN INTESTINAL BACTERIA. *The Lancet* 287, 1237–1238 (1966).
41. Barbut, F. *et al.* Epidemiology of Recurrences or Reinfections ofClostridium difficile-Associated Diarrhea. *J. Clin. Microbiol.* 38, 2386–2388 (2000).
42. van Nood, E. *et al.* Duodenal Infusion of Donor Feces for Recurrent Clostridium difficile. *N. Engl. J. Med.* 368, 407–415 (2013).
43. Rohlke, F., Surawicz, C. M. & Stollman, N. Fecal Flora Reconstitution for Recurrent Clostridium difficile Infection: Results and Methodology. *J. Clin. Gastroenterol.* 44, 567 (2010).
44. Garborg, K., Waagsbø, B., Stallemo, A., Matre, J. & Sundøy, A. Results of faecal donor instillation therapy for recurrent Clostridium difficile-associated diarrhoea. *Scand. J. Infect. Dis.* 42, 857–861 (2010).
45. Gough, E., Shaikh, H. & Manges, A. R. Systematic Review of Intestinal Microbiota Transplantation (Fecal Bacteriotherapy) for Recurrent Clostridium difficile Infection. *Clin. Infect. Dis.* 53, 994–1002 (2011).
46. Lawley, T. D. *et al.* Targeted Restoration of the Intestinal Microbiota with a Simple, Defined Bacteriotherapy Resolves Relapsing Clostridium difficile Disease in Mice. *PLOS Pathog.* 8, e1002995 (2012).
47. Sangster, W. *et al.* Bacterial and Fungal Microbiota Changes Distinguish C. difficile Infection from Other Forms of Diarrhea: Results of a Prospective Inpatient Study. *Front. Microbiol.* 7, (2016).
48. Lamendella, R. *et al.* Antibiotic Treatments for Clostridium difficile Infection Are Associated with Distinct Bacterial and Fungal Community Structures. *mSphere* 3, e00572-17 (2018).
49. Zuo, T. *et al.* Gut fungal dysbiosis correlates with reduced efficacy of fecal microbiota transplantation in Clostridium difficile infection. *Nat. Commun.* 9, 1–11 (2018).
50. Manian, F. A. & Bryant, A. Does Candida Species Overgrowth Protect Against Clostridium difficile Infection? *Clin. Infect. Dis.* 56, 464–465 (2013).
51. Blanco, N. *et al.* Clostridium difficile shows no trade-off between toxin and spore production within the human host. *J. Med. Microbiol.* 67, 631–640 (2018).
52. Raponi, G., Visconti, V., Brunetti, G. & Ghezzi, M. C. Clostridium difficile Infection and Candida Colonization of the Gut: Is There a Correlation? *Clin. Infect. Dis.* 59, 1648–1649 (2014).
53. The Human Microbiome Project Consortium. Structure, function and diversity of the healthy human microbiome. *Nature* 486, 207–214 (2012).

54. Yatsunenko, T. *et al.* Human gut microbiome viewed across age and geography. *Nature* 486, 222–227 (2012).
55. Dethlefsen, L. & Relman, D. A. Incomplete recovery and individualized responses of the human distal gut microbiota to repeated antibiotic perturbation. *Proc. Natl. Acad. Sci.* 108, 4554–4561 (2011).
56. Wu, G. D. *et al.* Linking Long-Term Dietary Patterns with Gut Microbial Enterotypes. *Science* 334, 105–108 (2011).
57. Carroll, I. M. *et al.* Molecular analysis of the luminal- and mucosal-associated intestinal microbiota in diarrhea-predominant irritable bowel syndrome. *Am. J. Physiol.-Gastrointest. Liver Physiol.* 301, G799–G807 (2011).
58. Turnbaugh, P. J. *et al.* A core gut microbiome in obese and lean twins. *Nature* 457, 480–484 (2009).
59. Chang, J. Y. *et al.* Decreased Diversity of the Fecal Microbiome in Recurrent Clostridium difficile—Associated Diarrhea. *J. Infect. Dis.* 197, 435–438 (2008).
60. Holling, C. S. Resilience and Stability of Ecological Systems. *Annu. Rev. Ecol. Syst.* 4, 1–23 (1973).
61. Gunderson, L. H. Ecological Resilience—In Theory and Application. *Annu. Rev. Ecol. Syst.* 31, 425–439 (2000).
62. Manichanh, C. *et al.* Reshaping the gut microbiome with bacterial transplantation and antibiotic intake. *Genome Res.* 20, 1411–1419 (2010).
63. Jakobsson, H. E. *et al.* Short-Term Antibiotic Treatment Has Differing Long-Term Impacts on the Human Throat and Gut Microbiome. *PLOS ONE* 5, e9836 (2010).
64. Mason, K. L. *et al.* Candida albicans and bacterial microbiota interactions in the cecum during recolonization following broad-spectrum antibiotic therapy. *Infect. Immun.* 80, 3371–3380 (2012).
65. Carabotti, M., Scirocco, A., Maselli, M. A. & Severi, C. The gut-brain axis: interactions between enteric microbiota, central and enteric nervous systems. *Ann. Gastroenterol. Q. Publ. Hell. Soc. Gastroenterol.* 28, 203–209 (2015).
66. Martin, C. R., Osadchiy, V., Kalani, A. & Mayer, E. A. The Brain-Gut-Microbiome Axis. *Cell. Mol. Gastroenterol. Hepatol.* 6, 133–148 (2018).
67. Carmody, R. N. *et al.* Diet Dominates Host Genotype in Shaping the Murine Gut Microbiota. *Cell Host Microbe* 17, 72–84 (2015).
68. Chassaing, B. *et al.* Dietary emulsifiers impact the mouse gut microbiota promoting colitis and metabolic syndrome. *Nature* 519, 92–96 (2015).
69. Munyaka, P. M., Rabbi, M. F., Khafipour, E. & Ghia, J.-E. Acute dextran sulfate sodium (DSS)-induced colitis promotes gut microbial dysbiosis in mice. *J. Basic Microbiol.* 56, 986–998 (2016).
70. Bharwani, A. *et al.* Structural & functional consequences of chronic psychosocial stress on the microbiome & host. *Psychoneuroendocrinology* 63, 217–227 (2016).
71. Marin, I. A. *et al.* Microbiota alteration is associated with the development of stress-induced despair behavior. *Sci. Rep.* 7, 43859 (2017).
72. Everard, A. *et al.* Cross-talk between Akkermansia muciniphila and intestinal epithelium controls diet-induced obesity. *Proc. Natl. Acad. Sci.* 110, 9066–9071 (2013).

73. Reigstad, C. S. *et al.* Gut microbes promote colonic serotonin production through an effect of short-chain fatty acids on enterochromaffin cells. *FASEB J. Off. Publ. Fed. Am. Soc. Exp. Biol.* 29, 1395–1403 (2015).
74. Olson, C. A. *et al.* The Gut Microbiota Mediates the Anti-Seizure Effects of the Ketogenic Diet. *Cell* 173, 1728-1741.e13 (2018).
75. Nishino, R. *et al.* Commensal microbiota modulate murine behaviors in a strictly contamination-free environment confirmed by culture-based methods. *Neurogastroenterol. Motil. Off. J. Eur. Gastrointest. Motil. Soc.* 25, 521–528 (2013).
76. Wikoff, W. R. *et al.* Metabolomics analysis reveals large effects of gut microflora on mammalian blood metabolites. *Proc. Natl. Acad. Sci.* 106, 3698–3703 (2009).
77. Le Gall, G. *et al.* Metabolomics of Fecal Extracts Detects Altered Metabolic Activity of Gut Microbiota in Ulcerative Colitis and Irritable Bowel Syndrome. *J. Proteome Res.* 10, 4208–4218 (2011).
78. O'Mahony, S. M., Clarke, G., Borre, Y. E., Dinan, T. G. & Cryan, J. F. Serotonin, tryptophan metabolism and the brain-gut-microbiome axis. *Behav. Brain Res.* 277, 32–48 (2015).
79. Asano, Y. *et al.* Critical role of gut microbiota in the production of biologically active, free catecholamines in the gut lumen of mice. *Am. J. Physiol. - Gastrointest. Liver Physiol.* 303, G1288–G1295 (2012).
80. Crumeyrolle-Arias, M. *et al.* Absence of the gut microbiota enhances anxiety-like behavior and neuroendocrine response to acute stress in rats. *Psychoneuroendocrinology* 42, 207–217 (2014).
81. Diaz Heijtz, R. *et al.* Normal gut microbiota modulates brain development and behavior. *Proc. Natl. Acad. Sci. U. S. A.* 108, 3047–3052 (2011).
82. Neufeld, K. M., Kang, N., Bienenstock, J. & Foster, J. A. Reduced anxiety-like behavior and central neurochemical change in germ-free mice. *Neurogastroenterol. Motil. Off. J. Eur. Gastrointest. Motil. Soc.* 23, 255–264, e119 (2011).
83. Guida, F. *et al.* Antibiotic-induced microbiota perturbation causes gut endocannabinoidome changes, hippocampal neuroglial reorganization and depression in mice. *Brain. Behav. Immun.* 67, 230–245 (2018).
84. Bravo, J. A. *et al.* Ingestion of Lactobacillus strain regulates emotional behavior and central GABA receptor expression in a mouse via the vagus nerve. *Proc. Natl. Acad. Sci. U. S. A.* 108, 16050–16055 (2011).
85. Sudo, N. *et al.* Postnatal microbial colonization programs the hypothalamic-pituitary-adrenal system for stress response in mice. *J. Physiol.* 558, 263–275 (2004).
86. Ait-Belgnaoui, A. *et al.* Probiotic gut effect prevents the chronic psychological stress-induced brain activity abnormality in mice. *Neurogastroenterol. Motil. Off. J. Eur. Gastrointest. Motil. Soc.* 26, 510–520 (2014).
87. Bercik, P. *et al.* Chronic gastrointestinal inflammation induces anxiety-like behavior and alters central nervous system biochemistry in mice. *Gastroenterology* 139, 2102-2112.e1 (2010).
88. Kato, K. *et al.* Randomized placebo-controlled trial assessing the effect of bifidobacteria-fermented milk on active ulcerative colitis. *Aliment. Pharmacol. Ther.* 20, 1133–1141 (2004).

89. Nobaek, S., Johansson, M. L., Molin, G., Ahrné, S. & Jeppsson, B. Alteration of intestinal microflora is associated with reduction in abdominal bloating and pain in patients with irritable bowel syndrome. *Am. J. Gastroenterol.* 95, 1231–1238 (2000).
90. Saggioro, A. Probiotics in the treatment of irritable bowel syndrome. *J. Clin. Gastroenterol.* 38, S104-106 (2004).
91. Slykerman, R. F. *et al.* Effect of Lactobacillus rhamnosus HN001 in Pregnancy on Postpartum Symptoms of Depression and Anxiety: A Randomised Double-blind Placebo-controlled Trial. *EBioMedicine* 24, 159–165 (2017).
92. Huang, R., Wang, K. & Hu, J. Effect of Probiotics on Depression: A Systematic Review and Meta-Analysis of Randomized Controlled Trials. *Nutrients* 8, 483 (2016).
93. Prantera, C. & Scribano, M. L. Probiotics and Crohn's disease. *Dig. Liver Dis. Off. J. Ital. Soc. Gastroenterol. Ital. Assoc. Study Liver* 34 Suppl 2, S66-67 (2002).
94. Kuisma, J. *et al.* Effect of Lactobacillus rhamnosus GG on ileal pouch inflammation and microbial flora. *Aliment. Pharmacol. Ther.* 17, 509–515 (2003).
95. Niv, E., Naftali, T., Hallak, R. & Vaisman, N. The efficacy of Lactobacillus reuteri ATCC 55730 in the treatment of patients with irritable bowel syndrome--a double blind, placebo-controlled, randomized study. *Clin. Nutr. Edinb. Scotl.* 24, 925–931 (2005).
96. Brown, R. E. *An Introduction to Neuroendocrinology*. (Cambridge University Press, 1994).
97. Sapolsky, R. M., Romero, L. M. & Munck, A. U. How do glucocorticoids influence stress responses? Integrating permissive, suppressive, stimulatory, and preparative actions. *Endocr. Rev.* 21, 55–89 (2000).
98. de Kloet, E. R., Oitzl, M. S. & Joëls, M. Functional implications of brain corticosteroid receptor diversity. *Cell. Mol. Neurobiol.* 13, 433–455 (1993).
99. Escoter-Torres, L. *et al.* Fighting the Fire: Mechanisms of Inflammatory Gene Regulation by the Glucocorticoid Receptor. *Front. Immunol.* 10, (2019).
100. Kumar, R. & Thompson, E. B. Gene regulation by the glucocorticoid receptor: Structure:function relationship. *J. Steroid Biochem. Mol. Biol.* 94, 383–394 (2005).
101. Dallman, M. F. *et al.* Feast and Famine: Critical Role of Glucocorticoids with Insulin in Daily Energy Flow. *Front. Neuroendocrinol.* 14, 303–347 (1993).
102. Peckett, A. J., Wright, D. C. & Riddell, M. C. The effects of glucocorticoids on adipose tissue lipid metabolism. *Metabolism* 60, 1500–1510 (2011).
103. Munck, A. Glucocorticoid Inhibition of Glucose Uptake by Peripheral Tissues: Old and New Evidence, Molecular Mechanisms, and Physiological Significance. *Perspect. Biol. Med.* 14, 265–289 (1971).
104. Brinkmann, V. & Kristofic, C. Regulation by corticosteroids of Th1 and Th2 cytokine production in human CD4+ effector T cells generated from CD45RO- and CD45RO+ subsets. *J. Immunol. Baltim. Md 1950* 155, 3322–3328 (1995).
105. Ramírez, F., Fowell, D. J., Puklavec, M., Simmonds, S. & Mason, D. Glucocorticoids promote a TH2 cytokine response by CD4+ T cells in vitro. *J. Immunol. Baltim. Md 1950* 156, 2406–2412 (1996).

106. Scheinman, R. I., Cogswell, P. C., Lofquist, A. K. & Baldwin, A. S. Role of transcriptional activation of I kappa B alpha in mediation of immunosuppression by glucocorticoids. *Science* 270, 283–286 (1995).
107. Auphan, N., DiDonato, J. A., Rosette, C., Helmberg, A. & Karin, M. Immunosuppression by glucocorticoids: inhibition of NF-kappa B activity through induction of I kappa B synthesis. *Science* 270, 286–290 (1995).
108. Johnson, J. D. *et al.* Catecholamines mediate stress-induced increases in peripheral and central inflammatory cytokines. *Neuroscience* 135, 1295–1307 (2005).
109. Takaki, A., Huang, Q. H., Somogyvári-Vigh, A. & Arimura, A. Immobilization stress may increase plasma interleukin-6 via central and peripheral catecholamines. *Neuroimmunomodulation* 1, 335–342 (1994).
110. den Boon, F. S. & Sarabdjitsingh, R. A. Circadian and ultradian patterns of HPA-axis activity in rodents: Significance for brain functionality. *Best Pract. Res. Clin. Endocrinol. Metab.* 31, 445–457 (2017).
111. Chung, S. *et al.* Cooperative roles of the suprachiasmatic nucleus central clock and the adrenal clock in controlling circadian glucocorticoid rhythm. *Sci. Rep.* 7, 46404 (2017).
112. Slieker, L. J. *et al.* Regulation of Expression of ob mRNA and Protein by Glucocorticoids and cAMP. *J. Biol. Chem.* 271, 5301–5304 (1996).
113. Gaunitz, F., Heise, K., Schumann, R. & Gebhardt, R. Glucocorticoid induced expression of glutamine synthetase in hepatoma cells. *Biochem. Biophys. Res. Commun.* 296, 1026–1032 (2002).
114. Wang, M. The role of glucocorticoid action in the pathophysiology of the Metabolic Syndrome. *Nutr. Metab.* 2, 3 (2005).
115. Bao, A.-M., Meynen, G. & Swaab, D. F. The stress system in depression and neurodegeneration: Focus on the human hypothalamus. *Brain Res. Rev.* 57, 531–553 (2008).
116. Arborelius, L., Owens, M. J., Plotsky, P. M. & Nemeroff, C. B. The role of corticotropin-releasing factor in depression and anxiety disorders. *J. Endocrinol.* 160, 1–12 (1999).
117. Kallen, V. L. *et al.* Associations between HPA axis functioning and level of anxiety in children and adolescents with an anxiety disorder. *Depress. Anxiety* 25, 131–141 (2008).
118. Pasquali, R., Vicennati, V., Cacciari, M. & Pagotto, U. The Hypothalamic-Pituitary-Adrenal Axis Activity in Obesity and the Metabolic Syndrome. *Ann. N. Y. Acad. Sci.* 1083, 111–128 (2006).
119. Debono, M., Ross, R. J. & Newell-Price, J. Inadequacies of glucocorticoid replacement and improvements by physiological circadian therapy. *Eur. J. Endocrinol.* 160, 719–729 (2009).
120. Devane, W. A., Dysarz, F. A., Johnson, M. R., Melvin, L. S. & Howlett, A. C. Determination and characterization of a cannabinoid receptor in rat brain. *Mol. Pharmacol.* 34, 605–613 (1988).
121. Matsuda, L. A., Lolait, S. J., Brownstein, M. J., Young, A. C. & Bonner, T. I. Structure of a cannabinoid receptor and functional expression of the cloned cDNA. *Nature* 346, 561–564 (1990).

122. Munro, S., Thomas, K. L. & Abu-Shaar, M. Molecular characterization of a peripheral receptor for cannabinoids. *Nature* 365, 61–65 (1993).
123. Hollister, L. E. Health aspects of cannabis. *Pharmacol. Rev.* 38, 1–20 (1986).
124. Devane, W. A. *et al.* Isolation and structure of a brain constituent that binds to the cannabinoid receptor. *Science* 258, 1946–1949 (1992).
125. Mechoulam, R. *et al.* Identification of an endogenous 2-monoglyceride, present in canine gut, that binds to cannabinoid receptors. *Biochem. Pharmacol.* 50, 83–90 (1995).
126. Bouaboula, M. *et al.* Activation of mitogen-activated protein kinases by stimulation of the central cannabinoid receptor CB1. *Biochem. J.* 312, 637–641 (1995).
127. Childers, S. R., Sexton, T. & Roy, M. B. Effects of anandamide on cannabinoid receptors in rat brain membranes. *Biochem. Pharmacol.* 47, 711–715 (1994).
128. Placzek, E. A., Okamoto, Y., Ueda, N. & Barker, E. L. Mechanisms for recycling and biosynthesis of endogenous cannabinoids anandamide and 2-arachidonylglycerol. *J. Neurochem.* 107, 987–1000 (2008).
129. Tanimura, A. *et al.* The Endocannabinoid 2-Arachidonoylglycerol Produced by Diacylglycerol Lipase α Mediates Retrograde Suppression of Synaptic Transmission. *Neuron* 65, 320–327 (2010).
130. Magotti, P. *et al.* Structure of human NAPE-PLD: regulation of fatty-acid ethanolamide biosynthesis by bile acids. *Struct. Lond. Engl. 1993* 23, 598–604 (2015).
131. Simon, G. M. & Cravatt, B. F. Anandamide Biosynthesis Catalyzed by the Phosphodiesterase GDE1 and Detection of Glycerophospho-N-acyl Ethanolamine Precursors in Mouse Brain. *J. Biol. Chem.* 283, 9341–9349 (2008).
132. Liu, J. *et al.* A biosynthetic pathway for anandamide. *Proc. Natl. Acad. Sci.* 103, 13345–13350 (2006).
133. Piomelli, D. *et al.* Pharmacological profile of the selective FAAH inhibitor KDS-4103 (URB597). *CNS Drug Rev.* 12, 21–38 (2006).
134. Mofford, D. M., Adams, S. T., Reddy, G. S. K. K., Reddy, G. R. & Miller, S. C. Luciferin Amides Enable in Vivo Bioluminescence Detection of Endogenous Fatty Acid Amide Hydrolase Activity. *J. Am. Chem. Soc.* 137, 8684–8687 (2015).
135. Moreno-Sanz, G. *et al.* Pharmacological characterization of the peripheral FAAH inhibitor URB937 in female rodents: interaction with the Abcg2 transporter in the blood-placenta barrier. *Br. J. Pharmacol.* 167, 1620–1628 (2012).
136. Bisogno, T. *et al.* Synthesis and Pharmacological Activity of a Potent Inhibitor of the Biosynthesis of the Endocannabinoid 2-Arachidonoylglycerol. *ChemMedChem* 4, 946–950 (2009).
137. Long, J. Z. *et al.* Dual blockade of FAAH and MAGL identifies behavioral processes regulated by endocannabinoid crosstalk in vivo. *Proc. Natl. Acad. Sci.* 106, 20270–20275 (2009).
138. Wang, J. *et al.* Functional Analysis of the Purified Anandamide-generating Phospholipase D as a Member of the Metallo-β-lactamase Family. *J. Biol. Chem.* 281, 12325–12335 (2006).
139. Sihag, J. & Jones, P. J. H. Dietary fatty acid profile influences circulating and tissue fatty acid ethanolamide concentrations in a tissue-specific manner in male Syrian

hamsters. *Biochim. Biophys. Acta BBA - Mol. Cell Biol. Lipids* 1864, 1563–1579 (2019).
140. Artmann, A. *et al.* Influence of dietary fatty acids on endocannabinoid and N-acylethanolamine levels in rat brain, liver and small intestine. *Biochim. Biophys. Acta BBA - Mol. Cell Biol. Lipids* 1781, 200–212 (2008).
141. Wood, J. T. *et al.* Dietary docosahexaenoic acid supplementation alters select physiological endocannabinoid-system metabolites in brain and plasma. *J. Lipid Res.* 51, 1416–1423 (2010).
142. Hill, M. N. *et al.* Suppression of amygdalar endocannabinoid signaling by stress contributes to activation of the hypothalamic-pituitary-adrenal axis. *Neuropsychopharmacol. Off. Publ. Am. Coll. Neuropsychopharmacol.* 34, 2733–2745 (2009).
143. Barna, I., Zelena, D., Arszovszki, A. C. & Ledent, C. The role of endogenous cannabinoids in the hypothalamo-pituitary-adrenal axis regulation: in vivo and in vitro studies in CB1 receptor knockout mice. *Life Sci.* 75, 2959–2970 (2004).
144. Cota, D. *et al.* Requirement of Cannabinoid Receptor Type 1 for the Basal Modulation of Hypothalamic-Pituitary-Adrenal Axis Function. *Endocrinology* 148, 1574–1581 (2007).
145. Gray, J. M. *et al.* Corticotropin-Releasing Hormone Drives Anandamide Hydrolysis in the Amygdala to Promote Anxiety. *J. Neurosci.* 35, 3879–3892 (2015).
146. Hill, M. N. *et al.* Recruitment of prefrontal cortical endocannabinoid signaling by glucocorticoids contributes to termination of the stress response. *J. Neurosci. Off. J. Soc. Neurosci.* 31, 10506–10515 (2011).
147. Haller, J., Bakos, N., Szirmay, M., Ledent, C. & Freund, T. F. The effects of genetic and pharmacological blockade of the CB1 cannabinoid receptor on anxiety. *Eur. J. Neurosci.* 16, 1395–1398 (2002).
148. Haller, J., Varga, B., Ledent, C. & Freund, T. F. CB1 cannabinoid receptors mediate anxiolytic effects: convergent genetic and pharmacological evidence with CB1-specific agents. *Behav. Pharmacol.* 15, 299–304 (2004).
149. Litvin, Y., Phan, A., Hill, M. N., Pfaff, D. W. & McEwen, B. S. CB1 receptor signaling regulates social anxiety and memory. *Genes Brain Behav.* 12, 479–489 (2013).
150. Scherma, M. *et al.* The endogenous cannabinoid anandamide has effects on motivation and anxiety that are revealed by fatty acid amide hydrolase (FAAH) inhibition. *Neuropharmacology* 54, 129–140 (2008).
151. Moreira, F. A., Kaiser, N., Monory, K. & Lutz, B. Reduced anxiety-like behaviour induced by genetic and pharmacological inhibition of the endocannabinoid-degrading enzyme fatty acid amide hydrolase (FAAH) is mediated by CB1 receptors. *Neuropharmacology* 54, 141–150 (2008).
152. Naidu, P. S. *et al.* Evaluation of fatty acid amide hydrolase inhibition in murine models of emotionality. *Psychopharmacology (Berl.)* 192, 61–70 (2007).
153. J, H. *et al.* Interactions between environmental aversiveness and the anxiolytic effects of enhanced cannabinoid signaling by FAAH inhibition in rats. *Psychopharmacology (Berl.)* 204, 607–616 (2009).
154. Rubino, T. *et al.* Role in anxiety behavior of the endocannabinoid system in the prefrontal cortex. *Cereb. Cortex N. Y. N 1991* 18, 1292–1301 (2008).

155. Movahed, P. *et al.* Endogenous unsaturated C18 N-acylethanolamines are vanilloid receptor (TRPV1) agonists. *J. Biol. Chem.* 280, 38496–38504 (2005).
156. Raboune, S. *et al.* Novel endogenous N-acyl amides activate TRPV1-4 receptors, BV-2 microglia, and are regulated in brain in an acute model of inflammation. *Front. Cell. Neurosci.* 8, 195 (2014).
157. Terzian, A. L. B., Aguiar, D. C., Guimarães, F. S. & Moreira, F. A. Modulation of anxiety-like behaviour by Transient Receptor Potential Vanilloid Type 1 (TRPV1) channels located in the dorsolateral periaqueductal gray. *Eur. Neuropsychopharmacol.* 19, 188–195 (2009).
158. Rossi, S. *et al.* Interleukin-1β causes anxiety by interacting with the endocannabinoid system. *J. Neurosci. Off. J. Soc. Neurosci.* 32, 13896–13905 (2012).
159. Moreira, F. A., Aguiar, D. C., Terzian, A. L. B., Guimarães, F. S. & Wotjak, C. T. Cannabinoid type 1 receptors and transient receptor potential vanilloid type 1 channels in fear and anxiety-two sides of one coin? *Neuroscience* 204, 186–192 (2012).
160. Bandelow, B. & Michaelis, S. Epidemiology of anxiety disorders in the 21st century. *Dialogues Clin. Neurosci.* 17, 327–335 (2015).
161. Baxter, A. J., Scott, K. M., Vos, T. & Whiteford, H. A. Global prevalence of anxiety disorders: a systematic review and meta-regression. *Psychol. Med.* 43, 897–910 (2013).
162. Leonardo, E. D. & Hen, R. Anxiety as a Developmental Disorder. *Neuropsychopharmacology* 33, 134–140 (2008).
163. Ait-Belgnaoui, A. *et al.* Prevention of gut leakiness by a probiotic treatment leads to attenuated HPA response to an acute psychological stress in rats. *Psychoneuroendocrinology* 37, 1885–1895 (2012).
164. Gareau, M. G., Jury, J., MacQueen, G., Sherman, P. M. & Perdue, M. H. Probiotic treatment of rat pups normalises corticosterone release and ameliorates colonic dysfunction induced by maternal separation. *Gut* 56, 1522–1528 (2007).
165. Messaoudi, M. *et al.* Assessment of psychotropic-like properties of a probiotic formulation (Lactobacillus helveticus R0052 and Bifidobacterium longum R0175) in rats and human subjects. *Br. J. Nutr.* 105, 755–764 (2011).
166. Ohland, C. L. *et al.* Effects of Lactobacillus helveticus on murine behavior are dependent on diet and genotype and correlate with alterations in the gut microbiome. *Psychoneuroendocrinology* 38, 1738–1747 (2013).
167. Li, J. *et al.* Fungi in Gastrointestinal Tracts of Human and Mice: from Community to Functions. *Microb. Ecol.* 75, 821–829 (2018).
168. Schulze, J. & Sonnenborn, U. Yeasts in the gut: from commensals to infectious agents. *Dtsch. Arzteblatt Int.* 106, 837–842 (2009).
169. Blaschke-Hellmessen, R. [Vertical transmission of Candida and its consequences]. *Mycoses* 41 Suppl 2, 31–36 (1998).
170. Tiraboschi, I. C. N. *et al.* Congenital candidiasis: confirmation of mother-neonate transmission using molecular analysis techniques. *Med. Mycol.* 48, 177–181 (2010).
171. Brown, D. H., Jr., Giusani, A. D., Chen, X. & Kumamoto, C. A. Filamentous growth of Candida albicans in response to physical environmental cues and its regulation by the unique CZF1 gene. *Mol Microbiol* 34, 651–62 (1999).

172. Walf, A. A. & Frye, C. A. The use of the elevated plus maze as an assay of anxiety-related behavior in rodents. *Nat. Protoc.* 2, 322–328 (2007).
173. Can, A. *et al.* The Mouse Forced Swim Test. *J. Vis. Exp. JoVE* (2012) doi:10.3791/3638.
174. Caporaso, J. G. *et al.* Ultra-high-throughput microbial community analysis on the Illumina HiSeq and MiSeq platforms. *ISME J.* 6, 1621–1624 (2012).
175. Caporaso, J. G. *et al.* QIIME allows analysis of high-throughput community sequencing data. *Nat. Methods* 7, 335–336 (2010).
176. Chong, J., Wishart, D. S. & Xia, J. Using MetaboAnalyst 4.0 for Comprehensive and Integrative Metabolomics Data Analysis. *Curr. Protoc. Bioinforma.* 68, e86 (2019).
177. Xia, J., Psychogios, N., Young, N. & Wishart, D. S. MetaboAnalyst: a web server for metabolomic data analysis and interpretation. *Nucleic Acids Res.* 37, W652–W660 (2009).
178. Alipour, M. *et al.* A Balanced IL-1β Activity Is Required for Host Response to Citrobacter rodentium Infection. *PLOS ONE* 8, e80656 (2013).
179. Sokol, H. *et al.* Card9 Mediates Intestinal Epithelial Cell Restitution, T-Helper 17 Responses, and Control of Bacterial Infection in Mice. *Gastroenterology* 145, 591-601.e3 (2013).
180. Erb Downward, J. R., Falkowski, N. R., Mason, K. L., Muraglia, R. & Huffnagle, G. B. Modulation of post-antibiotic bacterial community reassembly and host response by Candida albicans. *Sci Rep* 3, 2191 (2013).
181. Segata, N. *et al.* Metagenomic biomarker discovery and explanation. *Genome Biol.* 12, R60 (2011).
182. Hascoët, M. & Bourin, M. The Forced Swimming Test in Mice: A Suitable Model to Study Antidepressants. in *Mood and Anxiety Related Phenotypes in Mice* 85–118 (Humana Press, Totowa, NJ, 2009). doi:10.1007/978-1-60761-303-9_6.
183. Kalueff, A. V. & Nutt, D. J. Role of GABA in anxiety and depression. *Depress. Anxiety* 24, 495–517 (2007).
184. Kalueff, A. V., Wheaton, M. & Murphy, D. L. What's wrong with my mouse model?: Advances and strategies in animal modeling of anxiety and depression. *Behav. Brain Res.* 179, 1–18 (2007).
185. Nutt, D. J., Ballenger, J. C., Sheehan, D. & Wittchen, H.-U. Generalized anxiety disorder: comorbidity, comparative biology and treatment. *Int. J. Neuropsychopharmacol.* 5, 315–325 (2002).
186. Faravelli, C. *et al.* Childhood stressful events, HPA axis and anxiety disorders. *World J. Psychiatry* 2, 13–25 (2012).
187. Landgraf, R., Wigger, A., Holsboer, F. & Neumann, I. D. Hyper-Reactive Hypothalamo-Pituitary-Adrenocortical Axis in Rats Bred for High Anxiety-Related Behaviour. *J. Neuroendocrinol.* 11, 405–407 (1999).
188. Myers, B. & Greenwood-Van Meerveld, B. Elevated corticosterone in the amygdala leads to persistant increases in anxiety-like behavior and pain sensitivity. *Behav. Brain Res.* 214, 465–469 (2010).
189. Sotnikov, S. *et al.* Blunted HPA axis reactivity reveals glucocorticoid system dysbalance in a mouse model of high anxiety-related behavior. *Psychoneuroendocrinology* 48, 41–51 (2014).

190. Hill, M. N. & Tasker, J. G. Endocannabinoid signaling, glucocorticoid-mediated negative feedback, and regulation of the hypothalamic-pituitary-adrenal axis. *Neuroscience* 204, 5–16 (2012).
191. Atkinson, H. C. *et al.* Regulation of the hypothalamic-pituitary-adrenal axis circadian rhythm by endocannabinoids is sexually diergic. *Endocrinology* 151, 3720–3727 (2010).
192. Crowe, M. S., Nass, S. R., Gabella, K. M. & Kinsey, S. G. The endocannabinoid system modulates stress, emotionality, and inflammation. *Brain. Behav. Immun.* 42, 1–5 (2014).
193. Hermanson, D. J. *et al.* Substrate-selective COX-2 inhibition decreases anxiety via endocannabinoid activation. *Nat. Neurosci.* 16, 1291–1298 (2013).
194. Di, S., Malcher-Lopes, R., Halmos, K. C. & Tasker, J. G. Nongenomic Glucocorticoid Inhibition via Endocannabinoid Release in the Hypothalamus: A Fast Feedback Mechanism. *J. Neurosci.* 23, 4850–4857 (2003).
195. Dosoky, N. S., Guo, L., Chen, Z., Feigley, A. V. & Davies, S. S. Dietary Fatty Acids Control the Species of N-Acyl-Phosphatidylethanolamines Synthesized by Therapeutically Modified Bacteria in the Intestinal Tract. *ACS Infect. Dis.* 4, 3–13 (2018).
196. Joosten, M. M., Balvers, M. G., Verhoeckx, K. C., Hendriks, H. F. & Witkamp, R. F. Plasma anandamide and other N-acylethanolamines are correlated with their corresponding free fatty acid levels under both fasting and non-fasting conditions in women. *Nutr. Metab.* 7, 49 (2010).
197. Lin, L. *et al.* Dietary fatty acids augment tissue levels of n-acylethanolamines in n-acylphosphatidylethanolamine phospholipase D (NAPE-PLD) knockout mice. *J. Nutr. Biochem.* 62, 134–142 (2018).
198. Ntambi, J. M. & Bené, H. Polyunsaturated fatty acid regulation of gene expression. *J. Mol. Neurosci.* 16, 6 (2001).
199. Lee, K. N., Pariza, M. W. & Ntambi, J. M. Conjugated Linoleic Acid Decreases Hepatic Stearoyl-CoA Desaturase mRNA Expression. *Biochem. Biophys. Res. Commun.* 248, 817–821 (1998).
200. Oosterveer, M. H. *et al.* High Fat Feeding Induces Hepatic Fatty Acid Elongation in Mice. *PLOS ONE* 4, e6066 (2009).
201. Massillon, D., Barzilai, N., Hawkins, M., Prus-Wertheimer, D. & Rossetti, L. Induction of hepatic glucose-6-phosphatase gene expression by lipid infusion. *Diabetes* 46, 153–157 (1997).
202. Massillon, D., Arinze, I. J., Xu, C. & Bone, F. Regulation of Glucose-6-phosphatase Gene Expression in Cultured Hepatocytes and H4IIE Cells by Short-chain Fatty Acids ROLE OF HEPATIC NUCLEAR FACTOR-4α. *J. Biol. Chem.* 278, 40694–40701 (2003).
203. Chen, G. Liver lipid molecules induce PEPCK-C gene transcription and attenuate insulin action. *Biochem. Biophys. Res. Commun.* 361, 805–810 (2007).
204. Kajikawa, S., Harada, T., Kawashima, A., Imada, K. & Mizuguchi, K. Highly purified eicosapentaenoic acid prevents the progression of hepatic steatosis by repressing monounsaturated fatty acid synthesis in high-fat/high-sucrose diet-fed mice. *Prostaglandins Leukot. Essent. Fatty Acids* 80, 229–238 (2009).

205. Su, H., Zhou, D., Pan, Y.-X., Wang, X. & Nakamura, M. T. Compensatory induction of Fads1 gene expression in heterozygous Fads2-null mice and by diet with a high n-6/n-3 PUFA ratio. *J. Lipid Res.* 57, 1995–2004 (2016).
206. Rosenblat, M., Volkova, N., Roqueta-Rivera, M., Nakamura, M. T. & Aviram, M. Increased macrophage cholesterol biosynthesis and decreased cellular paraoxonase 2 (PON2) expression in Delta6-desaturase knockout (6-DS KO) mice: beneficial effects of arachidonic acid. *Atherosclerosis* 210, 414–421 (2010).
207. Osei-Hyiaman, D. *et al.* Endocannabinoid activation at hepatic CB_1 receptors stimulates fatty acid synthesis and contributes to diet-induced obesity. *J. Clin. Invest.* 115, 1298–1305 (2005).
208. Volat, F. E. *et al.* Depressed levels of prostaglandin F2α in mice lacking Akr1b7 increase basal adiposity and predispose to diet-induced obesity. *Diabetes* 61, 2796–2806 (2012).
209. Overbergh, L., Valckx, D., Waer, M. & Mathieu, C. Quantification of murine cytokine mRNAs using real time quantitative reverse transcriptase PCR. *Cytokine* 11, 305–312 (1999).
210. Fegley, D. *et al.* Characterization of the fatty acid amide hydrolase inhibitor cyclohexyl carbamic acid 3'-carbamoyl-biphenyl-3-yl ester (URB597): effects on anandamide and oleoylethanolamide deactivation. *J. Pharmacol. Exp. Ther.* 313, 352–358 (2005).
211. Danandeh, A. *et al.* Effects of fatty acid amide hydrolase inhibitor URB597 in a rat model of trauma-induced long-term anxiety. *Psychopharmacology (Berl.)* 235, 3211–3221 (2018).
212. Clapper, J. R. *et al.* Anandamide suppresses pain initiation through a peripheral endocannabinoid mechanism. *Nat. Neurosci.* 13, 1265–1270 (2010).
213. Moreira, F. A., Aguiar, D. C., Terzian, A. L. B., Guimarães, F. S. & Wotjak, C. T. Cannabinoid type 1 receptors and transient receptor potential vanilloid type 1 channels in fear and anxiety—two sides of one coin? *Neuroscience* 204, 186–192 (2012).
214. Navarria, A. *et al.* The dual blocker of FAAH/TRPV1 N-arachidonoylserotonin reverses the behavioral despair induced by stress in rats and modulates the HPA-axis. *Pharmacol. Res.* 87, 151–159 (2014).
215. Micale, V. *et al.* Anxiolytic Effects in Mice of a Dual Blocker of Fatty Acid Amide Hydrolase and Transient Receptor Potential Vanilloid Type-1 Channels. *Neuropsychopharmacology* 34, 593–606 (2009).
216. Lyte, M., Li, W., Opitz, N., Gaykema, R. P. A. & Goehler, L. E. Induction of anxiety-like behavior in mice during the initial stages of infection with the agent of murine colonic hyperplasia Citrobacter rodentium. *Physiol. Behav.* 89, 350–357 (2006).
217. Bellocchio, L. *et al.* Activation of the sympathetic nervous system mediates hypophagic and anxiety-like effects of CB1 receptor blockade. *Proc. Natl. Acad. Sci.* 110, 4786–4791 (2013).
218. Lee, T. T.-Y., Hill, M. N., Hillard, C. J. & Gorzalka, B. B. Temporal changes in N-acylethanolamine content and metabolism throughout the peri-adolescent period. *Synap. N. Y. N* 67, 4–10 (2013).

219. Romeo, R. D. *et al.* Stress history and pubertal development interact to shape hypothalamic-pituitary-adrenal axis plasticity. *Endocrinology* 147, 1664–1674 (2006).
220. Eiland, L. & Romeo, R. D. Stress and the developing adolescent brain. *Neuroscience* 249, 162–171 (2013).
221. Romeo, R. D. *et al.* Pubertal shifts in adrenal responsiveness to stress and adrenocorticotropic hormone in male rats. *Psychoneuroendocrinology* 42, 146–152 (2014).
222. Netherton, C., Goodyer, I., Tamplin, A. & Herbert, J. Salivary cortisol and dehydroepiandrosterone in relation to puberty and gender. *Psychoneuroendocrinology* 29, 125–140 (2004).
223. Gunnar, M. R., Wewerka, S., Frenn, K., Long, J. D. & Griggs, C. Developmental changes in hypothalamus–pituitary–adrenal activity over the transition to adolescence: Normative changes and associations with puberty. *Dev. Psychopathol.* 21, 69–85 (2009).
224. Hube, B. *et al.* Secreted lipases of Candida albicans: cloning, characterisation and expression analysis of a new gene family with at least ten members. *Arch. Microbiol.* 174, 362–374 (2000).
225. Ibrahim, A. S. *et al.* Evidence implicating phospholipase as a virulence factor of Candida albicans. *Infect. Immun.* 63, 1993–1998 (1995).
226. Fu, Y. *et al.* Cloning and characterization of a gene (LIP1) which encodes a lipase from the pathogenic yeast Candida albicans. *Microbiology,* 143, 331–340 (1997).
227. Mauvoisin, D. & Mounier, C. Hormonal and nutritional regulation of SCD1 gene expression. *Biochimie* 93, 78–86 (2011).
228. Leone, V. *et al.* Effects of diurnal variation of gut microbes and high-fat feeding on host circadian clock function and metabolism. *Cell Host Microbe* 17, 681–689 (2015).
229. Kim, J., Carlson, M. E., Kuchel, G. A., Newman, J. W. & Watkins, B. A. Dietary DHA reduces downstream endocannabinoid and inflammatory gene expression and epididymal fat mass while improving aspects of glucose use in muscle in C57BL/6J mice. *Int. J. Obes. 2005* 40, 129–137 (2016).
230. Yamada, D., Takeo, J., Koppensteiner, P., Wada, K. & Sekiguchi, M. Modulation of fear memory by dietary polyunsaturated fatty acids via cannabinoid receptors. *Neuropsychopharmacol. Off. Publ. Am. Coll. Neuropsychopharmacol.* 39, 1852–1860 (2014).
231. Ferraz, A. C. *et al.* Chronic ω-3 fatty acids supplementation promotes beneficial effects on anxiety, cognitive and depressive-like behaviors in rats subjected to a restraint stress protocol. *Behav. Brain Res.* 219, 116–122 (2011).
232. Clouard, C., Gerrits, W. J., van Kerkhof, I., Smink, W. & Bolhuis, J. E. Dietary Linoleic and α-Linolenic Acids Affect Anxiety-Related Responses and Exploratory Activity in Growing Pigs. *J. Nutr.* 145, 358–364 (2015).
233. Lessa, F. C. *et al.* Burden of Clostridium difficile infection in the United States. *N Engl J Med* 372, 825–34 (2015).
234. Schenck, L. P., Beck, P. L. & MacDonald, J. A. Gastrointestinal dysbiosis and the use of fecal microbial transplantation in Clostridium difficile infection. *World J Gastrointest Pathophysiol* 6, 169–80 (2015).

235. Solomon, K. The host immune response to Clostridium difficile infection. *Ther Adv Infect Dis* 1, 19–35 (2013).
236. Shields, K., Araujo-Castillo, R. V., Theethira, T. G., Alonso, C. D. & Kelly, C. P. Recurrent Clostridium difficile infection: From colonization to cure. *Anaerobe* 34, 59–73 (2015).
237. Youngster, I. *et al.* Oral, capsulized, frozen fecal microbiota transplantation for relapsing Clostridium difficile infection. *JAMA* 312, 1772–8 (2014).
238. Kassam, Z., Lee, C. H., Yuan, Y. & Hunt, R. H. Fecal microbiota transplantation for Clostridium difficile infection: systematic review and meta-analysis. *Am J Gastroenterol* 108, 500–8 (2013).
239. Li, Y. T., Cai, H. F., Wang, Z. H., Xu, J. & Fang, J. Y. Systematic review with meta-analysis: long-term outcomes of faecal microbiota transplantation for Clostridium difficile infection. *Aliment Pharmacol Ther* (2015) doi:10.1111/apt.13492.
240. De Leon, L. M., Watson, J. B. & Kelly, C. R. Transient flare of ulcerative colitis after fecal microbiota transplantation for recurrent Clostridium difficile infection. *Clin Gastroenterol Hepatol* 11, 1036–8 (2013).
241. Alang, N. & Kelly, C. R. Weight gain after fecal microbiota transplantation. *Open Forum Infect Dis* 2, ofv004 (2015).
242. Zelante, T. *et al.* Tryptophan catabolites from microbiota engage aryl hydrocarbon receptor and balance mucosal reactivity via interleukin-22. *Immunity* 39, 372–85 (2013).
243. Carvalho, A. *et al.* Dectin-1 isoforms contribute to distinct Th1/Th17 cell activation in mucosal candidiasis. *Cell Mol Immunol* 9, 276–86 (2012).
244. De Luca, A. *et al.* IL-22 defines a novel immune pathway of antifungal resistance. *Mucosal Immunol* 3, 361–73 (2010).
245. Quintin, J. *et al.* Candida albicans infection affords protection against reinfection via functional reprogramming of monocytes. *Cell Host Microbe* 12, 223–32 (2012).
246. Sherman, F. Getting started with yeast. *Methods Enzym.* 194, 3–21 (1991).
247. Sorg, J. A. & Sonenshein, A. L. Inhibiting the initiation of Clostridium difficile spore germination using analogs of chenodeoxycholic acid, a bile acid. *J Bacteriol* 192, 4983–90 (2010).
248. Sorg, J. A. & Sonenshein, A. L. Bile salts and glycine as cogerminants for Clostridium difficile spores. *J Bacteriol* 190, 2505–12 (2008).
249. Wilson, K. H., Kennedy, M. J. & Fekety, F. R. Use of sodium taurocholate to enhance spore recovery on a medium selective for Clostridium difficile. *J Clin Microbiol* 15, 443–6 (1982).
250. Caporaso, J. G. *et al.* Ultra-high-throughput microbial community analysis on the Illumina HiSeq and MiSeq platforms. *ISME J.* 6, 1621–1624 (2012).
251. Reeves, A. E. *et al.* The interplay between microbiome dynamics and pathogen dynamics in a murine model of Clostridium difficile Infection. *Gut Microbes* 2, 145–58 (2011).
252. Shen, A. Clostridium difficile toxins: mediators of inflammation. *J Innate Immun* 4, 149–58 (2012).
253. Yang, G. *et al.* Expression of recombinant Clostridium difficile toxin A and B in Bacillus megaterium. *BMC Microbiol* 8, 192 (2008).

254. Schubert, A. M., Sinani, H. & Schloss, P. D. Antibiotic-Induced Alterations of the Murine Gut Microbiota and Subsequent Effects on Colonization Resistance against Clostridium difficile. *MBio* 6, e00974 (2015).
255. Schubert, A. M. *et al.* Microbiome data distinguish patients with Clostridium difficile infection and non-C. difficile-associated diarrhea from healthy controls. *MBio* 5, e01021-14 (2014).
256. Shahinas, D. *et al.* Toward an understanding of changes in diversity associated with fecal microbiome transplantation based on 16S rRNA gene deep sequencing. *MBio* 3, (2012).
257. Reeves, A. E., Koenigsknecht, M. J., Bergin, I. L. & Young, V. B. Suppression of Clostridium difficile in the gastrointestinal tracts of germfree mice inoculated with a murine isolate from the family Lachnospiraceae. *Infect Immun* 80, 3786–94 (2012).
258. Nerandzic, M. M., Mullane, K., Miller, M. A., Babakhani, F. & Donskey, C. J. Reduced acquisition and overgrowth of vancomycin-resistant enterococci and Candida species in patients treated with fidaxomicin versus vancomycin for Clostridium difficile infection. *Clin Infect Dis* 55 Suppl 2, S121-6 (2012).
259. Hsu, M. S., Wang, J. T., Huang, W. K., Liu, Y. C. & Chang, S. C. Prevalence and clinical features of Clostridium difficile-associated diarrhea in a tertiary hospital in northern Taiwan. *J Microbiol Immunol Infect* 39, 242–8 (2006).
260. McFarland, L. V. Deciphering meta-analytic results: a mini-review of probiotics for the prevention of paediatric antibiotic-associated diarrhoea and Clostridium difficile infections. *Benef Microbes* 6, 189–94 (2015).
261. Johnson, S. *et al.* Is primary prevention of Clostridium difficile infection possible with specific probiotics? *Int J Infect Dis* 16, e786-92 (2012).
262. O'Horo, J. C., Jindai, K., Kunzer, B. & Safdar, N. Treatment of recurrent Clostridium difficile infection: a systematic review. *Infection* 42, 43–59 (2014).
263. Nakagawa, T. *et al.* Endogenous IL-17 as a factor determining the severity of Clostridium difficile infection in mice. *J Med Microbiol* 65, 821–7 (2016).
264. Hasegawa, M. *et al.* Interleukin-22 regulates the complement system to promote resistance against pathobionts after pathogen-induced intestinal damage. *Immunity* 41, 620–32 (2014).
265. Wang, L., Cao, J., Li, C. & Liping, Z. IL-27/IL-27receptor signaling provides protection in Clostridium difficile-induced colitis. *J Infect Dis* (2017) doi:10.1093/infdis/jix581.
266. Buonomo, E. L. *et al.* Role of interleukin 23 signaling in Clostridium difficile colitis. *J Infect Dis* 208, 917–20 (2013).
267. Rubino, S. J., Geddes, K. & Girardin, S. E. Innate IL-17 and IL-22 responses to enteric bacterial pathogens. *Trends Immunol* 33, 112–8 (2012).
268. Lee, J. S. *et al.* Interleukin-23-Independent IL-17 Production Regulates Intestinal Epithelial Permeability. *Immunity* 43, 727–38 (2015).
269. Caplan, M. S. *et al.* Bifidobacterial supplementation reduces the incidence of necrotizing enterocolitis in a neonatal rat model. *Gastroenterology* 117, 577–583 (1999).
270. Fanning, S. *et al.* Bifidobacterial surface-exopolysaccharide facilitates commensal-host interaction through immune modulation and pathogen protection. *Proc. Natl. Acad. Sci.* 109, 2108–2113 (2012).

271. O'Hara, A. M. *et al.* Functional modulation of human intestinal epithelial cell responses by Bifidobacterium infantis and Lactobacillus salivarius. *Immunology* 118, 202–215 (2006).
272. Underwood, M. A. *et al.* Bifidobacterium longum subsp. infantis in experimental necrotizing enterocolitis: alterations in inflammation, innate immune response, and the microbiota. *Pediatr. Res.* 76, 326–333 (2014).
273. Wang, H. *et al.* Bifidobacteria may be beneficial to intestinal microbiota and reduction of bacterial translocation in mice following ischaemia and reperfusion injury. *Br. J. Nutr.* 109, 1990–1998 (2013).
274. Derrien, M., Vaughan, E. E., Plugge, C. M. & de Vos, W. M. Akkermansia muciniphila gen. nov., sp. nov., a human intestinal mucin-degrading bacterium. *Int. J. Syst. Evol. Microbiol.* 54, 1469–1476 (2004).
275. Kang, C. *et al.* Extracellular Vesicles Derived from Gut Microbiota, Especially Akkermansia muciniphila, Protect the Progression of Dextran Sulfate Sodium-Induced Colitis. *PLOS ONE* 8, e76520 (2013).
276. Reunanen, J. *et al.* Akkermansia muciniphila Adheres to Enterocytes and Strengthens the Integrity of the Epithelial Cell Layer. *Appl. Environ. Microbiol.* 81, 3655–3662 (2015).
277. Derrien, M. *et al.* Modulation of Mucosal Immune Response, Tolerance, and Proliferation in Mice Colonized by the Mucin-Degrader Akkermansia muciniphila. *Front. Microbiol.* 2, (2011).
278. van Leeuwen, P. T. *et al.* Interspecies Interactions between Clostridium difficile and Candida albicans. *mSphere* 1, e00187-16 (2016).
279. Kimball, E. S., Wallace, N. H., Schneider, C. R., D'Andrea, M. R. & Hornby, P. J. Vanilloid receptor 1 antagonists attenuate disease severity in dextran sulphate sodium-induced colitis in mice. *Neurogastroenterol. Motil. Off. J. Eur. Gastrointest. Motil. Soc.* 16, 811–818 (2004).
280. Kihara, N. *et al.* Vanilloid receptor-1 containing primary sensory neurones mediate dextran sulphate sodium induced colitis in rats. *Gut* 52, 713–719 (2003).
281. Hasenoehrl, C., Taschler, U., Storr, M. & Schicho, R. The gastrointestinal tract – a central organ of cannabinoid signaling in health and disease. *Neurogastroenterol. Motil.* 28, 1765–1780 (2016).
282. Izzo, A. A. *et al.* Cannabinoid CB1-receptor mediated regulation of gastrointestinal motility in mice in a model of intestinal inflammation. *Br. J. Pharmacol.* 134, 563–570.
283. Marzo, V. D. & Izzo, A. A. Endocannabinoid overactivity and intestinal inflammation. *Gut* 55, 1373–1376 (2006).
284. Karwad, M. A. *et al.* The role of CB1 in intestinal permeability and inflammation. *FASEB J. Off. Publ. Fed. Am. Soc. Exp. Biol.* 31, 3267–3277 (2017).
285. Muccioli, G. G. *et al.* The endocannabinoid system links gut microbiota to adipogenesis. *Mol. Syst. Biol.* 6, 392 (2010).
286. Sam, A. H., Salem, V. & Ghatei, M. A. Rimonabant: From RIO to Ban. *J. Obes.* 2011, (2011).
287. Cani, P. D. *et al.* Endocannabinoids — at the crossroads between the gut microbiota and host metabolism. *Nat. Rev. Endocrinol.* 12, 133–143 (2016).

288. Ihenetu, K., Molleman, A., Parsons, M. E. & Whelan, C. J. Inhibition of interleukin-8 release in the human colonic epithelial cell line HT-29 by cannabinoids. *Eur. J. Pharmacol.* 458, 207–215 (2003).
289. Kimball, E. S., Schneider, C. R., Wallace, N. H. & Hornby, P. J. Agonists of cannabinoid receptor 1 and 2 inhibit experimental colitis induced by oil of mustard and by dextran sulfate sodium. *Am. J. Physiol.-Gastrointest. Liver Physiol.* 291, G364–G371 (2006).
290. Lunn, C. A., Reich, E.-P. & Bober, L. Targeting the CB2 receptor for immune modulation. *Expert Opin. Ther. Targets* 10, 653–663 (2006).
291. Alhouayek, M., Lambert, D. M., Delzenne, N. M., Cani, P. D. & Muccioli, G. G. Increasing endogenous 2-arachidonoylglycerol levels counteracts colitis and related systemic inflammation. *FASEB J.* 25, 2711–2721 (2011).
292. Rousseaux, C. *et al.* Lactobacillus acidophilus modulates intestinal pain and induces opioid and cannabinoid receptors. *Nat. Med.* 13, 35–37 (2007).
293. Jamshidi, N. & Taylor, D. A. Anandamide administration into the ventromedial hypothalamus stimulates appetite in rats. *Br. J. Pharmacol.* 134, 1151–1154 (2001).
294. Rodríguez de Fonseca, F. *et al.* An anorexic lipid mediator regulated by feeding. *Nature* 414, 209–212 (2001).
295. Fu, J. *et al.* Oleylethanolamide regulates feeding and body weight through activation of the nuclear receptor PPAR-alpha. *Nature* 425, 90–93 (2003).
296. Schwabe, R. F. Endocannabinoids promote hepatic lipogenesis and steatosis through CB1 receptors. *Hepatology* 42, 959–961 (2005).
297. Matias, I., Belluomo, I. & Cota, D. The Fat Side of the Endocannabinoid System: Role of Endocannabinoids in the Adipocyte. *Cannabis Cannabinoid Res.* 1, 176–185 (2016).
298. Mehrpouya-Bahrami, P. *et al.* Blockade of CB1 cannabinoid receptor alters gut microbiota and attenuates inflammation and diet-induced obesity. *Sci. Rep.* 7, 1–16 (2017).
299. Massa, F. *et al.* Alterations in the Hippocampal Endocannabinoid System in Diet-Induced Obese Mice. *J. Neurosci.* 30, 6273–6281 (2010).
300. Mallat, A., Teixeira-Clerc, F., Deveaux, V., Manin, S. & Lotersztajn, S. The endocannabinoid system as a key mediator during liver diseases: new insights and therapeutic openings. *Br. J. Pharmacol.* 163, 1432–1440 (2011).
301. Caraceni, P. *et al.* Circulating and hepatic endocannabinoids and endocannabinoid-related molecules in patients with cirrhosis. *Liver Int.* 30, 816–825 (2010).
302. Blüher, M. *et al.* Dysregulation of the peripheral and adipose tissue endocannabinoid system in human abdominal obesity. *Diabetes* 55, 3053–3060 (2006).
303. Engeli, S. *et al.* Activation of the Peripheral Endocannabinoid System in Human Obesity. *Diabetes* 54, 2838–2843 (2005).
304. Schofield, D. A., Westwater, C., Warner, T. & Balish, E. Differential Candida albicans lipase gene expression during alimentary tract colonization and infection. *FEMS Microbiol. Lett.* 244, 359–365 (2005).
305. Paraje, M. G., Correa, S. G., Renna, M. S., Theumer, M. & Sotomayor, C. E. Candida albicans-secreted lipase induces injury and steatosis in immune and parenchymal cells. *Can. J. Microbiol.* 54, 647–659 (2008).

306. Roustan, J. L., Rascon Chu, A., Moulin, G. & Bigey, F. A novel lipase/acyltransferase from the yeast Candida albicans: expression and characterisation of the recombinant enzyme. *Appl. Microbiol. Biotechnol.* 68, 203–212 (2005).
307. Niewerth, M. & Korting, H. C. Phospholipases of Candida albicans. *Mycoses* 44, 361–367 (2001).
308. Naglik, J. R. *et al.* Differential Expression of Candida albicans Secreted Aspartyl Proteinase and Phospholipase B Genes in Humans Correlates with Active Oral and Vaginal Infections. *J. Infect. Dis.* 188, 469–479 (2003).
309. KOTHAVADE, R. J. & PANTHAKI, M. H. Evaluation of phospholipase activity of Candida albicans and its correlation with pathogenicity in mice. *J. Med. Microbiol.* 47, 99–102 (1998).
310. Leidich, S. D. *et al.* Cloning and Disruption of caPLB1, a Phospholipase B Gene Involved in the Pathogenicity of Candida albicans. *J. Biol. Chem.* 273, 26078–26086 (1998).
311. Mukherjee, P. K. *et al.* Reintroduction of the PLB1 gene into Candida albicans restores virulence in vivo. *Microbiology,* 147, 2585–2597 (2001).
312. Jones, P. J. H., Lin, L., Gillingham, L. G., Yang, H. & Omar, J. M. Modulation of plasma N-acylethanolamine levels and physiological parameters by dietary fatty acid composition in humans. *J. Lipid Res.* 55, 2655–2664 (2014).
313. Mitchell, R. W. & Hatch, G. M. Fatty acid transport into the brain: of fatty acid fables and lipid tails. *Prostaglandins Leukot. Essent. Fatty Acids* 85, 293–302 (2011).
314. Martin, G. G. *et al.* Sterol Carrier Protein-2/Sterol Carrier Protein-x/Fatty Acid Binding Protein-1 Ablation Impacts Response of Brain Endocannabinoid to High-Fat Diet. *Lipids* 54, 583–601 (2019).
315. McPartland, J. M., Matias, I., Di Marzo, V. & Glass, M. Evolutionary origins of the endocannabinoid system. *Gene* 370, 64–74 (2006).
316. Merkel, O., Schmid, P. C., Paltauf, F. & Schmid, H. H. O. Presence and potential signaling function of N-acylethanolamines and their phospholipid precursors in the yeast Saccharomyces cerevisiae. *Biochim. Biophys. Acta BBA - Mol. Cell Biol. Lipids* 1734, 215–219 (2005).
317. Allen, J. A., Halverson-Tamboli, R. A. & Rasenick, M. M. Lipid raft microdomains and neurotransmitter signalling. *Nat. Rev. Neurosci.* 8, 128–140 (2007).
318. Maccarrone, M. *et al.* Lipid rafts regulate 2-arachidonoylglycerol metabolism and physiological activity in the striatum. *J. Neurochem.* 109, 371–381 (2009).
319. Bari, M., Battista, N., Fezza, F., Finazzi-Agrò, A. & Maccarrone, M. Lipid Rafts Control Signaling of Type-1 Cannabinoid Receptors in Neuronal Cells IMPLICATIONS FOR ANANDAMIDE-INDUCED APOPTOSIS. *J. Biol. Chem.* 280, 12212–12220 (2005).
320. Lewis, B. B. *et al.* Loss of Microbiota-Mediated Colonization Resistance to Clostridium difficile Infection With Oral Vancomycin Compared With Metronidazole. *J. Infect. Dis.* 212, 1656–1665 (2015).
321. Theriot, C. M. *et al.* Antibiotic-induced shifts in the mouse gut microbiome and metabolome increase susceptibility to Clostridium difficile infection. *Nat. Commun.* 5, 1–10 (2014).

322. Khanna, S. *et al.* A Novel Microbiome Therapeutic Increases Gut Microbial Diversity and Prevents Recurrent Clostridium difficile Infection. *J. Infect. Dis.* 214, 173–181 (2016).
323. Costello, E. K., Stagaman, K., Dethlefsen, L., Bohannan, B. J. M. & Relman, D. A. The application of ecological theory towards an understanding of the human microbiome. *Science* 336, 1255–1262 (2012).
324. Bairey, E., Kelsic, E. D. & Kishony, R. High-order species interactions shape ecosystem diversity. *Nat. Commun.* 7, 1–7 (2016).
325. Mineur, Y. S., Belzung, C. & Crusio, W. E. Effects of unpredictable chronic mild stress on anxiety and depression-like behavior in mice. *Behav. Brain Res.* 175, 43–50 (2006).
326. Roth, M. K. *et al.* Effects of chronic plus acute prolonged stress on measures of coping style, anxiety, and evoked HPA-axis reactivity. *Neuropharmacology* 63, 1118–1126 (2012).
327. Kim, J.-G., Jung, H.-S., Kim, K.-J., Min, S.-S. & Yoon, B.-J. Basal blood corticosterone level is correlated with susceptibility to chronic restraint stress in mice. *Neurosci. Lett.* 555, 137–142 (2013).